EFFECT OF BRINE ON MECHANICAL PROPERTIES OF MARBLE, SILTSTONE AND SANDSTONE

NONGPLOY PUANGTHONG

A Thesis Submitted in Partial Fulfillment of the Requirements for the
Degree of Master of Engineering in Civil, Transportation and
Geo-resources Engineering
Suranaree University of Technology
Academic Year 2023

ผลกระทบของน้ำเกลือต่อสมบัติเชิงกลของหินอ่อน หินทรายแป้งและหินทราย

นางสาวน้องพลอย พวงทอง

วิทยานิพนธ์นี้เป็นส่วนหนึ่งของการศึกษาตามหลักสูตรปริญญาวิศวกรรมศาสตรมหาบัณฑิต

สาขาวิชาวิศวกรรมโยธา ขนส่ง และทรัพยากรธรณี

มหาวิทยาลัยเทคโนโลยีสุรนารี

ปีการศึกษา 2566

EFFECT OF BRINE ON MECHANICAL PROPERTIES OF MARBLE, SILTSTONE AND SANDSTONE

Suranaree University of Technology has approved this thesis submitted in partial fulfillment of the requirements for a Master's Degree.

Thesis Examining Committee

....

(Assoc. Prof. Dr. Pornkasem Jongpradist)

Chairperson

....

(Emeritus Prof. Dr. Kittitep Fuenkajorn)

Member (Thesis Advisor)

....

(Asst. Prof. Dr. Prachya Tepnarong)

Member

....

(Assoc. Prof. Dr. Yupaporn Ruksakulpiwat)

Vice Rector for Academic Affairs and Quality Assurance

....

(Assoc. Prof. Dr. Pornsiri Jongkol)

Dean of Institute of Engineering

น้องพลอย พวงทอง : ผลกระทบของน้ำเกลือต่อสมบัติเชิงกลของหินอ่อน หินทรายแป้ง และหินทราย (EFFECT OF BRINE ON MECHANICAL PROPERTIES ON MARBLE, SILTSTONE AND SANDSTONE)
อาจารย์ที่ปรึกษา : ศาสตราจารย์ (เกียรติคุณ) ดร.กิตติเทพ เฟื่องขจร, 125 หน้า.

คำสำคัญ: การเสื่อมสภาพของหิน/การตกผลึกของเกลือ/น้ำเกลือโซเดียมคลอไรด์/ระยะเวลาแช่/ความแข็งของหิน

การศึกษานี้มีวัตถุประสงค์เพื่อประเมินผลกระทบของการแช่ในน้ำเกลือโซเดียมคลอไรด์ (NaCl) ต่อสมบัติเชิงกลของหินทรายแป้ง หินทราย และหินอ่อน ซึ่งเป็นหินที่นิยมนำมาใช้เป็นหินประดับอาคารในภาคตะวันออกเฉียงเหนือของประเทศไทย ตัวอย่างหินถูกแช่ในน้ำเกลือความเข้มข้นสูงสุดเป็นเวลา 240 วัน ทุกๆ 60 วัน มีการวัดปริมาณการแทรกซึมของของเหลว ความแข็งแรง และความยืดหยุ่นของตัวอย่างหิน ผลการทดสอบชี้ให้เห็นว่า หลังจาก 240 วัน หินทรายแป้งและหินทรายสามารถดูดซึมน้ำเกลือได้สูงสุดถึง 6% และ 9% ตามลำดับ ในขณะที่หินอ่อนดูดซึมได้น้อยกว่า 0.1% แรงดันของเหลวที่เกิดขึ้นในรูพรุนของหินส่งผลต่อการลดลงของความแข็งแรงในการกดอัด ความแข็งแรงในการดึงและความยืดหยุ่นของหินตามระยะเวลาการแช่ที่เพิ่มขึ้น นอกจากนี้ เมื่อนำตัวอย่างหินออกจากน้ำเกลือมาตากแห้งเป็นเวลา 30 วัน ยังคงพบว่าความแข็งแรงและความยืดหยุ่นของหินทรายแป้งและหินทรายลดลงอีก สาเหตุมาจากการเกิดและขยายตัวของรอยแตกและรอยแตกขนาดจุลภาค อันเนื่องมาจากผลึกเกลือที่ตกค้างอยู่ภายในรูพรุนของหิน การศึกษานี้เสนอสูตรทางคณิตศาสตร์แบบเลขชี้กำลัง (exponential equations) เพื่อทำนายการลดลงของความแข็งแรงและความยืดหยุ่นของหินในระยะยาวจากผลการทดลองในห้องปฏิบัติการ

สาขาวิชา เทคโนโลยีธรณี
ปีการศึกษา 2566

ลายมือชื่อนักศึกษา น้องพลอย
ลายมือชื่ออาจารย์ที่ปรึกษา ....

NONGPLOY PUANGTHONG: EFFECT OF BRINE ON MECHANICAL PROPERTIES OF MARBLE, SILTSTONE AND SANDSTONE. THESIS ADVISOR: EMERITUS PROF. DR. KITTITEP FUENKAJORN, Ph.D., P.E., 125 PP.

Keyword: Rock deterioration/ Salt crystallization/ Sodium chloride brine/ Submerged duration/ Rock strengths

The objective of this study is to determine the effects of NaCl brine submersion on mechanical properties of siltstone, sandstone and marble that have been used as decorating stones in the northeast of Thailand. Rock specimens are submerged under saturated brine for up to 240 days. Every 60 days interval, their liquid contents, strengths and elasticity are determined. Results indicate that after 240 days siltstone and sandstone specimens can absorb brine and water up to 6% and 9% by weight, where less than 0.1% can be absorbed by marble. Due to the effect of pore pressure compressive and tensile strengths and elasticity of the rocks continue to decrease with increasing submersion duration. When left air-dried for 30 days further reduction of rock strengths and elasticity are observed from the siltstone and sandstone. This is due to initiation and propagation of fissures and micro cracks caused by the growth of remaining salt crystals left in the pore spaces. Exponential equations are proposed to predict the ultimate reductions of rock strength and elasticity based on the laboratory test results.

School of Geotechnology Student's Signature ....

Academic Year 2023 Advisor's Signature ....

ACKNOWLEDGEMENTS

I wish to acknowledge the funding support from Suranaree University of Technology (SUT).

I would like to express thanks to Emeritus Prof. Dr. Kittitep Fuenkajorn, thesis advisor, who gave a critical review. I appreciate his encouragement, suggestions, and comments during the research period. I would like to express thanks to Assoc. Prof. Dr. Pornkasem Jongpradist and Asst. Prof. Dr. Prachya Tepnarong for their valuable suggestions and comments on my research works as thesis committee members. Grateful thanks are given to all staffs of Geomechanics Research Unit, Institute of Engineering who supported my work.

Finally, I most gratefully acknowledge my parents for all their support and encouragement throughout the period of this study.

Nongploy Puangthong

TABLE OF CONTENTS

Page

TABLE OF CONTENTS (Continued)

TABLE OF CONTENTS (Continued)

Page

TABLE OF CONTENTS (Continued)

Page

LIST OF TABLES

LIST OF FIGURES

Figure **Page**

LIST OF FIGURES (Continued)

LIST OF FIGURES (Continued)

LIST OF FIGURES (Continued)

SYMBOLS AND ABBREVIATIONS

$w_{\%}$	=	Percent of liquid/salt contents
w_b	=	Weight of wet specimens submerged in saturated brine
w_{brine}	=	Brine contents
w_i	=	Weight of initial specimen
w_s	=	Weight of specimens after left air-dried for 30 days
w_{salt}	=	Salt contents
w_{sat}	=	Weight of soaked specimen
w_w	=	Weight of wet specimens submerged in distilled water
w_{water}	=	Water contents
t	=	Time
σ_B	=	Brazilian tensile strength
σ_c	=	Uniaxial compressive strength
E	=	Young's modulus
ν	=	Poisson's ratio

CHAPTER I

INTRODUCTION

1.1 Background and Rationale

Rock salt near ground surface in the Maha Sarakham formation, northeast of Thailand, has caused damage to housing structures, particularly near the edges of the basins where salt depth is less than 50 m. The shallow salt beds are mostly covered by silty and sandy soils (Figure 1.1). Detailed description of the salt and geology of the basins are given by Warren (2016). During rainy season the saline groundwater can reach the ground surface and can cause flooding in some low areas. The groundwater subsides during dry season and salt crystals and powder are left on the top soil and in decorating stones forming housing terrace and pavement. Marble, siltstone and sandstone are widely used in the area. This calls for the study of the effect of saline groundwater and remaining salt crystals on the long-term integrity of these rocks.

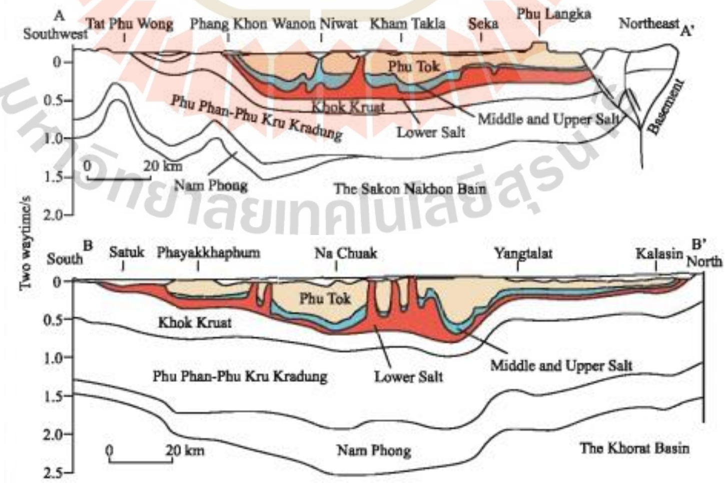

Figure 1.1 Subsurface structure of the Maha Sarakham Formation (Warren, 2016)

1.2 Research Objectives

The objective of this study is to determine the effects of NaCl brine submersion on mechanical properties of siltstone, sandstone and marble that have been used as decorating stones in the northeast of Thailand. The findings are useful to predict the lifespan or deterioration and strength and stiffness of each rock types that exposes to saline environment under long period.

1.3 Scope and Limitations

The scope and limitations of this study include as follows:

1) The rock specimens are prepared from Khao Khad marble, Phu Phan siltstone and Phu Phan sandstones.

2) The diameters of specimens are 45 mm with a length of 90 mm for uniaxial compression tests and 54 mm with a length of 27 mm for Brazilian tension tests.

3) The specimens are tested under water, brine, and salt conditions.

4) Saturated brine is prepared by dissolving sodium chloride in distilled water with a concentration of 33.91% by weight.

5) The saturation periods are 60, 120, 180 and 240 days.

6) Uniaxial compressive strength test are conducted following ASTM D7012-14 standard practice.

7) Brazilian tensile strength test are conducted following ASTM D3967-05 standard practice.

8) Mineral compositions are determined for different saturation periods using X-ray diffraction following the STP 479 standard practice.

1.4 Research Methodology

The research methodology shown in Figure 1.2 comprises 9 steps; including literature review, sample preparation, laboratory simulation of rock deterioration, uniaxial compression strength test, Brazilian tensile strength test, X-ray diffraction analysis, results analysis, discussions, conclusions and thesis writing.

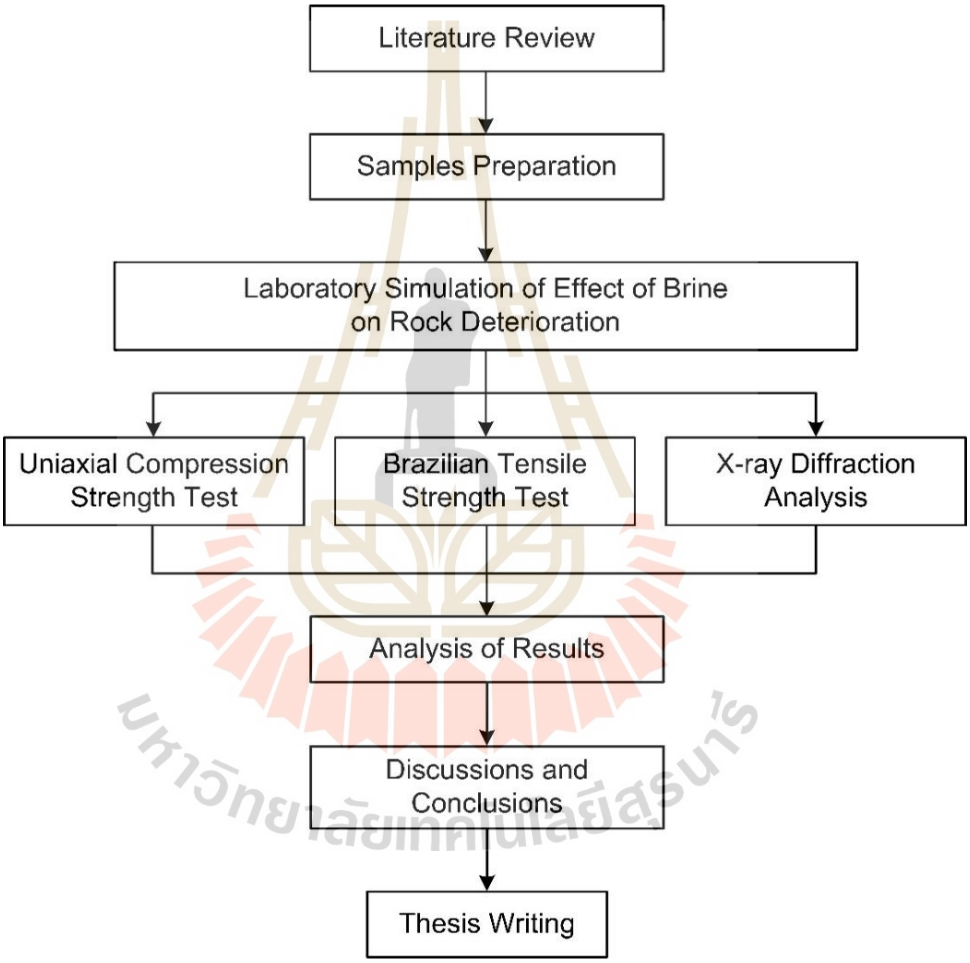

Figure 1.2 Research methodology.

1.4.1 Literature review

Literature review is conducted to study the effects of salt weathering on the mechanical properties of decorating rocks under compression and tension conditions and the effect of time on rocks properties under brine conditions. The sources of information are from journals, technical reports, and conference papers.

1.4.2 Samples preparation

The rock samples are prepared from marble of Khao Khad formation, siltstone and sandstones of Phu Phan formation. The rock samples are prepared to obtain cylinders with diameters of 45 mm and lengths of 90 mm for uniaxial compression tests, and 54 mm in diameter with a length of 27 mm for Brazilian tensile tests.

1.4.3 Laboratory simulation of deterioration

The simulation of rock deterioration is investigated under water, brine and salt conditions. These conditions are performed on water and NaCl brine (33.91% by weight). The test procedure are as follows:

1) Water conditions; Submerging in distilled water for 240 days. Samples are taken out for physical and mechanical testing every 60 days.

2) Brine conditions; Submerging in NaCl brine for 240 days. Samples are taken out for physical and mechanical testing every 60 days.

3) Salt condition; Submerging in NaCl brine for every 60 days, samples are placed under room temperature and left air-dried for 30 days before testing.

1.4.4 Uniaxial compressive strength test

The uniaxial compressive strength test and calculation follow the ASTM D7012-14 standard practice. The testing is performed by increasing the axial stress to the rock specimens. The results are used to determine the compressive strength, elastic modulus, and Poisson’s ratio, revealing the effect of rock deterioration initially and after every cycle under water, brine, and salt conditions.

1.4.5 Brazilian tensile strength test

The Brazilian tensile strength test and calculation follow the ASTM D3967-05 standard practice. The test is performed to determine the effect of rock deterioration on rock tensile strength. Testing is conducted initially and after every cycle under water, brine, and salt conditions.

1.4.6 X-ray diffraction (XRD) analysis

The XRD analysis is performed on finely ground rock powder pressed into coherent pellets. The analysis is conducted initially and after every 60 days of simulation on rock deterioration. The results can be used to identify the effects of rock deterioration due to NaCl brine influence on mineral compositions, which may affect rock properties.

1.4.7 Results and analysis

The results obtained from the liquid/salt contents, uniaxial compression test and Brazilian tension test on rock specimens are compared and analyzed to develop the mathematical relationship between them.

1.4.8 Discussions and Conclusions

This section describes the results compared with previous studies, and the prediction of long-term effects on the rock mechanical properties.

1.4.9 Thesis writing

All research activities, methods and results will be documented and carried out in the dissertation. The research or findings will be published in a conference or journal process.

1.5 Thesis content

This research thesis is divided into seven chapters. Chapter 1 includes background and rational, research objectives, scope and limitations and research methodology. Chapter 2 presents summary result of literature review to improve an understanding of the effect of brine on mechanical properties of decorating rocks. Chapter 3 describes sample preparation. Chapter 4 describes laboratory testing and methods for rock duration simulations. Chapter 5 describes the results of rock duration simulations. Chapter 6 presents analysis of test result. Chapter 7 presents the discussion, conclusions, and recommendations for future studies.

CHAPTER II

LITERATURE REVIEW

2.1 Introduction

This chapter summarizes of literature review carried out to improve an understanding brine weathering process of rock. The topics reviewed include effect of salt weathering on rocks, effect of brine on compressive strength, effect of time on rocks deterioration, effects of brine on Brazilian tensile strength and effect of pore pressure on rocks properties.

2.2 Effects of salt weathering on rocks

Salt weathering is one of the main processes causing serious deterioration of structure, culture heritage made from stones, brick. Such as Angkor monuments in Cambodia, show in Figure 2.1 (Hosono et al., 2006), Angkor temples in Cambodia (Xu et al., 2018), the Tuscany architecture in Italy (Andreotti et al., 2018) and Dazu rock carvings in Chongqing (Yan et al., 2022). And some decorating rock as building dolostones (Benavente et al., 2007) (Figure 2.2), limestone (Vazquez and Lux, 2023), sandstone, (Shukla et al., 2012; Rathnaweera et al., 2014). The mechanisms of salt transport and consequent weathering patterns are controlled by the petrographic characteristics of the porous rock, type of salt (e.g. sodium chloride, sodium sulfate, nitrate) salt concentration, and moisture content. That can be conclude as follows:

1) One of the crucial mechanisms of porous rocks deterioration is salt crystallization in their pores. Crystal growth within pores creates maximum pressure and this produces great stress which in turn damages the rock matrix (Benavente et al., 2007 and Keppert et al., 2015)

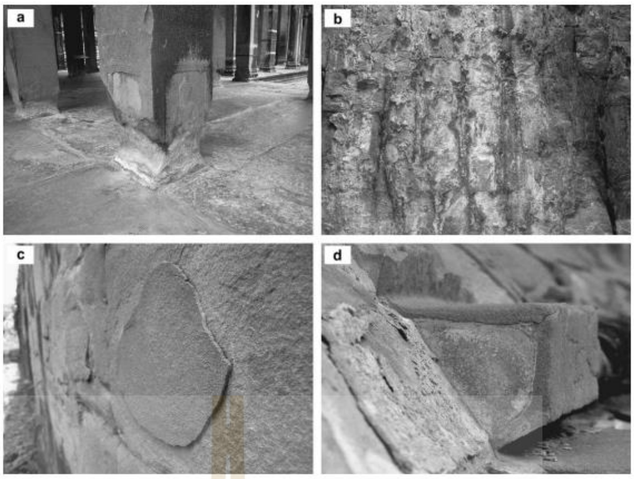

Figure 2.1 Representative images of the salt weathering process affecting sandstone at Angkor monuments in Cambodia. (a) Lower part of a pillar, (b) northern interior wall, (c) stone surface of the northern side, and (d) stone surface of the eastern side (Hosono et al., 2006).

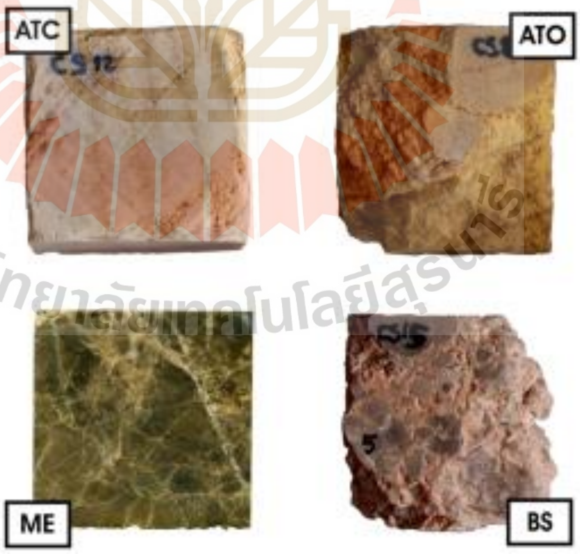

Figure 2.2 Weathering deterioration processes; ATC: Amarillo Triana Claro; ATO: Amarillo Triana Oscuro; ME: Marrón Emperador; BS: Beige Serpiente. (Benavente et al., 2007)

The role of pore size distribution in the damage caused by salt crystallization is verry significant. Rock with high porosity, coupled with crystal growth, is considered to have a high potential for causing rock damage (Celik and Kacmaz, 2016).

2) Various types of salt can originate from different sources, but sodium chloride (NaCl) and sodium sulfate (Na_2SO_4) are most commonly considered. Important sources of NaCl salt include seawater, groundwater, rock salts, and deicing salts. Other sourced of Na_2SO_4 salt include rainwater and atmospheric pollution (Oguchi and Yu, 2021). Several reviews suggest that NaCl salt is less damaging to rock compared to Na_2SO_4 due to the greater reactivity of sulfates with rock (Cooke, 1979; Celik and Aygün, 2019; Celik and Sert, 2020; Scrivano and Gaggero, 2020; Oguchi and Yu, 2021; Alveset et al., 2021)

3) High salt concentrations significantly increase the energy required for crystal growth compared to low concentration (Seo et al, 2019). As a result, crystals tend to grow larger in size (see Figure 2.3). These conditions profoundly affect the strength and deterioration of rock. Consequently, crystals tend to grow within larger pores until the pressure within the rock reaches a critical point, leading to rock fracture (Wellman and Wilson, 1968).

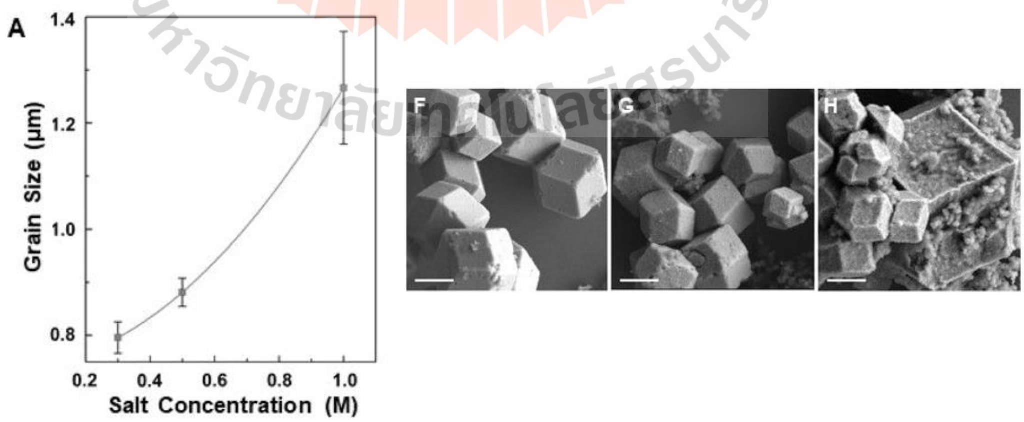

Figure 2.3 SEM images of increase crystal size with increasing salt concentration at (F) 0.3, (G) 0.5, and (H) 1 M NaCl. (Seo et al., 2019).

4) Moisture is a factor in salt weathering. Moisture can act as a carrier for salt, depositing it into pores and cracks, as only salts dissolved in water can penetrate and move through porous materials. When the moisture content of porous materials reaches its maximum, deterioration is often observed (Snethlage and Wendler, 1997).

Mechanisms for salt weathering include crystallization, hydration, and thermal expansion (Wang and An, 2016). Most research has concluded that the main cause of structural deterioration due to salt solution is salt crystallization in pore spaces (Dunning and Huf., 1983), as shown in Figure 2.4. The salt crystals grown to fill the pore space (Figure 2.4a) and they continue to develop and expand until cracks form within the pore spaces due to crystallization pressure (Figure 2.4b), Subsequently, salt crystals begin to merge, forming wider cracks (Figure 2.4c), the cracks are finally revealed (Figure 2.4d), and eventually cause rock deterioration (Zehnder and Arnold, 1989). Crystallization pressure arises from the volume expansion of salt within the pore spaces. (Ruiz-Agudo et al., 2006). Desaenuad et al. (2016) studied crystallization pressure and found that the pressure from crystal expansion was approximately 0.03 ± 0.007 N, causing deterioration of sandstone sculptures at the Lecce Historical Center in Italy (Figure 2.5). When sandstone samples are analyzed under Scanning Electron Microscope (SEM), salt crystallization is observed in the gaps between quartz and cracks. This crack are caused by crystallization pressure and expansion of salt in the pore space.

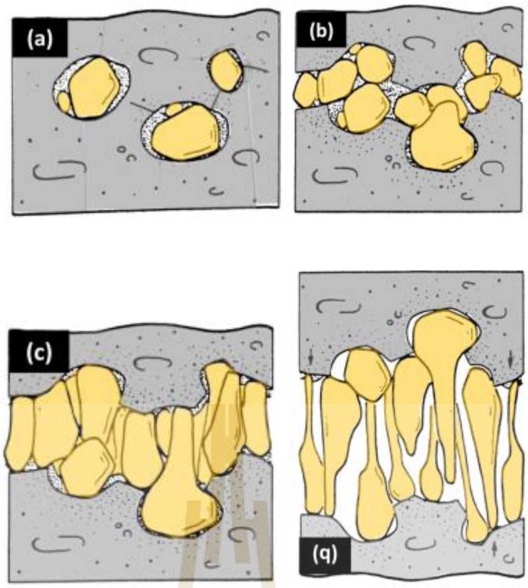

Figure 2.4 Model of salt crystallization in pore spaces. (Zehnder and Arnold., 1989)

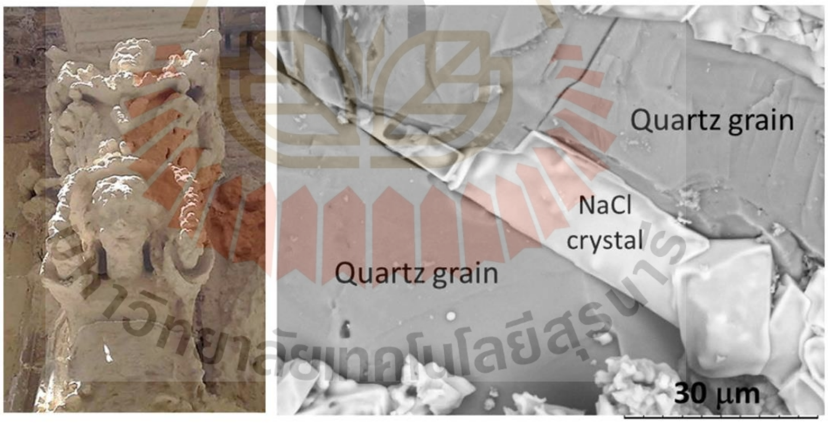

Figure 2.5 Left: Deterioration of a historical stone sculpture in Lecce, Italy. Right: SEM image of NaCl crystals. (Desaenuad et al., 2016).

2.3 Effects of brine on compressive strength

Most researchers have studied the behavior of brine-saturated rocks of different concentrations on compressive strength of a variety of rocks, such as sandstone (Shukla et al., 2012; Rathnaweera et al., 2014; De Silva et al., 2018; Huang et al., 2019;) Coal (Sampath et al., 2018), Shale (Zhou et al., 2021), and gypsum (Liang et al., 2012). Zhang et al. (2018) concluded that the brine concentration affects compressive strength of rocks and has a non-monotonic variation (U-shaped) relationship, (Figure 2.6). Under lower brine concentrations of 0 - 5% by weight, resulting in a reduction of compressive strength of approximately 8 - 27% compared with water condition. The reduced strength caused by the dissolution of cementing clay minerals in the sandstone (De Silva et al., 2018). When the brine concentration was increased to 10% by weight, resulting is increasing in compressive strength due to the crystallization of NaCl molecules from brine in pore spaces adding to the rock strength. Shukla et al. (2012) show that the increase of compressive strength may be due to crystallization of salts within the pore spaces. Therefore, compared to very porous rocks (such as sandstone), the effect of concentration in brine is even higher.

From triaxial compressive strength test result, the effect of confining pressure and brine concentration on the triaxial compressive strength of sandstone depends on both confining pressure and brine concentration. Huang et al. (2018) explain that when the confining pressure and brine concentration increased, the triaxial compressive strength, elastic modulus, cohesion and internal friction angle all increased (Figure 2.7). Similar experimental results have been obtained by Rathnaweera et al. (2015) that the brine saturating can effect on the stress-strain behavior of saline reservoir rock.

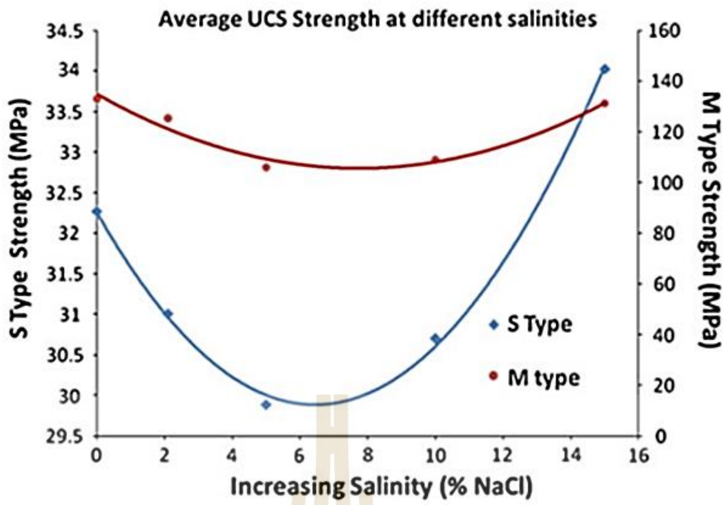

Figure 2.6 Average uniaxial strength at different brine concentrations. (Shukla et al., 2012).

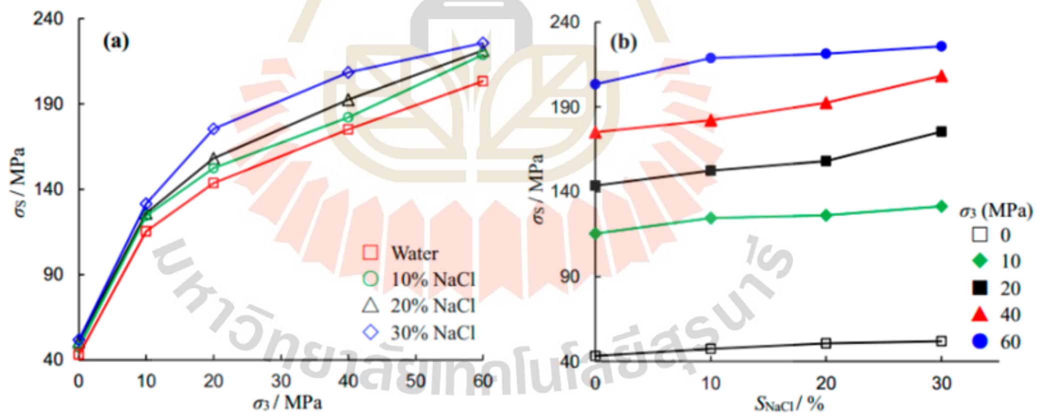

Figure 2.7 (a) Triaxial compressive strength versus confining pressure and (b) Triaxial compressive strength versus brine concentrations. (Huang et al., 2018).

2.4 Effect of time on rocks deterioration

The duration of immersion in brine is another reason for the deterioration of the mechanical properties of precious stones as water weakens the stone's adhesion (Li and Wang 2019). Effects of time on gypsum Liang et al. (2012) in the sandstone Dinesh et al. (2021) for 30 to 60 days have been studied. Their conclusions are that the mechanical properties (compressive strength, shear strength and Elastic parameters) decrease with increasing immersion time (Figures 2.8 and 2.9) due to increased salt crystallization, causing expansion stresses to fracture within the rock. As the salinity increases, there are effects of corrosion reaction on quartz and clay minerals. Tang and Wang (1999) describe that brine corrosion mechanism can affect rocks properties by decreases and accelerates cracks formation within rock.

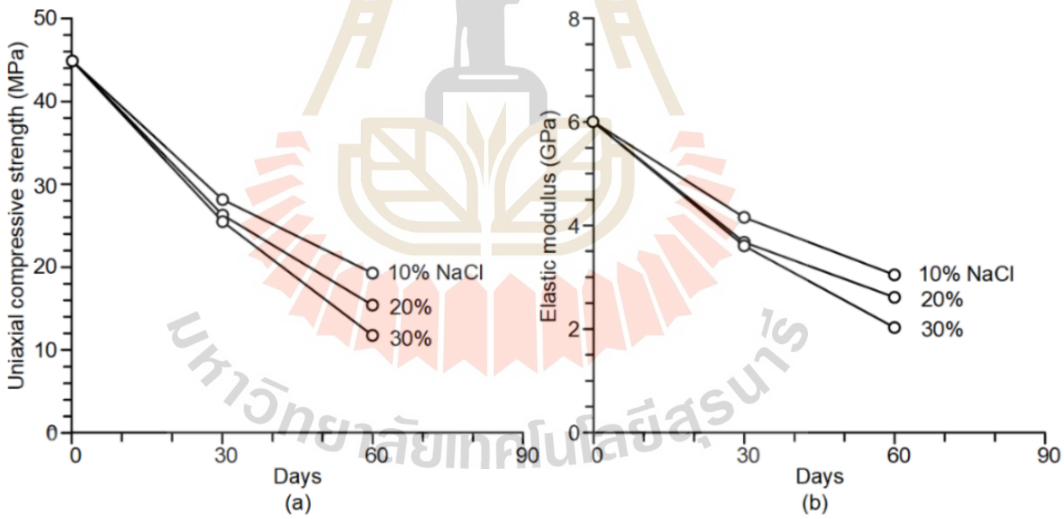

Figure 2.8 Uniaxial compressive strength (a) and elastic modulus (b) of saline saturated sandstone for 60 days (Dinesh et al., 2021).

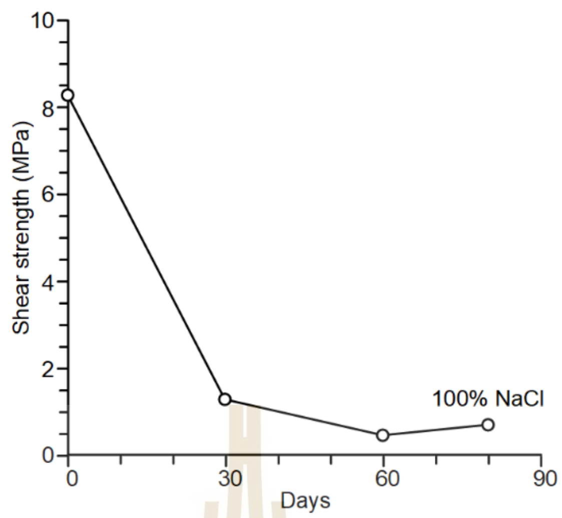

Figure 2.9 Shear strength of saline saturated gypsum for 90 days (Li and Wang, 2019).

2.5 Effects of brine on Brazilian tensile strength

Tensile strength is an important parameter in rock because rocks are much weaker in tension than in compression. De Silva et al. (2018) investigated effect of salinity under Brazilian tensile strength tests under varying NaCl brine concentrations (5, 7.5, 10, 12.5%). The result show that the tensile strength reduces with the concentration of NaCl lower than 0-10% in saturated brine, caused by the dissolution of cementing clay minerals in the rock matrix. Huang et al. (2019) investigated the influence of brine salinity on Brazilian tensile strength (BTS) under different concentrations of 0, 10, 20 and 30% by weight. The result shows that when the brine concentration increases up to 10 percent, the tensile strength of sandstone increases (Figure 2.9). This behavior is similar with the uniaxial compressive strength.

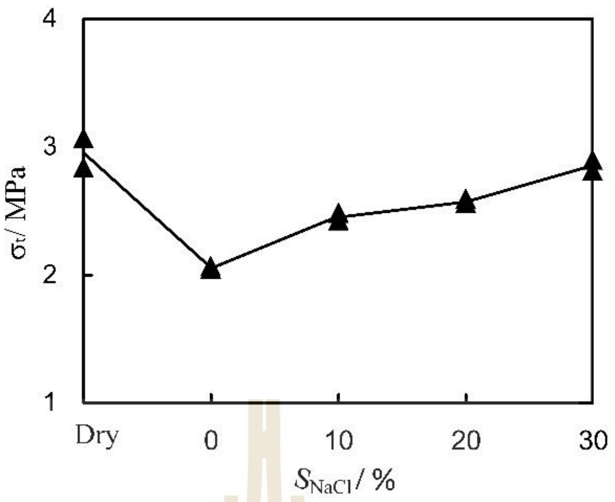

Figure 2.10 Tensile mechanical parameters of saturated sandstone specimens. (Huang et al., 2019).

2.6 Effect of pore pressure on rocks properties

Most researchers have studied the effect of pore pressure on compressive strength of a variety of rocks, such as sandstone (Vásárhelyi, 2003; Vásárhelyi and Van 2006), gypsum (Yilmaz, 2010), and limestone (Vásárhelyi et al., 2005). Khamrat et. al, (2016) investigated effect of pore pressure on the compressive strengths and elasticity of 6 rock type, under dry and wet conditions. The results show that the strength from the wet specimens decrease with increasing pore pressure. When the pore pressure increase, the elastic modulus decreased and Poisson's ratio slightly increased. Hawkins and McConnell (1992) investigated the influence of water content on the strength and deformability of 35 different British sandstones. The results show that the compressive strength decrease with increasing water content. Due to the strength of rock is very sensitive to the water content an increase in water content after only 1% from the dry condition can effect on strength as shown in Figure 2.11 (Vásárhelyi and Van, 2006). The water content can decrease the elastic modulus and increase Poisson's ratio of the rock (Vásárhelyi B, 2003; Vásárhelyi B, 2005). Additionally, tensile strength under saturated conditions is lower than under dry conditions, similar to compressive strength (Vásárhelyi B, 2005).

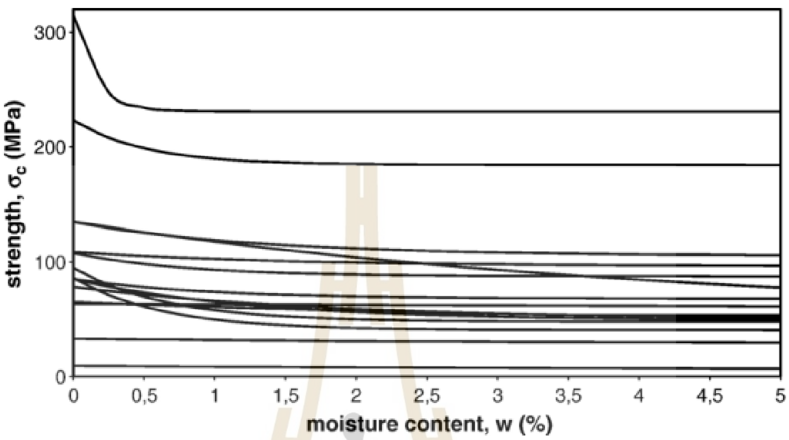

Figure 2.11 Relationships between strength as function of water content of 15 different rock type (Vásárhelyi and Van, 2006).

CHAPTER III

SAMPLE PREPARATION

3.1 Introduction

This chapter describes the rock sample preparation for simulation of rock deterioration under distilled water and saturated brine submersion. Uniaxial compression test and Brazilian tension test will be used as an indicator for the rock deterioration.

3.2 Sample preparation

The rock specimens used in this study are Khoa Khad marble, Phu Phan siltstone and Phu Phan sandstone. They are widely used as construction and decorating stones in Thailand. For each rock type, thirty specimens are prepared to obtained cylindrical specimens with dimensions of 45 mm in diameter and 90 mm in height for uniaxial compression test (Figure 3.1). Similarly, forty-five specimens were prepared to obtain cylindrical disk specimen with diameter of 54 mm and thickness of 27 mm to carry out the Brazilian tension test (Figure 3.2). Tables A.1 through A.11 in Appendix A shows the dimensions and weigh of the specimens.

Saturated brine is prepared by mixing distilled water with pure sodium chloride powder (NaCl) in plastic container. NaCl powder is added until no future dissolution occurs. The solution is continuously stirred. The container is left opened to allowed evaporation. The process is performed at 30±1°C. Approximately 39.1% by weight of NaCl powder is used to obtained fully saturation. The brine density is measured by hydrometer (ASTM D1298). The density is 1.21 g/cc.

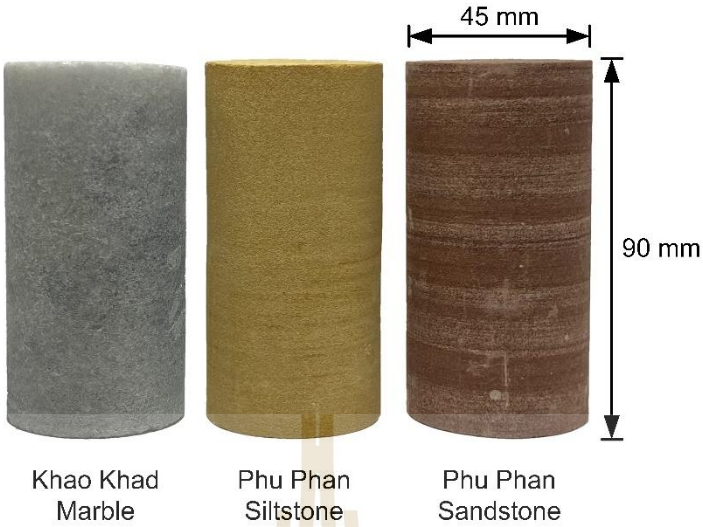

Figure 3.1 Examples of specimens prepared for simulation of deterioration based on uniaxial compressive strength as indicator.

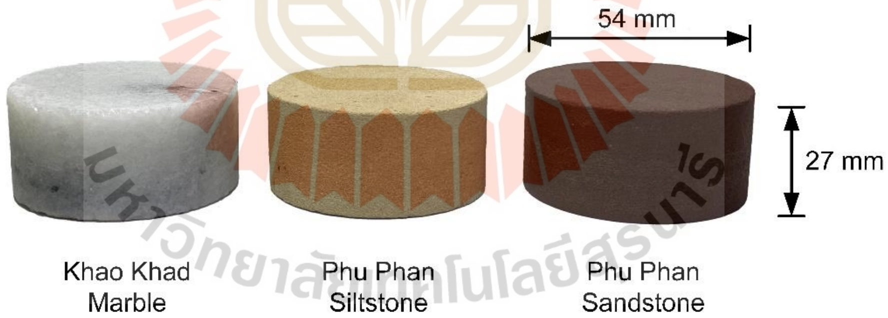

Figure 3.2 Examples of specimens prepared for simulation of deterioration based on tensile strength as indicator.

3.3 X-ray diffraction analysis

Some rock specimens are ground to obtain powder with particle sizes of less than 0.25 mm (mesh #60) (Figure 3.3). The powder specimen is used to determine mineral compositions by X-ray diffraction (XRD) analysis. Table 3.1 gives the mineral compositions of the rock samples from X-ray diffraction following the STP 479 standard practice.

Figure 3.3 Rock powder specimens prepared for XRD-diffraction analysis.

Table 3.1 Mineral compositions of rock samples before deterioration simulation from X-ray diffraction analysis.

Rock Type	Mineral compositions (weight%)
Khao Khad Marble	55.75% calcite, 11.40% ankerite, 9.04% actinolite, 7.16% huntite, 5.79% tremolite, 4.84% dolomite, 2.4% chalcopyrite, 1.65% Wollastonite, 1.43% Diopside
Phu Phan Siltstone	70.04% Quartz, 26.06% Clay Minerals, 2.21% Feldspar, 1.33% Mica, 0.19% pyrite, 0.16% siderite
Phu Phan Sandstone	50.99% Quartz, 40.96% Feldspar, 5.3% Clay Minerals, 1.19% Mica, 1.05% calcite, 0.39% pyrite, 0.12% Hematite

CHAPTER IV

LABORATORY TESTING

4.1 Introduction

This chapter describes the mechanical and physical test methods performed to assess the rock properties under various submersion durations. X-ray diffraction analysis is determined the mineral compositions of rock specimen after liquid submersion to compared with those under initial condition.

4.2 Simulation of rock deterioration

Rock specimens are submerged under distilled water and saturated brine. They are divided into 3 sets, as shown in Figure 4.1. The figure also depicts test plan throughout 240 days. For each set, there are eight specimens for the uniaxial compression tests (UCS) and twelve specimens for the Brazilian tension tests (BZ). Sets I and II are submerged under distilled water and saturated brine in the plastic containers, as shown in Figure 4.2. Every 60 days, 2 specimens are taken out for uniaxial compression test and 3 specimens for Brazilian tension test. Sets III specimens are submerged under saturated brine. Every 60 days the specimens are taken out and left air-dried at room temperature for 30 days, as shown in Figure 4.3, and then they are subjected to the two mechanical tests, as described above. The specimens are removed from the containers only minutes before testing to avoid moisture loss. Excess liquid on specimen surface is removed. The weights are measured to determine the liquid content and density in according to ASTM D2216-19. The mechanical testing is subsequently performed.

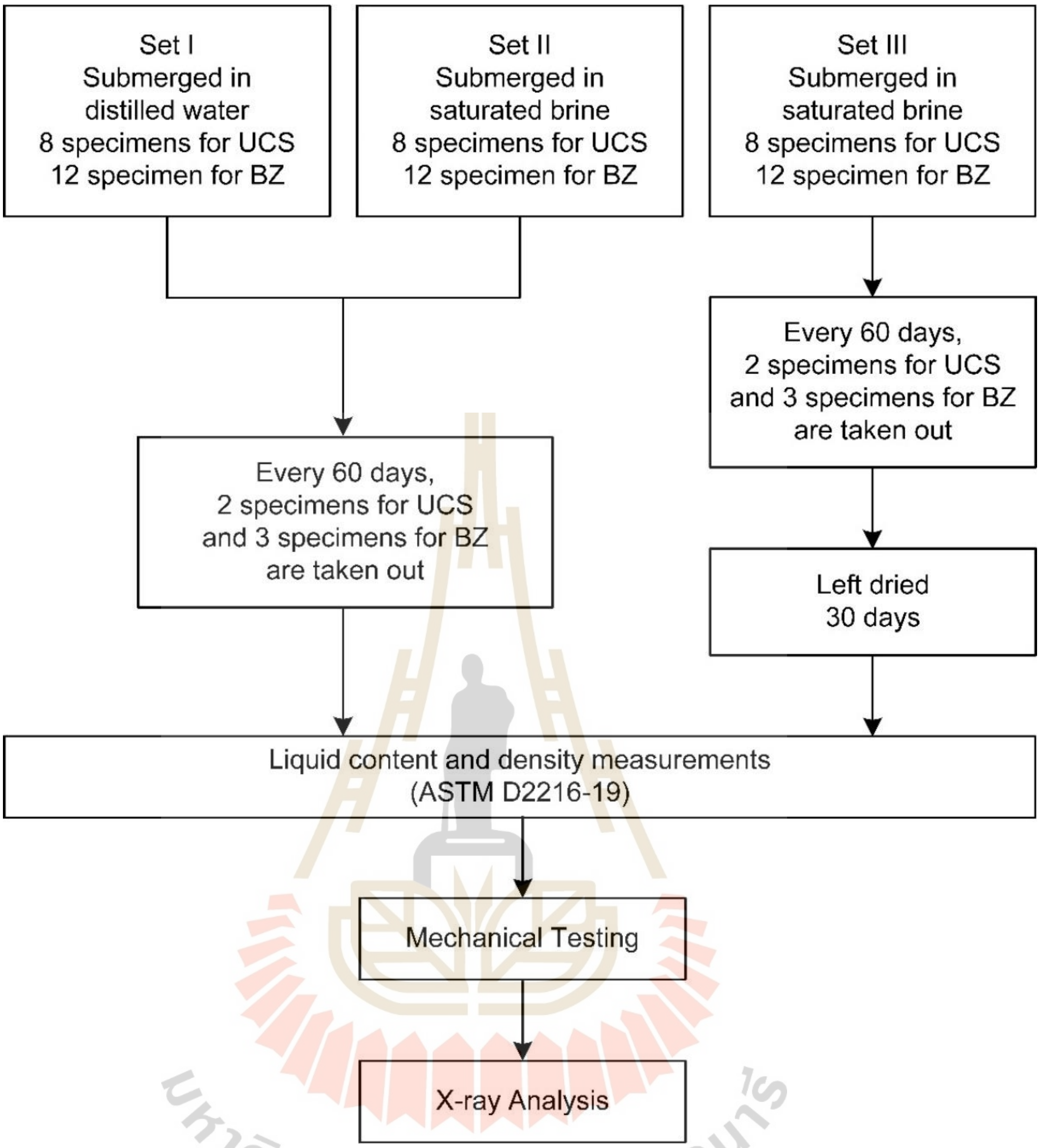

Figure 4.1 Test diagram for simulation of rock deterioration.

Figure 4.2 Specimens submerged in plastic containers.

Figure 4.3 Specimen of set III left air-dried at room temperature for 30 days.

4.3 Physical testing

4.3.1 Moisture contents

The moisture contents of specimens from sets I and II are measured immediately after they have been removed from the liquid container. The specimen weights are measured to the measurement 0.01 g using AND Model FX-2000i. The liquid content is determined in accordance with ASTM D2216-19 standard :

$$W_{water} = ((W_w - W_i)/W_i) \times 100\% \quad (4.1)$$

$$W_{brine} = ((W_b - W_i)/W_i) \times 100\% \quad (4.2)$$

where W_{water} is water content (% by weight), W_i is weight of initial specimen (g), W_w is weight of wet specimens submerged in distilled water (g), W_{brine} is brine content (% by weight) and W_b is weight of wet specimens submerged in saturated brine (g).

The salt content of specimens from set III after left air-dried for 30 days is determined. The salt content can be calculated by :

$$W_{salt} = ((W_s - W_i)/W_i) \times 100\% \quad (4.3)$$

where W_{salt} is salt content (% by weight), W_i is weight of initial specimen (g), W_s is weight of specimens after left air-dried for 30 days (g).

4.3.2 Density

The wet density of specimens from sets I and II are calculated from weight of rock after removing from liquid container divided by the volume of specimen. Set III specimens are calculated from weight of rock after they have left air-dried 30 days divided by the specimen volume. The density is calculating density in accordance with ASTM D2216-19 standard.

4.4 Mechanical testing

4.4.1 Uniaxial compression tests

Immediately after the liquid contents have been determined, uniaxial compression tests are performed on cylindrical specimen from sets I and II. The test procedure and calculation follow ASTM D7012-14e1 standard. The specimen strength and elastic parameters are determined for each 60 days interval. Set III specimens are tested after being air dried for 30 days. The elastic modulus is obtained from the tangent of axial stress-strain curve at about 40% to 50% of rock strength. The Poisson's ratio is determined from the lateral and axial strains. The test method is performed according to ASTM D7012-14e1. Post-failure characteristics are observed and recorded. Figure 4.4 shows that arrangement for the uniaxial compression test.

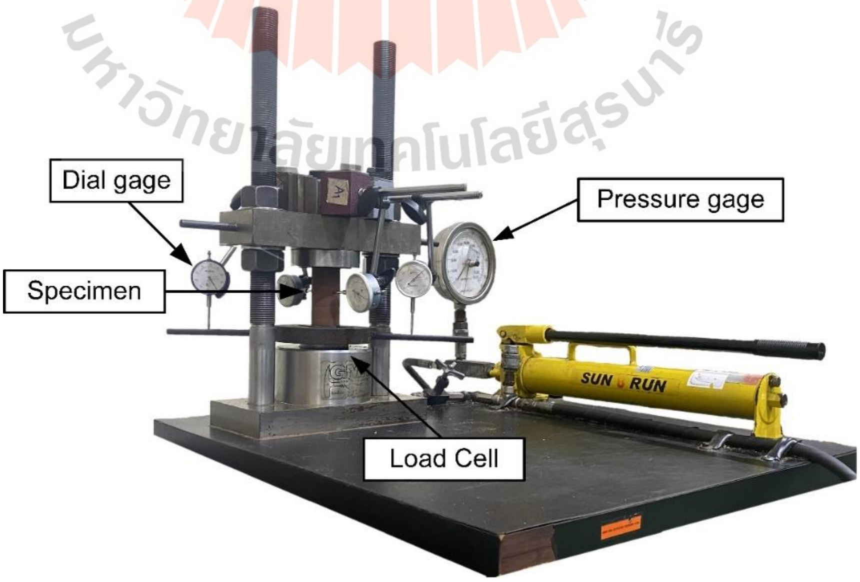

Figure 4.4 Uniaxial compression test arrangement.

4.4.2 Brazilian tensile tests

Similar to the uniaxial compression specimens, the Brazilian disk specimens from sets I and II are immediately subjected to diametral loading after their liquid contents have been measured. The test method and calculation are performed in according to ASTM D3967-05. Post-test characteristics are observed and recorded. Figure 4.5 shows the arrangement for the Brazilian tensile test.

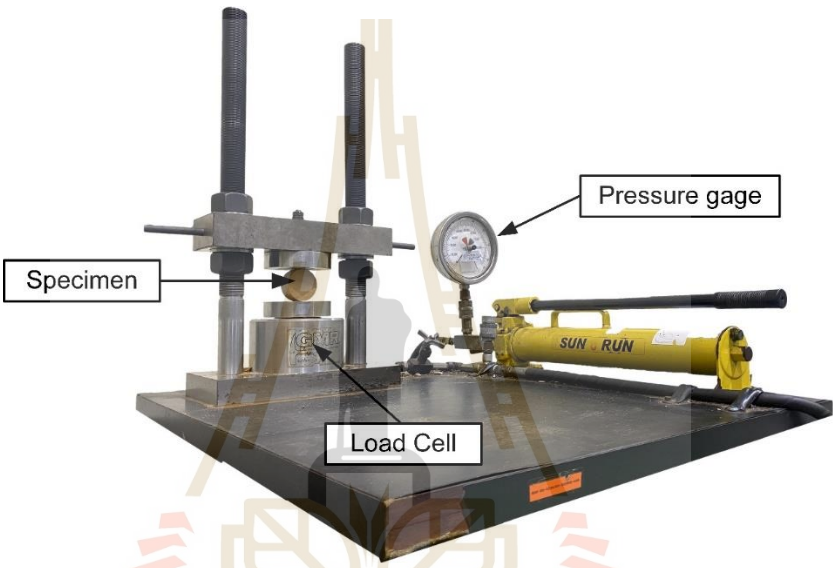

Figure 4.5 Brazilian tension test arrangement.

4.5 X-ray diffraction tests

The cylindrical specimens after subjecting to the uniaxial compression test is ground to obtain powder with particle sizes of less than 0.25 mm (mesh #60). The results are used to determine whether the alteration of mineral compositions of specimen has occurred during liquid submersion. X-ray diffractometer-Bruker D8 ADVANCE (Figure 4.6) is used. Every mineral exhibits a typical ‘X-ray fingerprint’, which is stored in databases This fingerprint is utilized in the DIFFRAC.EVA software for composition identification.

Figure 4.6 X-ray diffractometer-Bruker D8 ADVANCE.

CHAPTER V

TEST RESULTS

5.1 Introduction

This chapter describes the results of rock deterioration simulations. The degrees of deterioration are determined by the changes of specimen liquid and salt contents, density, compressive and Brazilian tensile strengths and deformation moduli, and mineral compositions. These indicators have been monitored from the initial conditions through every 60 days of the simulations.

5.2 Liquid/salt contents

The liquid and salt contents from 0-240 days with 60 days interval are summarized in Table 5.1. Appendix B gives liquid and salt contents for all tested specimens. The results indicate that moisture contents tend to increase with increasing submerging duration. This is true for all rock types, as shown in Figure 5.1. Sandstone specimens tend to absorb more liquid a the other two rocks. The lowest moisture contents is shown by marble for about 0.1%. Under distilled water (set I) all specimens gives greater liquid contents than those under brine (set II) probably due to that water can penetrate through the connective voids better than brine can. The salt content specimens for set III are measured after have been left air-dried for 30 days. Salt contents increase with submerging duration. This agrees with a similar study conducted by Taye et al. (2022), who study the influence of salt (NaCl) brine on clay rocks.

Table 5.1 Liquid/salt contents of rock specimens under all test conditions.

Rock Type	Conditions	Submerging Duration (Days)			
		60	120	180	240
		Liquid/salt contents (%)			
Khao Khad Marble	Water	0.02	0.04	0.05	0.09
	Brine	0.02	0.02	0.04	0.08
	Salt	0.02	0.02	0.04	0.08
Phu Phan Siltstone	Water	3.76	4.67	5.68	6.35
	Brine	3.32	4.47	5.32	5.79
	Salt	1.31	2.19	2.54	2.72
Phu Phan Sandstone	Water	4.87	6.59	7.94	8.99
	Brine	4.22	5.94	6.26	6.42
	Salt	1.22	2.86	4.58	5.19

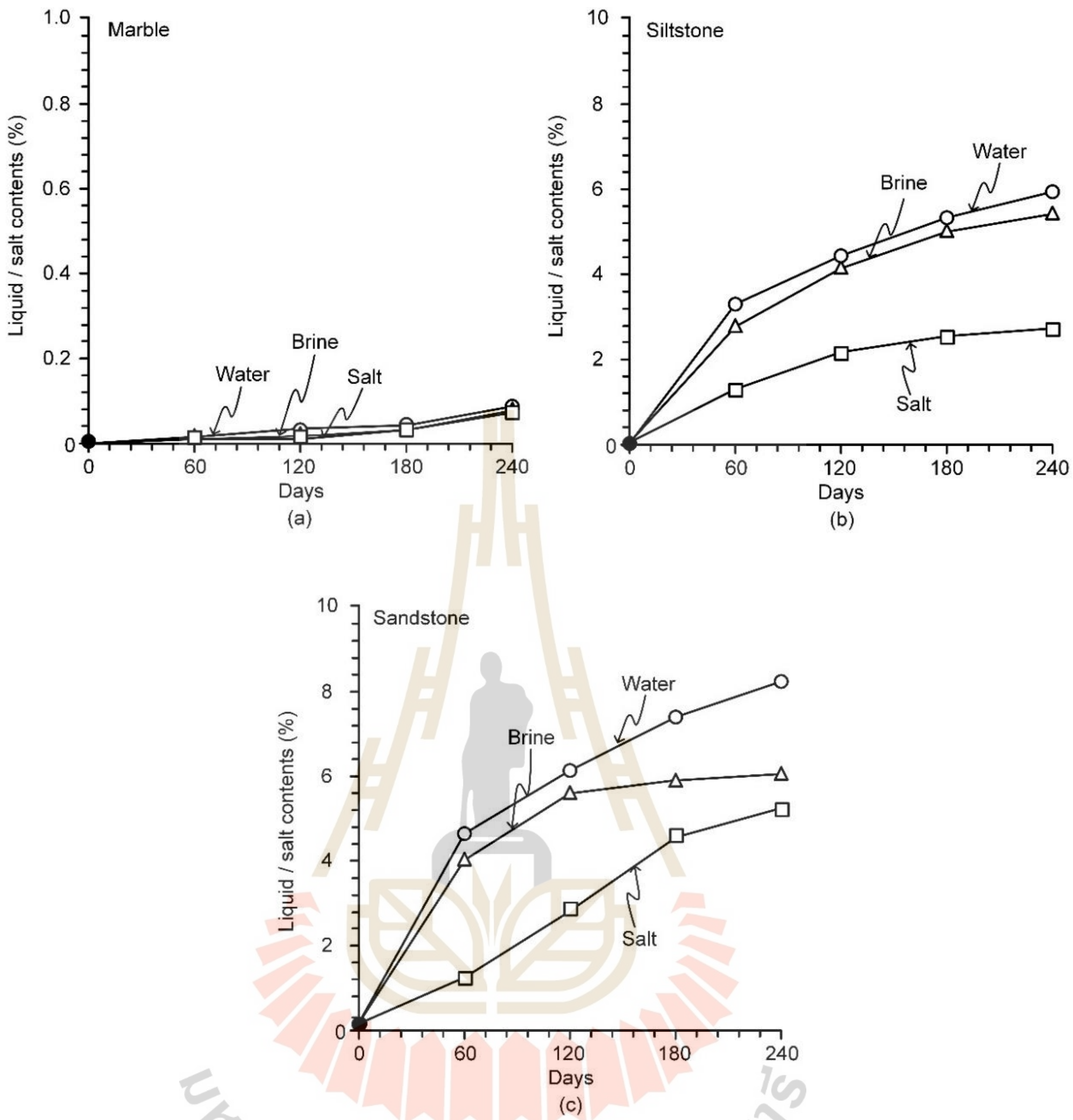

Figure 5.1 Liquid and salt contents as a function of submerging duration for marble (a), siltstone (b), and sandstone (c).

5.3 Specimen density

The density from 0-240 days with 60 days interval are summarized in Table 5.2. Appendix C gives the results for all tested specimens. The wet density tends to increase with increasing submerging duration similar to those of the liquid content. This holds true for all rock types and test conditions, as shown in Figure 5.2. Marble specimens show slight increase of the density due to the liquid absorption less than 0.1%.

Table 5.2 Specimen density of rock specimens under all test conditions.

Rock Type	Conditions	Submerging Duration (Days)			
		60	120	180	240
		Density (g/cc)			
Khao Khad Marble	Water	2.70	2.70	2.71	2.72
	Brine	2.72	2.73	2.74	2.74
	Salt	2.71	2.72	2.73	2.73
Phu Phan Siltstone	Water	2.30	2.33	2.35	2.36
	Brine	2.43	2.44	2.46	2.47
	Salt	2.34	2.34	2.36	2.38
Phu Phan Sandstone	Water	2.36	2.38	2.39	2.41
	Brine	2.40	2.45	2.46	2.49
	Salt	2.38	2.40	2.42	2.45

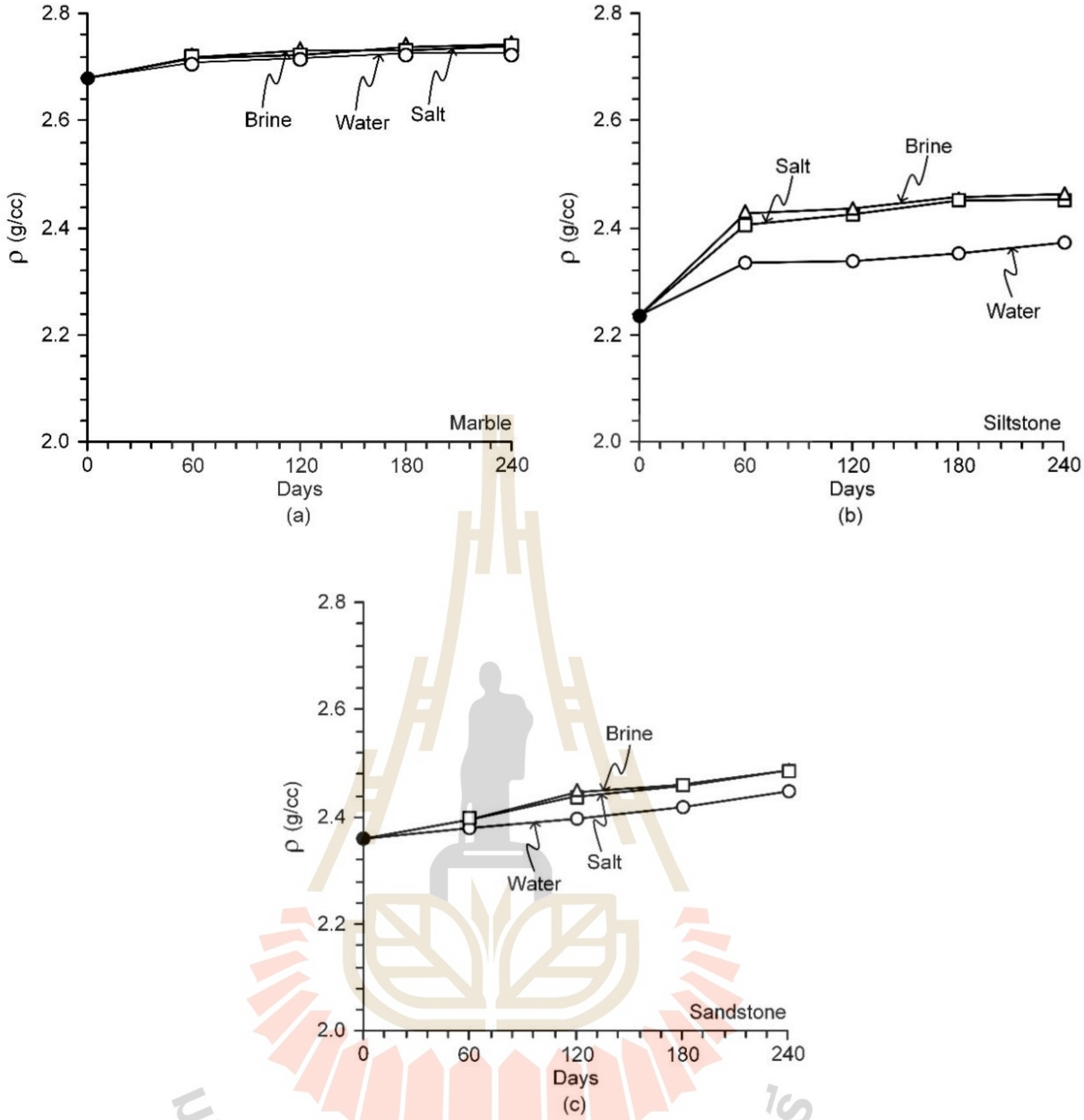

Figure 5.2 Density as a function of submerging duration for marble (a), siltstone (b), and sandstone (c).

5.4 Uniaxial compression test results

After determining the liquid contents and density, uniaxial compression tests are conducted on cylindrical specimens of all rock types. Figure 5.3 shows some post-test specimens from uniaxial compression tests under distilled water (set I), brine (set II), and salt (set III) conditions. The specimens exhibit a combination of multiple shear and longitudinal failures. No distinctive difference of mode of failure of specimens from different test conditions and submerging periods. Appendix D show the stress-strain curves at the initial (0 day) and 240 days under different conditions. All specimens show dilation immediately before failure occurs. Appendix E provides uniaxial compression test results for all specimens. Average compressive strengths are summarized in Table 5.3 and plotted in Figure 5.4. The results indicate that strength decreases from the initial condition (without liquid submersion) to the increase of submerging durations. This is due to the effect of pore pressure, which coincides with test results obtained from other researches (e.g. Hawkins and McConnell (1992); Khamrat et al., 2016; Vásárhelyi, 2003). Specimens with water exhibit a higher effect of pore pressure than those with brine because their pore spaces contain a larger volume of the liquid, as evidenced by the liquid contents measured prior to the mechanical testing. The lowest strength for all rock types is obtained from specimens containing salt crystals (set III).

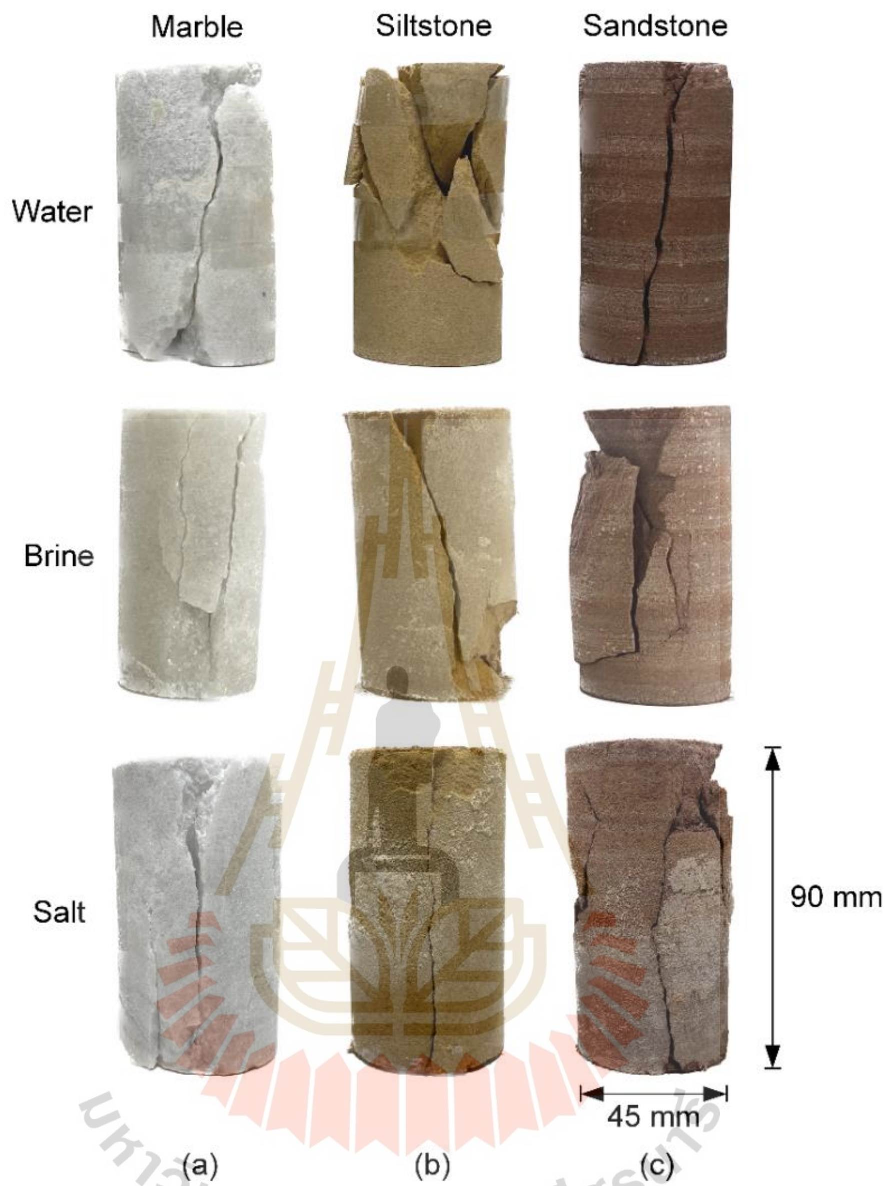

Figure 5.3 Some post-test specimens of submerging of uniaxial compression tests for marble (a), siltstone (b), and sandstone (c), after submerging in liquid for 240 days.

Table 5.3 Compressive strengths of rock specimens under all test conditions.

Rock Type	Conditions	Submerging Duration (Days)			
		60	120	180	240
		Compressive strengths (MPa)			
Khao Khad Marble	Water	47.49	42.08	36.73	32.72
	Brine	48.98	44.27	40.79	40.82
	Salt	43.09	39.95	35.42	31.25
Phu Phan Siltstone	Water	37.68	34.09	30.33	26.48
	Brine	39.87	36.96	34.12	28.68
	Salt	34.76	29.95	26.93	22.32
Phu Phan Sandstone	Water	44.47	38.93	33.83	32.24
	Brine	45.26	41.78	37.78	38.49
	Salt	40.48	35.94	32.02	30.44

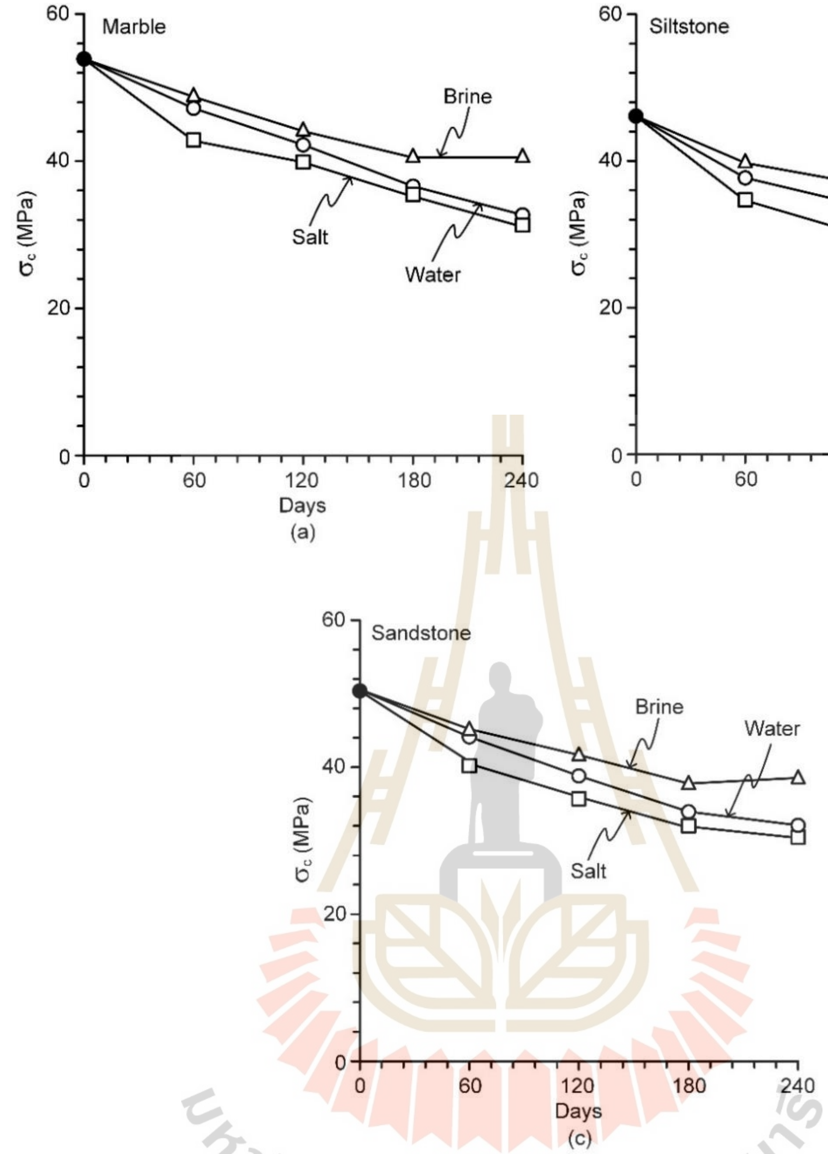

Figure 5.4 Uniaxial compressive strengths as a function of submerging duration for marble (a), siltstone (b), and sandstone (c).

The elastic modulus and Poisson's ratio are determined from the tangent of the stress-strain curve at approximately 40-50% of the rock strength. Average elasticity and Poisson's ratio are summarized in Tables 5.4 and 5.5. The elastic modulus exhibits a similar trend with that of the compressive strength, decreasing with an increasing submersion duration (Figure 5.5). Figure 5.6 shows the increase of Poisson's ratio due to the rise in lateral dilation of specimens under axial loading. This is caused by the liquid pressure trapped in the pore spaces. Longer submersion durations result in higher internal liquid pressure and, consequently, greater lateral dilation.

Table 5.4 Elastic moduli of rock specimens under all test conditions.

Rock Type	Conditions	Submerging Duration (Days)			
		60	120	180	240
		Elastic modulus (GPa)			
Khao Khad Marble	Water	10.37	8.45	7.47	7.23
	Brine	10.26	8.65	7.85	7.63
	Salt	7.90	6.68	6.10	5.93
Phu Phan Siltstone	Water	7.86	6.04	5.43	5.13
	Brine	7.84	6.74	5.87	5.50
	Salt	5.85	4.34	3.90	3.80
Phu Phan Sandstone	Water	4.64	4.19	3.60	3.40
	Brine	5.55	4.86	4.20	4.00
	Salt	4.10	3.52	3.13	3.02

Table 5.5 Poisson’s ratios of rock specimens under all test conditions.

Rock Type	Conditions	Submerging Duration (Days)			
		60	120	180	240
		Poisson’s ratio			
Khao Khad Marble	Water	0.20	0.25	0.27	0.27
	Brine	0.23	0.28	0.28	0.28
	Salt	0.19	0.23	0.24	0.26
Phu Phan Siltstone	Water	0.25	0.26	0.27	0.28
	Brine	0.26	0.27	0.28	0.28
	Salt	0.24	0.25	0.25	0.26
Phu Phan Sandstone	Water	0.25	0.27	0.27	0.28
	Brine	0.26	0.28	0.28	0.28
	Salt	0.23	0.25	0.26	0.26

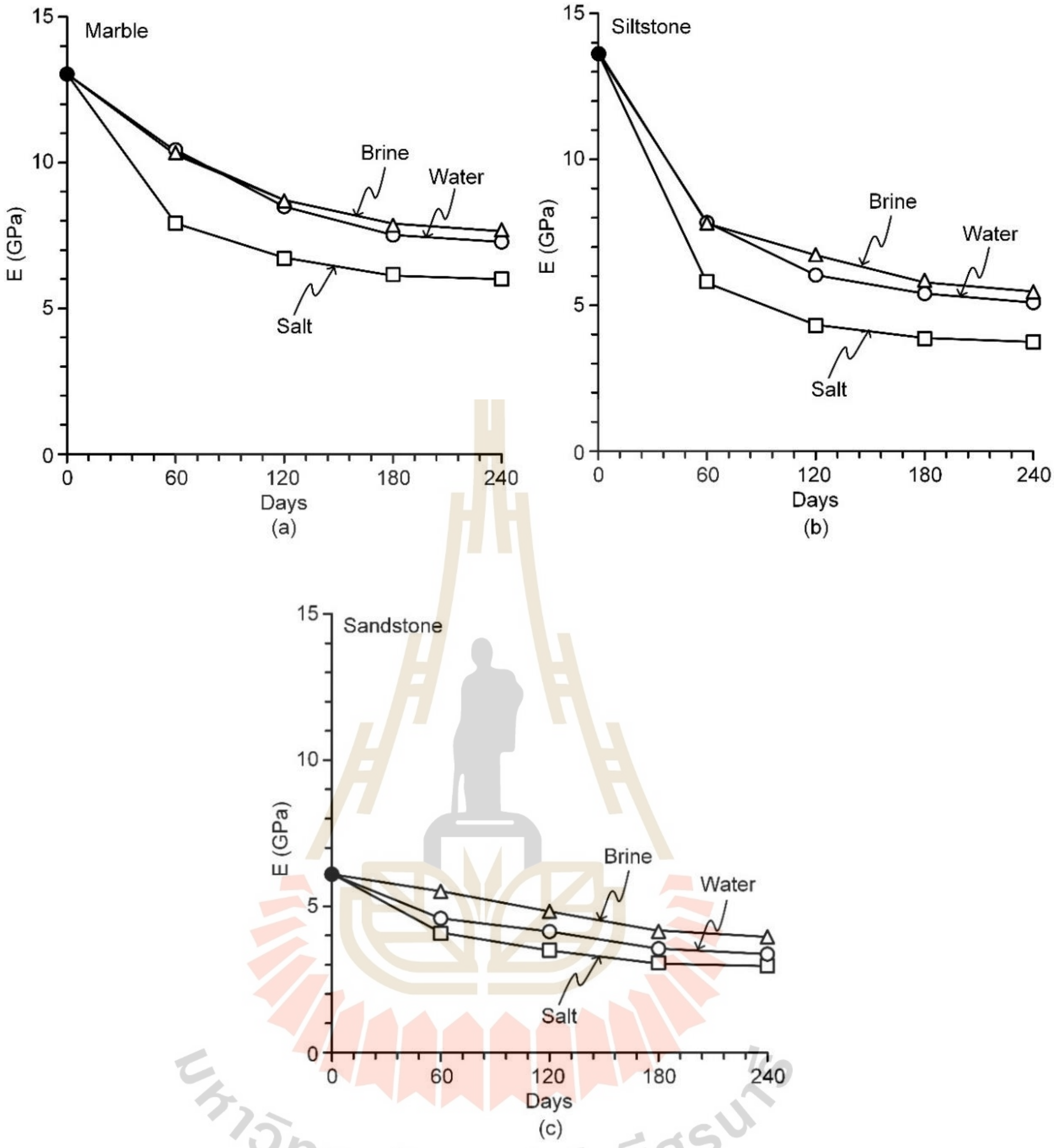

Figure 5.5 Elastic moduli (E) as a function of submerging duration for marble (a), siltstone (b), and sandstone (c).

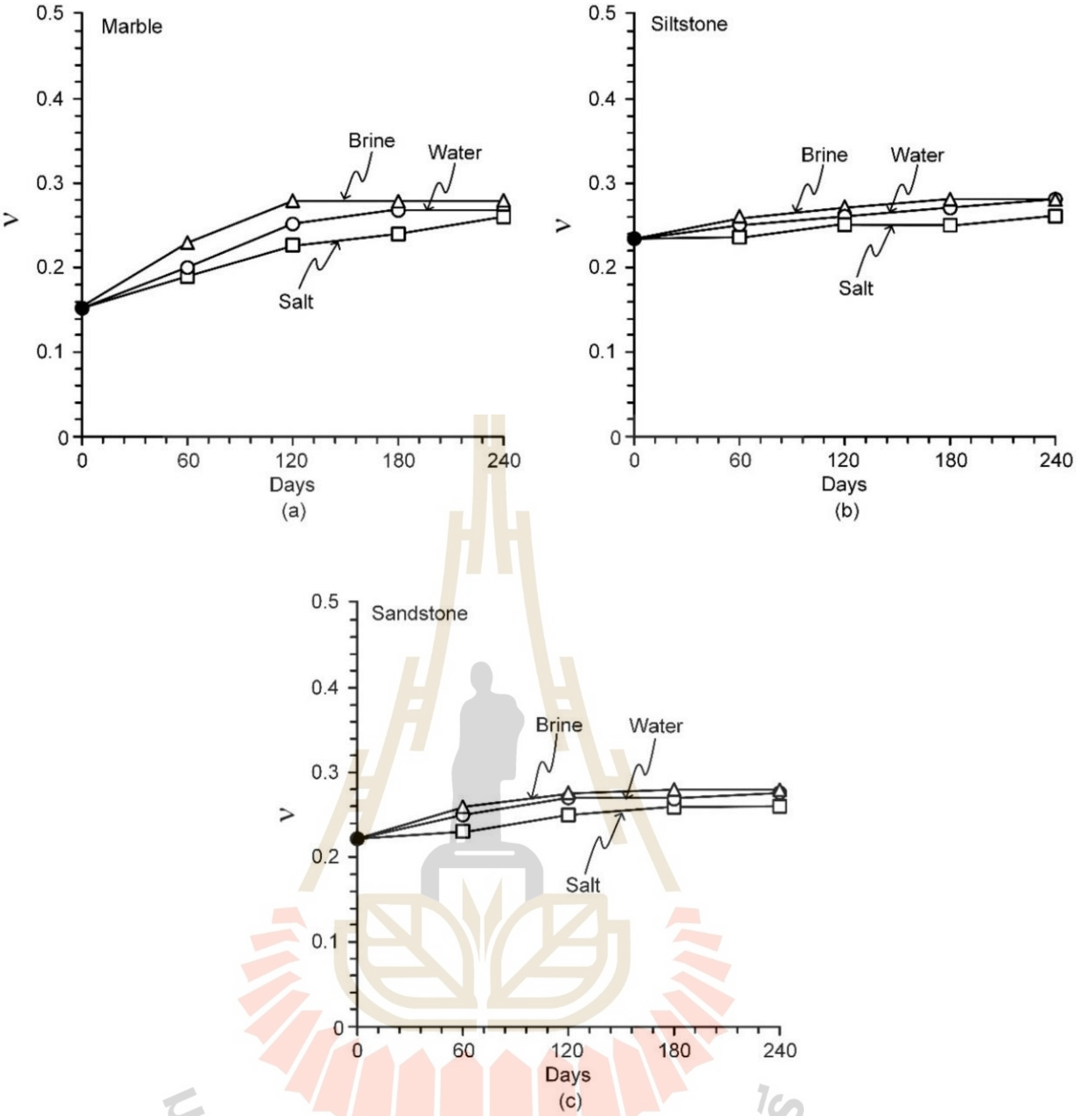

Figure 5.6 Poisson's ratios as a function of submerging duration for marble (a), siltstone (b), and sandstone (c).

5.5 Brazilian tensile strengths

Similar to the uniaxial compression specimens, the Brazilian disk specimens after submerging in distilled water (set I) and brine (set II) for 60, 120 180 and 240 days are immediately subjected to diametral loading after measuring their liquid contents. The Brazilian tensile strength results are summarized in Table 5.6, with detailed information given in Appendix F. Figure 5.7 plots the Brazilian tensile strengths as a function of submersion duration for all rock types, revealing a notable decrease of the tensile strength with increasing submersion duration. Pore pressure is the main factor inducing the decrease in tensile strengths of specimens with higher liquid contents. New micro-cracks and fissures induced by salt crystal growth in the pore space of specimens from the salt condition (set III) can further reduce the rock's tensile strength, making it lower than those tested under water and brine conditions. This behavior occurs for all rock types and test durations.

Table 5.6 Tensile strengths of rock specimens under all test conditions.

Rock Type	Conditions	Submerging Duration (Days)			
		60	120	180	240
		Tensile strengths (MPa)			
Khao Khad Marble	Water	4.98	4.42	4.20	3.94
	Brine	5.06	4.67	4.40	4.12
	Salt	4.47	4.14	4.03	3.80
Phu Phan Siltstone	Water	2.20	1.72	1.38	1.49
	Brine	2.47	2.06	1.73	1.83
	Salt	2.10	1.67	1.28	1.30
Phu Phan Sandstone	Water	2.27	1.87	1.58	1.46
	Brine	3.10	2.73	2.32	2.09
	Salt	2.11	1.66	1.46	1.39

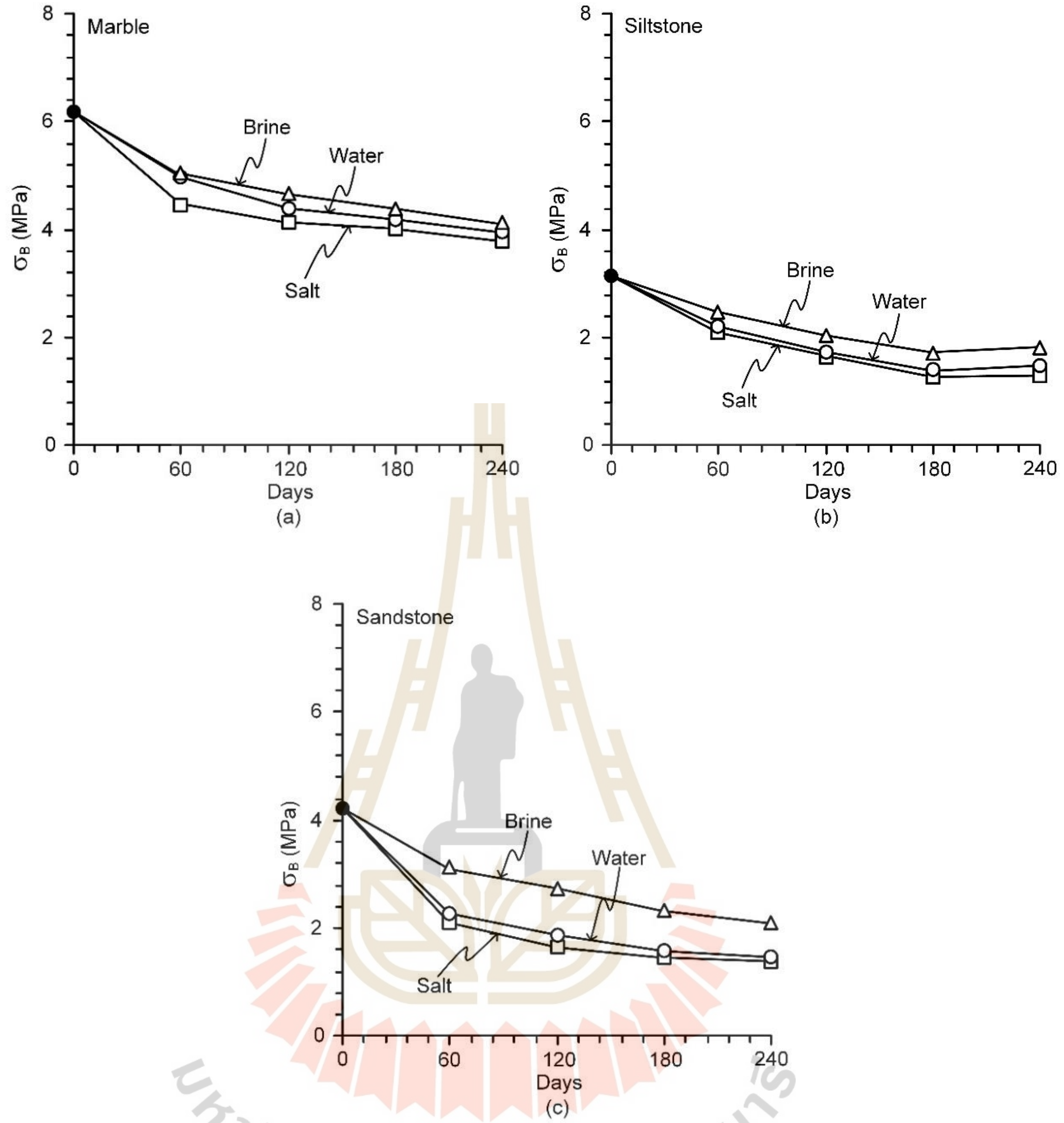

Figure 5.7 Brazilian tensile strengths as a function of submerging duration for marble (a), siltstone (b), and sandstone (c).

5.6 X-ray Diffraction (XRD) Analysis

Mineral compositions of rock specimens are determined by X-ray diffraction analysis (XRD). Before submerging in the liquid, siltstone and sandstone are primarily composed of quartz and feldspar, while marble predominantly contains calcite and dolomite (Table 5.7 through 5.9). XRD results from different submersion durations and liquid types do not show a significant change in the amounts of these main mineral compositions. As shown in Fig. 5.8 the combined weight percentages of quartz and feldspar remain effectively unchanged for siltstone and sandstone. Marble also exhibits similar amounts of calcite and dolomite in specimens subjected to different test conditions, although small differences in weight percentages of these key minerals can be observed. These variations are likely due to the intrinsic variability among the specimens. In summary, the minerals composing the tested sandstone, siltstone and marble tend to be chemically insensitive to the water and brine, at least within the test period of 240 days.

Table 5.7 Mineral compositions of marble specimens obtained from XRD analysis.

Condition	Time	Calcite	Dolomite	Ankerite	Huntite	Wollastonite	Diopside	Chalcopyrite	Actinolite	Tremolite	Halite
Initial	0	55.75	4.84	11.40	7.16	1.65	1.43	2.4	9.04	5.79	-
Water	60	58.55	4.68	10.12	6.92	1.30	1.01	4.77	7.09	5.55	-
	120	58.44	4.51	10.53	5.72	2.20	1.00	4.74	7.64	5.22	-
	180	59.20	4.23	10.16	5.64	2.45	1.08	4.87	7.36	5.01	-
	240	58.18	3.13	11.43	5.58	1.65	1.18	3.73	10.3	4.81	-
Salt	60	60.27	5.14	9.28	5.82	1.78	1.81	3.63	7.38	4.54	0.35
	120	67.43	3.10	8.23	3.55	1.59	1.34	3.09	6.71	4.52	0.44
	180	73.14	2.48	3.82	4.27	1.80	1.21	3.99	6.42	2.01	0.86
	240	72.34	2.61	8.42	2.96	0.54	1.11	2.09	6.14	2.65	1.14

Table 5.8 Mineral compositions of siltstone specimens obtained from XRD analysis.

Condition	Time	Quartz	Clay Minerals	Feldspar	Mica	Siderite	Pyrite	Halite
Initial	0	70.04	26.06	2.21	1.33	0.16	0.19	-
Water	60	70.25	25.53	2.22	1.60	0.12	0.19	-
	120	72.03	24.1	2.07	1.44	0.16	0.22	-
	180	76.37	19.55	2.15	1.69	0.12	0.11	-
	240	84.82	11.29	2.18	1.40	0.09	0.23	-
Salt	60	73.31	19.36	2.89	2.43	0.14	0.23	2.13
	120	72.78	17.80	4.79	2.72	0.16	0.23	2.22
	180	72.8	17.93	3.70	2.76	0.12	0.32	2.57
	240	75.04	16.89	3.62	1.36	0.12	0.12	2.76

Table 5.9 Mineral compositions of sandstone specimens obtained from XRD analysis.

Condition	Time	Quartz	Clay Minerals	Feldspar	Mica	Hematite	Calcite	Pyrite	Halite
Initial	0	50.99	5.30	40.96	1.19	0.12	1.05	0.39	-
Water	60	48.93	3.90	40.32	5.64	0.18	0.69	0.33	-
	120	54.72	4.03	35.2	5.42	0.26	0.33	0.06	-
	180	53.13	3.23	37.02	5.99	0.2	0.38	0.36	-
	240	60.70	2.76	31.59	4.44	0.19	0.18	0.14	-
Salt	60	51.27	4.05	38.47	3.90	0.11	0.87	0.37	0.97
	120	50.16	3.02	39.13	5.22	0.11	0.75	0.6	1.02
	180	58.05	3.83	31.42	4.19	0.15	0.18	0.45	1.74
	240	63.8	2.36	28.95	2.80	0.22	0.31	0.10	1.46

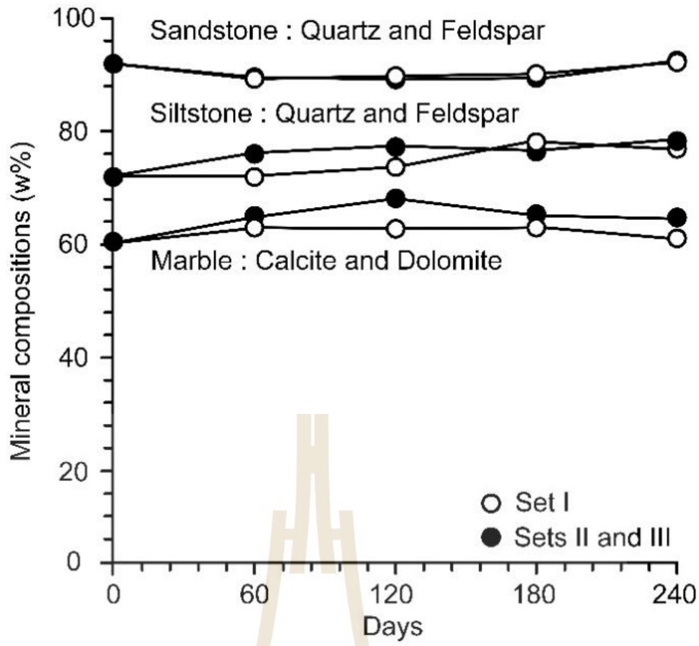

Figure 5.8 Main mineral compositions observed during 240 days of submersion.

CHAPTER VI

ANALYSIS OF TEST RESULTS

6.1 Introduction

The objective of this chapter is to determine the correlation between liquid/salt contents, submerging duration and mechanical properties of the test specimens. The finding can be useful to predict the rock properties for long-term under different submerging solutions. This chapter aims to analyze siltstone and sandstone only as the marble liquid/salt contents are less than 0.1%.

6.2 Correlation between liquid/salt contents and submerging duration

An attempt is made to correlate the liquid/salt contents with the submerging duration. The maximum liquid/salt contents defined in this study is the liquid/salt content at which it remains unchanged during submerging period. And hence the specimens are referred to as saturated specimens. This parameter can be used to predict minimum strength and stiffness as the submerged duration increases.

Based on the assumptions posed above, the maximum liquid/salt contents can be determined using Figures 6.1 and 6.2. Exponential relations are proposed to correlate the liquid content and duration as follows:

$$w_{\%} = A \cdot (1 - \exp(-B \cdot t)) \quad (6.1)$$

where $w_{\%}$ is percent of liquid/salt contents, A and B are constants and t is submerged duration (days). Regression analysis of the test data by SPSS software (Wendai, 2000) can determine A and B, as shown in Table 6.1. Good correlation is obtained ($R^2 > 0.9$).

The results show that it would require a duration of 400, 200, and 600 days under water, brine and salt for siltstone, and 200, 250, 300 days for sandstone to reach the saturation conditions.

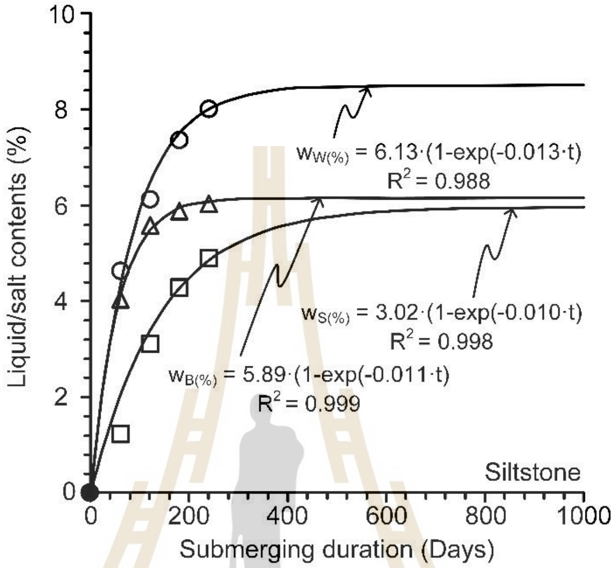

Figure 6.1 Liquid/salt contents as a function of submerging duration for siltstone.

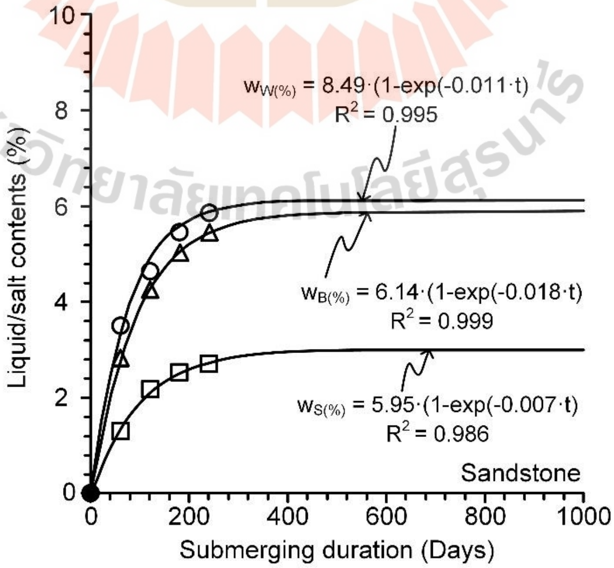

Figure 6.2 Liquid/salt contents as a function of submerging duration for sandstone.

Table 6.1 Constants A and B obtained from regression analysis of Equations (6.1).

Rock types	Conditions	A (%)	B (1/day)	Coefficient of determination	Maximum Liquid/salt content (%)
Siltstone	Water	6.13	0.013	0.988	6.13
	Brine	5.89	0.011	0.999	5.89
	Salt	3.02	0.010	0.998	3.02
Sandstone	Water	8.49	0.011	0.995	8.49
	Brine	6.14	0.018	0.999	6.14
	Salt	5.95	0.007	0.986	5.95

6.3 Correlation between mechanical properties and liquid/salt contents

6.3.1 Uniaxial compressive strength and liquid/salt contents

Exponential equation is proposed to represent the uniaxial compressive strength as a function of liquid/salt contents. The results indicate that compressive strength decreases as the liquid/salt contents increase under all test conditions. The relationships are shown in Figures 6.3 and 6.4. The following equation defines their relationship:

$$\sigma_c = C \cdot \exp(-D \cdot w_{\%}) \quad (6.2)$$

where σ_c is uniaxial compressive strength (MPa), $w_{\%}$ is liquid/salt contents (%), C and D are empirical constants. Their numerical values are shown in Table 6.2. Good correlation is obtained ($R^2 > 0.8$).

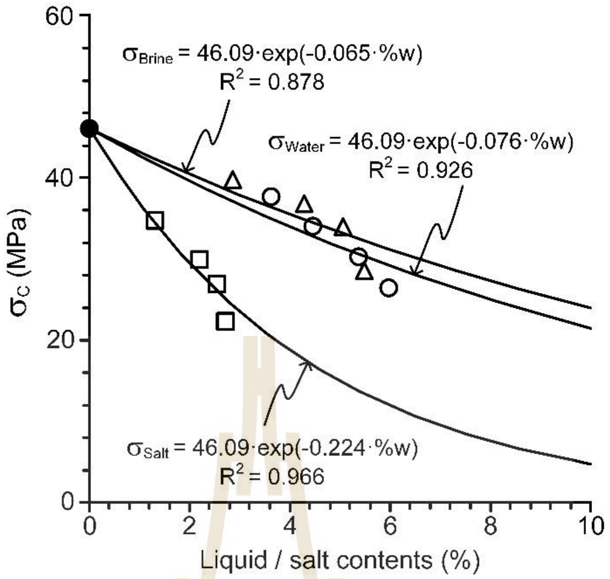

Figure 6.3 Uniaxial compressive strengths as a function of liquid/salt contents for siltstone.

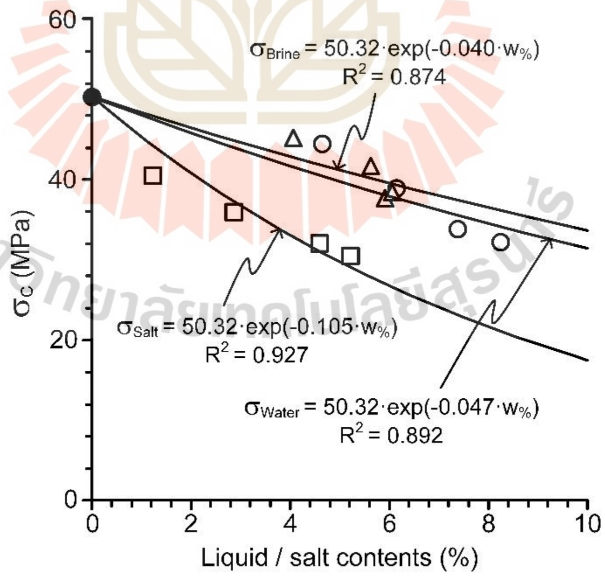

Figure 6.4 Uniaxial compressive strengths as a function of liquid/salt contents for sandstone.

Table 6.2 Constants C and D obtained from regression analysis of Equations (6.2).

Rock Types	Conditions	$\sigma_c = C \cdot \exp(-D \cdot w_{\%})$	
		C (MPa)	D
Siltstone	Water	46.09	0.076
	Brine		0.065
	Salt		0.224
Sandstone	Water	50.32	0.047
	Brine		0.040
	Salt		0.105

6.3.2 Elastic modulus and liquid/salt contents

The elastic modulus can also be correlated with liquid/salt contents using exponential equation. The results indicate that elastic moduli decrease with liquid/salt contents under all test conditions, as shown in Figures 6.5 and 6.6. The relationship can be shown as:

$$E = F \cdot \exp(-G \cdot w_{\%}) \qquad (6.3)$$

where E is elastic modulus (GPa), $w_{\%}$ is liquid/salt contents (%), F and G are empirical constants (Table 6.3). Good correlations are obtained for both rock types ($R^2 > 0.8$).

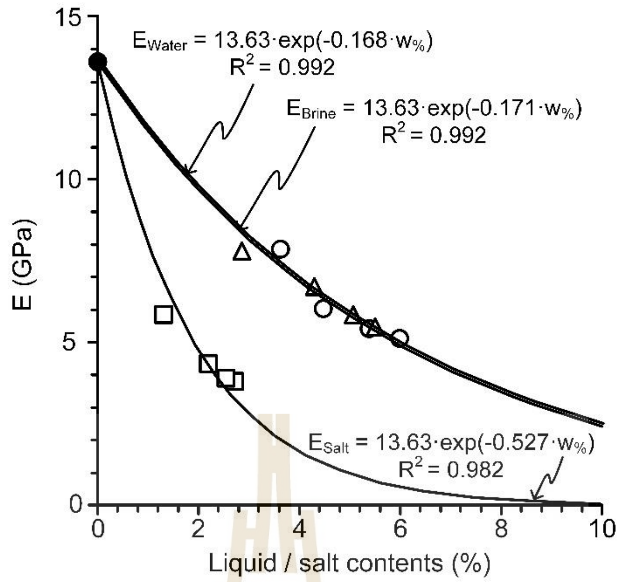

Figure 6.5 Elastic modulus (E) as a function of liquid/salt contents for siltstone.

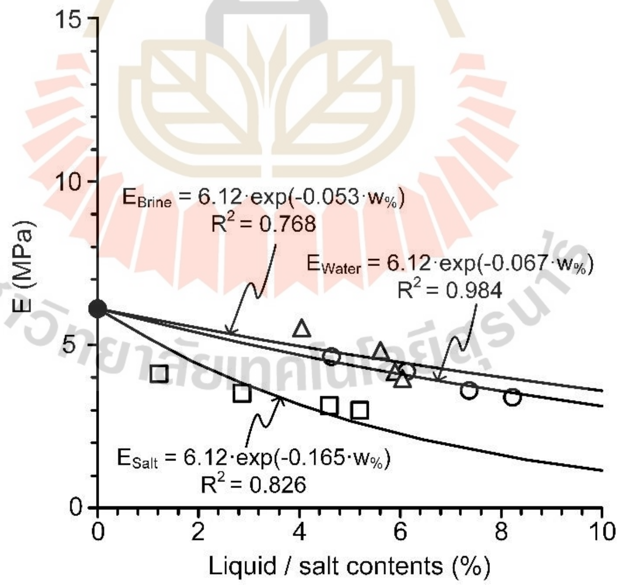

Figure 6.6 Elastic modulus (E) as a function of liquid/salt contents for sandstone.

Table 6.3 Constants F and G obtained from regression analysis of Equations (6.3).

Rock Types	Conditions	$E = F \cdot \exp(-G \cdot w_{\%})$	
		F (GPa)	G
Siltstone	Water	13.63	0.168
	Brine		0.171
	Salt		0.527
Sandstone	Water	6.12	0.067
	Brine		0.053
	Salt		0.165

6.3.3 Poisson's ratio and liquid/salt contents

Exponential relationship can best represent the changes of Poisson's ratio as a function of liquid/salt contents. The Poisson's ratio increases with liquid/salt contents. The relationships are shown in Figures 6.7 and 6.8. The relationship can be written as:

$$\nu = H \cdot \exp(I \cdot w_{\%}) \quad (6.4)$$

where ν is Poisson's ratio (MPa), $w_{\%}$ is liquid/salt contents (%), H and I are empirical constants (Table 6.4). Good correlation is obtained ($R^2 > 0.9$).

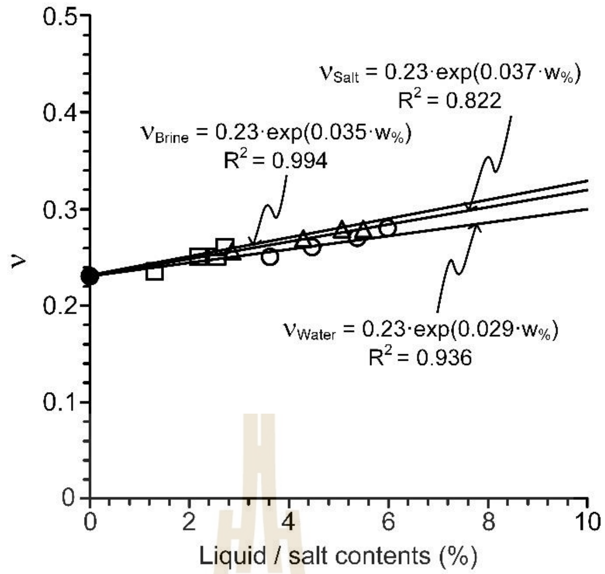

Figure 6.7 Poisson's ratio (ν) as a function of liquid/salt contents for siltstone.

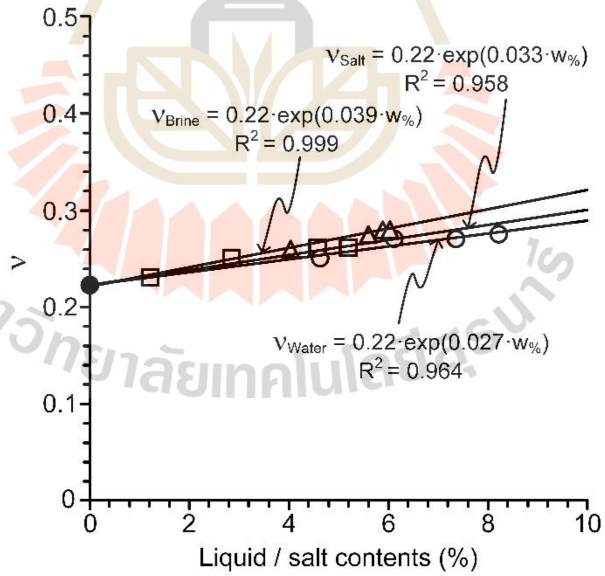

Figure 6.8 Poisson's ratio (ν) as a function of liquid/salt contents for sandstone.

Table 6.4 Constants H and I obtained from regression analysis of Equations (6.4).

Rock Types	Conditions	ν = H•exp(I•$w_{\%}$)	
		H	I
Siltstone	Water	0.23	0.029
	Brine		0.035
	Salt		0.037
Sandstone	Water	0.22	0.027
	Brine		0.039
	Salt		0.033

6.3.4 Brazilian tensile strength and liquid/salt contents

Exponential equation can represent the Brazilian tensile strength as a function of liquid/salt content. Similar to the uniaxial compressive strength results, the Brazilian tensile strength decreases as the liquid/salt contents increase under all test conditions. Their relationships are shown in Figure 6.9 and 6.10:

$$\sigma_B = J \cdot \exp(-K \cdot w_{\%}) \qquad (6.5)$$

where σ_B is Brazilian tensile strength (MPa), $w_{\%}$ is liquid/salt contents (%), J and K are empirical constants (Table 6.5). In each condition. Good correlation is obtained (R^2 > 0.8).

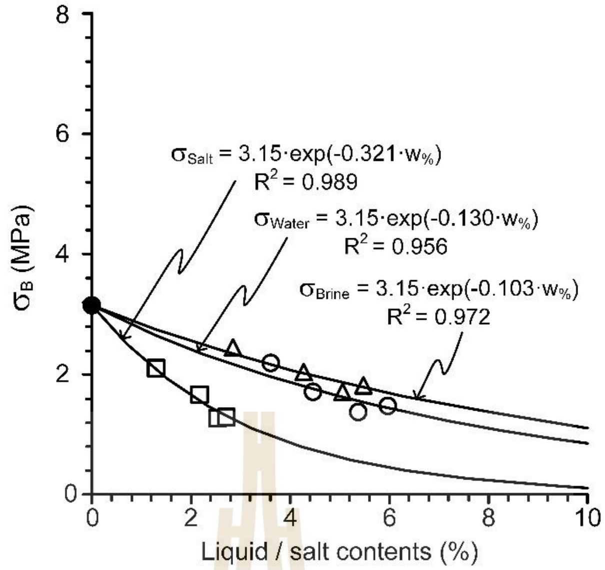

Figure 6.9 Brazilian tensile strengths as a function of liquid/salt contents for siltstone.

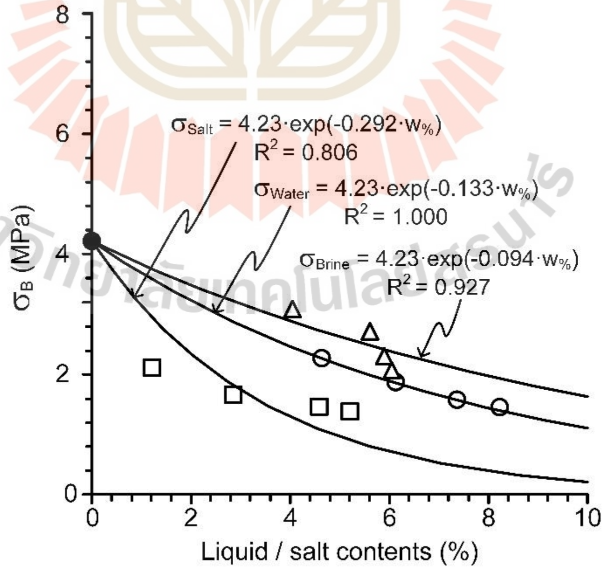

Figure 6.10 Brazilian tensile strengths as a function of liquid/salt contents for sandstone.

Table 6.5 Constants J and K obtained from regression analysis of Equations (6.5).

Rock Types	Conditions	$\sigma_B = J \cdot \exp(-K \cdot w_{\%})$	
		J (MPa)	K
Siltstone	Water	3.15	0.130
	Brine		0.103
	Salt		0.321
Sandstone	Water	4.23	0.133
	Brine		0.094
	Salt		0.292

6.4 Mechanical properties on saturated specimens

All correlations defined above can be used to predict the strengths, stiffness and dilation of the saturated siltstone and sandstone. This is achieved by substituting the maximum liquid/salt contents from Table 6.1 into Equations (6.2) through (6.5) and hence the long-term compressive strengths, elastic moduli, Poisson's ratio and tensile strengths can be obtained. It is implied that when specimens are saturated, the strength and stiffness are decreased from the initial condition. The mechanical properties show in Table 6.6 would represent the most severe condition where the specimens are subjected to long-term submersion in water and brine and when the brine is evaporated and becomes salt crystals in the pore spaces.

Table 6.6 Mechanical properties on saturated siltstone and sandstone.

Rock types	Conditions	Compressive strengths (MPa)	Elastic moduli (GPa)	Poisson's ratio	Brazilian tensile strengths (MPa)
Siltstone	Initial	46.1	13.6	0.23	3.2
	Water	28.9	4.9	0.28	1.4
	Brine	31.4	5.0	0.28	1.7
	Salt	23.5	2.8	0.26	1.2
Sandstone	Initial	50.3	6.1	0.22	4.2
	Water	33.8	3.5	0.28	1.4
	Brine	39.4	4.4	0.28	2.4
	Salt	26.9	2.3	0.27	0.7

CHAPTER VII

DISCUSSIONS AND CONCLUSIONS

7.1 Discussions

The effects of brine on the compressive strength and deformability are determined for cylindrical and disk specimens prepared from marble, siltstone and sandstone. The specimens are submerged under water, brine, and salt conditions for 240 days.

The compressive and tensile strengths and elastic parameters of the water submerging specimens are about 5-10% lower than those obtained from the brine submersion. This does not necessarily mean the brine causes less adverse effect to rock strengths and elasticity as compared to water. The strength and elasticity differences are due to the fact that the lower density and viscosity of water allow a larger amount of liquid to penetrate into the connective voids of the rocks, as compared to the higher density and viscosity of the brine. As a result, strength and elasticity reductions caused by the trapped water pore pressure is more severe than that of the brine pore pressure. The results obtained here agree reasonably with those of Khamrat et al. (2016) who find that the compressive strengths of saturated sandstone specimens decrease with increasing pore pressure. Hawkins and McConnell (1992) show that moisture content of British sandstone can decrease its mechanical properties, which agrees with the findings from other investigators on sandstones (Vásárhelyi and Van, 2006; Vásárhelyi, 2003).

For the brine submersion specimens, the real adverse effect occurs when they are left dried. The remaining recrystallized salt expands inside the pore spaces, and hence initiates new cracks and fissures or propagates the existing ones. This is a progressive process as additional brine penetrates under increasing the submersion period. This process is however irreversible. The compressive and tensile strengths of specimens with salt crystals in pore spaces are about 35% to 50% lower than those of the initial condition, and are lower than those tested under wet conditions. The results obtained here agree with those of Shukla et al. (2012) who demonstrate that brine exposure reduces the strength and elasticity of sandstone in the southeastern of Melbourne. This finding aligns with the previous research on the effects of brine on sandstone from the Gosford quarries in New South Wales (Rathnaweera et al., 2013) and silicate sandstone from the Sydney basin (De Silva et al., 2018).

The strength and stiffness of saturated siltstone and sandstone can be measured to determine long-term compressive strengths, elastic moduli, Poisson's ratio, and tensile strengths. It is implied that when specimens are saturated, the strength and stiffness are decreased from the initial condition. The results of this study agree with the findings obtained by Dinesh (2021), who shows that the strengths and elastic modulus of gypsum decrease with increasing immersion time in brine.

Approximate extrapolation of the compressive strength-time curves suggests that the three rock types could lose their strength within 5 to 6 years. Note that this approximation is based on that the rocks are continuously under saturated brine before drying. In actual condition, however, they would be subjected to yearly cycle of wet and dry which could extend their service life longer than the approximation above. Remediation of the salt crystals induced damage to these decorating rocks could be made by routinely washing these rocks with fresh water soon after they submerged under the brine.

Results from x-ray diffraction analysis show that there is no significant change of mineral compositions of the tested rock specimens from the initial condition through the end of 240 days of liquid submersion. This is probably due to the fact that the test period is relatively short. However, it does not mean that water and brine do not affect the mineral compositions of the rocks in long-term.

It should be noted that the Phu Phan sandstone and siltstone formation contains various characteristics of texture and mineral compositions as described by Murray (1993). As a results, the research findings obtained here may not represent the deterioration behavior for the entire rock formation.

Most decorating stones applications in the northeast of Thailand are for terraces and walkways where the stones are cut into thin slaps and laid flat on the ground surface. As a results, their tensile strength would be more important than other mechanical properties. Increasing their thickness would extend their service life, depending also on the applied load during application.

7.2 Conclusions

Conclusions drawn from this study can be summarized as follows.

1) Siltstone and sandstone can absorb water and brine up to 6 % to 9 % by weight while less than 0.1% can be absorbed by marble through the submersion period of 240 days.

2) For all tested rocks water can infiltrate the connective voids better than brine can. This results in lower strengths and elasticity of water submersion specimens than brine submersion specimens. This is due to a higher pore pressure effect for water submersion specimens than brine submersion specimens.

3) The reduction of rock strength and elasticity increases with increasing submersion duration.

4) After the brine submersion specimens have been left air-dried for 30 days, they yield the lower strength and elasticity than those of the wet specimens. This is due to the initiation and propagation of fissure and micro-cracks caused by the growth of the remaining salt crystals in the pore spaces.

5) X-ray diffraction analysis shows that within the maximum continuous period of submersion in both liquids for 240 days, all tested rocks show insignificant change of their mineral compositions.

6) Empirical equations are derived to correlate the liquid/salt content with submersion duration, and hence the ultimate strength and elasticity reduction can be predicted under long-term submersion period.

7.3 Recommendations for future studies

The recommendations for future studies are as follows:

1) More diverse rock types and brine concentrations are desirable for additional testing in order to truly assess all factors affecting the deterioration of rock from salt weathering process.

2) Longer test duration may be needed for deterioration simulation to obtain a better mathematical representation of their properties as affected by the deterioration simulated parameters. The results could review the effect of mineral alterations on the rock durability.

3) Cycle of wet, dry and heating should be added in the future test parameters. Their could simulated the actual rock deterioration under in-situ condition.

4) Non-invasive method should be developed to assess the physical and mechanical properties of these building and decorating stones during their service life. Such methods may include, for examples, seismic method (P- and S-wave measurements) and resistivity (as the salt contained rocks could provide a better conductivity than those without salt inclusions).

REFERENCES

Alves, C., Figueiredo, C. A. M., Sanjurjo-Sánchez, J., & Hernández, A. C. (2021). Salt weathering of natural stone: a review of comparative laboratory studies. *Heritage, 4,* 1554-1565.

American Society for Testing and Materials. (2014). *Annual Book of ASTM Standards: Standard Test Methods for Compressive Strength and Elastic Moduli of Intact Rock Core Specimens under Varying States of Stress and Temperatures* (Vol. 04.09). West Conshohocken, PA: ASTM International.

American Society for Testing and Materials. (2016). *Annual Book of ASTM Standards: Standard test method for splitting tensile strength of intact rock core specimens* (Vol. 04.08). West Conshohocken, PA: ASTM International.

American Society for Testing and Materials. (2016). *Annual Book of ASTM Standards: Standard Test Method for Density, Relative Density (Specific Gravity), or API Gravity of Crude Petroleum and Liquid Petroleum Products by Hydrometer Method* (Vol. 05.01). West Conshohocken, PA: ASTM International.

American Society for Testing and Materials. (2019). *Annual Book of ASTM Standards: Standard Test Method for Laboratory Determination of Water (Moisture) Content of Soil and Rock by Mass* (Vol. 04.08). West Conshohocken, PA: ASTM International.

Andreotti, S., Franzoni, E., & Fabbri, P. (2018). Poly(hydroxyalkanoate)s-based hydrophobic coatings for the protection of stone in cultural heritage. *Materials (Basel)*, *11*(1), 1-26.

Benavente, D., Martínez-Martínez, J., Cueto, N., & García-del-Cura, M. A. (2007). Salt weathering in dual-porosity building dolostones. *Engineering Geology*, *94*(3-4), 215-226.

Celik, M. Y., & Aygün, A. (2019). The effect of salt crystallization on degradation of volcanic building stones by sodium sulfates and sodium chlorides. *Bulletin of Engineering Geology and the Environment, 78,* 3509-3529.

Celik, M. Y., & Kacmaz, A. U. (2016). The investigation of static and dynamic capillary by water absorption in porous building stones under normal and salty water conditions. *Environ Earth Sci, 2016,* 1-19.

Celik, M. Y., & Sert, M. (2020). The role of different salt solutions and their concentration ratios in salt crystallization test on the durability of the Döğer tuff (Afyonkarahisar, Turkey) used as building stones of cultural heritages. *Bulletin of Engineering Geology and the Environment, 79,* 5553-5568.

Cooke, R.U. (1979). Laboratory simulation of salt weathering processes in arid environments. *Earth Surface Processes and Landforms, 4(4),* 347-359.

De Silva, V. R. S., Ranjith, P. G., Wu, B., & Perera, M. S. A. (2018). Micro-mechanics based numerical simulation of NaCl brine induced mechanical strength deterioration of sedimentary host-rock formations. *Engineering Geology*, *242*, 55-69.

Desaenuad, J., Bonn, D., & Shahidzadeh, N. (2016). The pressure induced by salt crystallization in confinement. *Scientific Reports*, *6*(1), 1-8.

Dinesh, P., Ranjith, P. G., Behera, M. R., & Muthu, N. (2021). Experimental and numerical (EFG method) studies on sedimentary rock under varied salinity conditions. *Rock Mechanics and Mining Sciences*, *148*, 1-21.

Dunning, J. D., & Huf, W. L. (1983). The effects of aqueous chemical environments on crack and hydraulic fracture propagation and morphologies. *Geophysical Research: Solid Earth*, *88*(B8), 6491-6499.

Hawkins, A. B., & McConnell, B. J. (1992). Sensitivity of sandstone strength and deformability to changes in moisture content. *Engineering Geology, 25,* 115-130.

Hosono, T., Uchida, E., Suda, C., Ueno, A., & Nakagawa, T. (2006). Salt weathering of sandstone at the Angkor monuments, Cambodia: identification of the origins of salts using sulfur and strontium isotopes. *Archaeological Science, 33*(11), 1541-1551.

Huang, Y. H., Yang, S. Q., Hall, M., & Zhang, Y. C. (2018). The effects of NaCl concentration and confining pressure on mechanical and acoustic behaviors of brine-saturated sandstone. *Energies*, *11*(2), 1-17.

Huang, Y. H., Yang, S. Q., Li, W. P., & Hall, M. R. (2019). Influence of super-critical CO2 on the strength and fracture behavior of brine-saturated sandstone specimens. *Rock Mechanics and Rock Engineering*, *53*(2), 653-670.

Keppert, M., Čáchová, J., Fort, J., Konáková, D., Pavlik, Z. & Černý, R. (2015). Damage of porous stones by salt crystallization. *WIT Transactions on Modelling and Simulation, 59*, 333-341.

Khamrat, S., Archeeploha, S., & Fuenkajorn, K. (2016). Pore pressure effects on strength and elasticity of ornamental stones. *Sci. Asia*, *42*, 121-135.

Li, D., & Wang, W. (2019). Quantitative analysis of the influence of saturation on rock strength reduction considering the distribution of water. *Geomechanics and Geophysics for Geo-Energy and Geo-Resources*, *5*(2), 197-207.

Liang, W., Yang, X., Gao, H., Zhang, C., Zhao, Y., & Dusseault, M. B. (2012). Experimental study of mechanical properties of gypsum soaked in brine. *Rock Mechanics and Mining Sciences*, *53*, 142-150.

Murray, C., Heggemann, H., Gouadain, J., Krisadasima, S. (1993). Geological history of the siliciclastic Mesozoic strata of the Khorat Group in the Phu Phan range area, northeastern Thailand. *International Symposium on Biostratigraphy of Mainland Southeast Asia: Facies and Paleontology,* 23-49.

Oguchi, C. T., & Yu, S. (2021). A review of theoretical salt weathering studies for stone heritage. *Earth and Planetary Science, 2021,* 1-23.

Rathnaweera, T. D., Ranjith, P. G., & Perera, M. S. A. (2014). Salinity-dependent strength and stress–strain characteristics of reservoir rocks in deep saline aquifers: An experimental study. *Fuel*, *122*, 1-11.

Rathnaweera, T. D., Ranjith, P. G., Perera, M. S. A., Lashin, A., & Al Arifi, N. (2015). Non-linear stress–strain behaviour of reservoir rock under brine saturation: An experimental study. *Measurement*, *71*, 56-72.

Ruiz-Agudo, E., Mees, F., Jacobs, P., & Rodriguez-Navarro, C. (2006). The role of saline solution properties on porous limestone salt weathering by magnesium and sodium sulfates. *Environmental Geology*, *52*(2), 269-281.

Sampath, K. H. S. M., Perera, M. S. A., Elsworth, D., Ranjith, P. G., Matthai, S. K., & Rathnaweera, T. (2018). Experimental investigation on the mechanical behavior of victorian brown coal under brine saturation. *Energy & Fuels*, *32*(5), 5799-5811.

Scrivano, S., & Gaggera, L. (2020). An experimental investigation into the salt-weathering susceptibility of building limestones. *Rock Mechanics and Rock Engineering, 53(12),* 5329–5343.

Seo, S. E., Girard, M., De La Cruz, M. O., & Mirkin, C. A. (2019). The importance of salt-enhanced electrostatic repulsion in colloidal crystal engineering with DNA. *ACS central science*, *5(1)*, 186-191.

Shukla, R., Ranjith, P. G., Choi, S. K., Haque, A., Yellishetty, M., & Hong, L. (2012). Mechanical behaviour of reservoir rock under brine saturation. *Rock Mechanics and Rock Engineering*, *46*(1), 83-93.

Snethlage, R., & Wendler, E. (1997). Moisture cycles and sandstone degradation. *Environmental Sciences Research Report ES, 20*, 7-24.

Tang, L. S., & Wang, S. J. (1999). Progress in the study on mechanical effect of the chemical action of water–rock on deformation and failure of rocks. *Advances in Earth Science*, *14*(5), 433-439.

Taye, B., Viles, H., & Zhang, H. (2022). Influence of salt (NaCl) on hydric and hygric dilatation of clay-rich rocks. *Cultural Heritage, 58*(2022), 137-145.

Vásárhelyi, B. (2003). Some observations regarding the strength and deformability of sandstones in dry and saturated conditions. *Bulletin of Engineering Geology and the Environment, 62,* 245-249.

Vásárhelyi, B., & Ván, P. (2006) Influence of water content on the strength of rock. *Engineering Grology, 84,* 70-74.

Vásárhelyi, B. (2005). Technical note statistical analysis of the influence of water content on the strength of the Miocene limestone. *Rock Mech. Rock Eng, 38(1),* 69-76.

Yilmaz, I. (2010). Influence of water content on the strength and deformability of gypsum. *International Journal of Rock Mechanics and Mining Sciences, 47(2),* 342-347.

Vazquez, P., & Lux, J. (2023). Salt crystallization on Crazannes limestone in a long-term storage environment. *Minerals, 13,* 1282.

Wang, Z. T., & An, Z. S. (2016). A simple theoretical approach to the thermal expansion mechanism of salt weathering. *Catena*, *147*, 695-698.

Warren, JK. (2016). *Evaporite: A Geological Compendium*. Springer. 83 p.

Wellman, H. W., & Wilson, A. T. (1965). Salt weathering, a neglected geological erosive agent in coastal and arid environments, *Nature, 205*, 1097–1098.

Wendai, L. (2000). *Regression analysis, linear regression and profit regression*. 13chapters. SPSS for Windows: statistical analysis: Publishing House of Electronics Industry, Beijing, China.

Xu, H. B., Tsukuda, M., Takahara, Y., Sato, T., Gu, J. D., & Katayama, Y. (2018). Lithoautotrophical oxidation of elemental sulfur by fungi including Fusarium solani isolated from sandstone Angkor temples. *International Biodeterioration and Biodegradation*, *126*, 95-102.

Yan, S., Xie, N., Liu, J., Li, L., Peng, L., & Jiang, S. (2022). Salt weathering of sandstone under dehydration and moisture absorption cycles: An experimental study on the sandstone from Dazu rock carvings. *Earth Surface Processes and Landforms*, *47*(4), 977-993.

Zehnder, K., & Arnold, A. (1989). Crystal growth in salt efflorescence. *Crystal Growth*, *97*(2), 513-521.

Zhang, X., Gamage, R., Perera, M., & Ranathunga, A. (2018). Effects of water and brine saturation on mechanical property alterations of brown coal. *Energies*, *11*(5), 1-17.

Zhou, J., Tian, S., Zhou, L., Xian, X., Zhang, C., Yang, K., Dong, Z., & Lu, Z. (2021). Effect of sub-/super-critical CO2 and brine exposure on the mechanical and acoustic emission characteristics of shale. *Natural Gas Science and Engineering*, *90*(2021), 1-14.

APPENDIX A

ROCK SPECIMEN DIMENSIONS

Table A.1 Specimens prepared for initial condition for uniaxial compression test.

Specimen No.	Diameter (mm)	Length (mm)	Weight (g)	Density (g/cc)
M-I-1	44.74	90.90	656.85	2.75
M-I-2	44.82	89.94	661.50	2.74
M-I-3	44.74	90.60	662.99	2.73
SY-I-1	44.68	89.78	539.94	2.23
SY-I-2	44.68	89.18	546.35	2.25
SY-I-3	44.68	89.72	549.86	2.24
SR-I-1	44.66	88.58	567.26	2.39
SR-I-2	44.68	88.74	576.06	2.40
SR-I-3	44.68	89.12	565.11	2.36

Table A.2 Specimens prepared for initial condition for Brazilian tension test.

Specimen No.	Diameter (mm)	Length (mm)	Weight (g)	Density (g/cc)
M-I-1	53.04	24.50	154.11	2.75
M-I-2	53.24	25.00	154.42	2.74
M-I-3	53.22	24.68	153.71	2.73
SY-I-1	53.32	25.32	126.92	2.24
SY-I-2	53.44	25.64	131.71	2.29
SY-I-3	53.28	23.42	118.13	2.26
SR-I-1	53.24	26.42	141.97	2.41
SR-I-2	53.12	24.46	130.51	2.41
SR-I-3	53.24	26.18	143.31	2.46

Table A.3 Specimens prepared for simulation of deterioration under distilled water and uniaxial compression test.

Specimen No.	Diameter (mm)	Length (mm)	Weight (g)	Density (g/cc)
M-W-1	44.72	89.32	378.44	2.70
M-W-2	44.62	88.74	374.58	2.70
M-W-3	44.72	89.98	381.28	2.70
M-W-4	44.68	88.92	377.40	2.71
M-W-5	44.68	90.60	381.98	2.69
M-W-6	44.68	90.62	383.54	2.70
M-W-7	44.70	90.58	382.82	2.69
M-W-8	44.68	90.28	379.28	2.68
SY-W-1	44.70	89.44	312.82	2.23
SY-W-2	44.70	89.44	313.24	2.23
SY-W-3	44.68	89.86	315.46	2.24
SY-W-4	44.64	89.46	313.78	2.24
SY-W-5	44.73	88.44	309.30	2.23
SY-W-6	44.68	86.82	304.73	2.24
SY-W-7	44.66	88.40	311.10	2.25
SY-W-8	44.70	89.42	313.76	2.24
SR-W-1	44.72	89.20	330.64	2.36
SR-W-2	44.68	88.48	327.48	2.36
SR-W-3	44.68	89.28	332.40	2.37
SR-W-4	44.68	89.28	330.78	2.36
SR-W-5	44.68	89.58	332.38	2.37
SR-W-6	44.68	88.84	330.28	2.37
SR-W-7	44.66	88.32	329.25	2.38
SR-W-8	44.68	88.95	330.08	2.37

Table A.4 Specimens prepared for simulation of deterioration under distilled water and Brazilian tension test.

Specimen No.	Diameter (mm)	Length (mm)	Weight (g)	Density (g/cc)
M-W-1-1	53.3	26.90	163.65	2.73
M-W-1-2	53.4	26.70	162.71	2.72
M-W-1-3	53.5	26.70	161.96	2.70
M-W-2-1	53.40	26.20	160.19	2.73
M-W-2-2	53.40	26.20	156.50	2.67
M-W-2-3	53.40	25.60	156.40	2.73
M-W-3-1	53.30	23.00	158.59	2.73
M-W-3-2	53.40	23.60	158.90	2.67
M-W-3-3	53.30	26.70	162.20	2.72
M-W-4-1	53.50	27.00	162.58	2.68
M-W-4-2	53.40	26.90	163.27	2.71
M-W-4-3	53.30	25.40	152.22	2.68
SY-W-1-1	53.10	26.00	128.58	2.23
SY-W-1-2	53.10	24.50	118.74	2.19
SY-W-1-3	53.40	26.00	130.80	2.25
SY-W-2-1	53.30	27.10	126.48	2.09
SY-W-2-2	53.40	25.10	126.61	2.25
SY-W-2-3	53.00	22.60	122.82	2.46
SY-W-3-1	53.40	25.90	126.31	2.18
SY-W-3-2	53.40	24.80	124.26	2.24
SY-W-3-3	53.30	25.70	125.47	2.19
SY-W-4-1	53.20	24.60	123.49	2.26
SY-W-4-2	53.40	25.50	128.71	2.25
SY-W-4-3	53.50	25.10	125.21	2.22

Table A.5 Specimens prepared for simulation of deterioration under distilled water and Brazilian tension test.

Specimen No.	Diameter (mm)	Length (mm)	Weight (g)	Density (g/cc)
SR-W-1-1	53.22	26.70	138.05	2.32
SR-W-1-2	53.16	26.76	144.84	2.44
SR-W-1-3	53.22	26.18	143.92	2.47
SR-W-2-1	53.30	25.24	135.56	2.41
SR-W-2-2	53.26	25.34	137.30	2.43
SR-W-2-3	53.16	24.52	130.61	2.40
SR-W-3-1	53.34	25.60	137.48	2.40
SR-W-3-2	53.84	26.70	143.35	2.36
SR-W-3-3	53.14	26.40	142.64	2.44
SR-W-4-1	53.20	25.80	135.20	2.36
SR-W-4-2	53.30	27.30	145.25	2.38
SR-W-4-3	53.10	26.80	141.55	2.38

Table A.6 Specimens prepared for simulation of deterioration under brine and uniaxial compression test.

Specimen No.	Diameter (mm)	Length (mm)	Weight (g)	Density (g/cc)
M-B-1	44.68	87.52	375.52	2.74
M-B-2	44.68	88.74	375.65	2.70
M-B-3	44.70	87.64	371.91	2.70
M-B-4	44.64	89.68	381.76	2.72
M-B-5	44.71	90.76	385.11	2.70
M-B-6	44.68	85.80	362.41	2.69
M-B-7	44.70	88.86	376.40	2.70
M-B-8	44.68	89.74	378.45	2.69
SY-B-1	44.68	89.42	314.23	2.24
SY-B-2	44.70	87.72	308.46	2.24
SY-B-3	44.68	89.96	316.10	2.24
SY-B-4	44.70	88.68	311.22	2.24
SY-B-5	44.68	88.64	311.40	2.24
SY-B-6	44.70	90.34	317.22	2.24
SY-B-7	44.72	88.56	311.56	2.24
SY-B-8	44.68	88.72	311.92	2.24
SR-B-1	44.68	89.32	327.10	2.33
SR-B-2	44.70	87.40	321.83	2.34
SR-B-3	44.70	89.40	331.63	2.36
SR-B-4	44.70	89.12	325.61	2.33
SR-B-5	44.68	89.02	330.64	2.37
SR-B-6	44.70	89.12	322.69	2.31
SR-B-7	44.74	89.42	332.40	2.36
SR-B-8	44.76	88.40	328.17	2.36

Table A.7 Specimens prepared for simulation of deterioration under brine and Brazilian tension test.

Specimen No.	Diameter (mm)	Length (mm)	Weight (g)	Density (g/cc)
M-B-1-1	53.40	26.20	161.22	2.75
M-B-1-2	53.40	26.60	160.40	2.69
M-B-1-3	53.40	26.10	159.34	2.72
M-B-2-1	53.40	26.00	158.33	2.72
M-B-2-2	53.50	25.00	151.88	2.70
M-B-2-3	53.70	26.40	156.78	2.62
M-B-3-1	53.30	26.50	161.31	2.73
M-B-3-2	53.50	27.40	162.13	2.63
M-B-3-3	53.40	25.70	156.37	2.72
M-B-4-1	53.60	25.60	156.10	2.70
M-B-4-2	53.40	26.60	160.28	2.69
M-B-4-3	53.40	26.40	158.71	2.68
SY-B-1-1	53.30	25.10	121.67	2.17
SY-B-1-2	53.20	24.90	124.35	2.25
SY-B-1-3	53.30	25.80	128.59	2.23
SY-B-2-1	53.30	25.20	122.34	2.17
SY-B-2-2	53.30	25.60	127.43	2.23
SY-B-2-3	53.30	26.10	131.71	2.26
SY-B-3-1	53.40	25.80	130.19	2.36
SY-B-3-2	53.40	24.80	123.76	2.35
SY-B-3-3	53.60	25.80	126.78	2.30
SY-B-4-1	53.20	23.70	118.17	2.24
SY-B-4-2	53.30	27.30	136.96	2.25
SY-B-4-3	53.40	23.40	117.14	2.61

Table A.8 Specimens prepared for simulation of deterioration under brine and Brazilian tension test.

Specimen No.	Diameter (mm)	Length (mm)	Weight (g)	Density (g/cc)
SR-B-1-1	53.30	26.60	142.32	2.40
SR-B-1-2	53.30	24.70	130.66	2.37
SR-B-1-3	53.30	27.00	142.51	2.36
SR-B-2-1	53.30	26.60	141.77	2.39
SR-B-2-2	53.30	26.20	139.11	2.38
SR-B-2-3	53.40	26.60	141.25	2.37
SR-B-3-1	53.20	27.00	145.25	2.52
SR-B-3-2	53.20	26.80	142.93	2.50
SR-B-3-3	53.30	25.00	134.68	2.51
SR-B-4-1	53.30	26.30	145.23	2.42
SR-B-4-2	53.30	25.50	141.41	2.43
SR-B-4-3	53.40	26.70	146.97	2.39

Table A.9 Specimens prepared for simulation of deterioration under brine and uniaxial compression test.

Specimen No.	Diameter (mm)	Length (mm)	Weight (g)	Density (g/cc)
M-S-1	44.70	87.64	371.45	2.70
M-S-2	44.64	89.68	379.08	2.70
M-S-3	44.50	89.70	376.70	2.70
M-S-4	44.80	88.90	378.48	2.70
M-S-5	44.68	85.80	364.60	2.71
M-S-6	44.68	89.36	379.74	2.71
M-S-7	44.68	89.74	382.72	2.72
M-S-8	44.70	90.56	386.51	2.72
SY-S-1	44.68	89.96	319.10	2.30
SY-S-2	44.70	88.68	317.22	2.30
SY-S-3	44.72	90.42	323.51	2.33
SY-S-4	44.70	89.90	321.96	2.33
SY-S-5	44.70	90.34	327.52	2.34
SY-S-6	44.70	89.54	318.38	2.35
SY-S-7	44.68	88.72	317.92	2.36
SY-S-8	44.70	89.72	323.61	2.35
SR-S-1	44.70	89.40	331.63	2.43
SR-S-2	44.70	83.12	325.61	2.58
SR-S-3	44.68	87.48	318.00	2.38
SR-S-4	44.62	89.22	321.86	2.38
SR-S-5	44.70	87.12	313.24	2.38
SR-S-6	44.72	89.22	317.02	2.39
SR-S-7	44.72	88.40	318.17	2.41
SR-S-8	44.68	89.64	320.48	2.41

Table A.10 Specimens prepared for simulation of deterioration under brine and Brazilian tension test.

Specimen No.	Diameter (mm)	Length (mm)	Weight (g)	Density (g/cc)
M-S-1-1	53.40	26.20	161.52	2.72
M-S-1-2	53.40	26.60	160.56	2.61
M-S-1-3	53.40	26.10	159.48	2.61
M-S-2-1	53.40	26.90	156.10	2.59
M-S-2-2	53.70	26.60	160.28	2.66
M-S-2-3	53.78	26.44	158.71	2.64
M-S-3-1	53.40	26.80	162.69	2.71
M-S-3-2	53.40	24.70	151.06	2.73
M-S-3-3	53.50	27.00	162.90	2.68
M-S-4-1	53.50	26.60	158.55	2.65
M-S-4-2	53.50	26.10	158.10	2.70
M-S-4-3	53.40	26.10	160.74	2.76
SY-S-1-1	53.30	25.10	128.21	2.39
SY-S-1-2	53.20	24.90	130.74	2.41
SY-S-1-3	53.30	25.80	135.46	2.39
SY-S-2-1	53.70	23.74	118.17	2.32
SY-S-2-2	53.74	27.46	136.96	2.31
SY-S-2-3	53.78	23.80	117.14	2.29
SY-S-3-1	53.30	25.80	131.56	2.22
SY-S-3-2	53.40	24.20	127.22	2.28
SY-S-3-3	53.40	25.30	131.60	2.25
SY-S-4-1	53.40	25.50	126.88	2.30
SY-S-4-2	53.30	25.20	124.45	2.29
SY-S-4-3	53.40	25.00	125.00	2.29

Table A.11 Specimens prepared for simulation of deterioration under brine and Brazilian tension test.

Specimen No.	Diameter (mm)	Length (mm)	Weight (g)	Density (g/cc)
SR-S-1-1	53.30	26.60	147.88	2.49
SR-S-1-2	53.30	24.70	142.12	2.58
SR-S-1-3	53.30	27.00	147.76	2.45
SR-S-2-1	53.20	27.12	142.65	2.46
SR-S-2-2	53.62	26.06	137.66	2.43
SR-S-2-3	53.62	26.54	139.10	2.41
SR-S-3-1	53.30	26.30	145.23	2.42
SR-S-3-2	53.30	25.50	141.41	2.43
SR-S-3-3	53.40	26.70	146.97	2.39
SR-S-4-1	53.30	25.50	135.83	2.43
SR-S-4-2	53.30	25.90	137.43	2.43
SR-S-4-3	53.40	25.00	132.80	2.42

APPENDIX B

LIQUID AND SALT CONTENTS

Table B.1 Liquid and salt contents of marble for uniaxial compression test.

Conditions	Duration (Days)	Specimen No.	Liquid/salt contents (%)	Average (%)
Initial	0	M-I-1	0.00	0.00
		M-I-2		
		M-I-3		
Water	60	M-W-1	0.03	0.02
		M-W-2	0.01	
	120	M-W-3	0.03	0.04
		M-W-4	0.04	
	180	M-W-5	0.05	0.05
		M-W-6	0.05	
	240	M-W-7	0.09	0.09
		M-W-8	0.08	
Brine	60	M-B-1	0.02	0.02
		M-B-2	0.02	
	120	M-B-3	0.02	0.02
		M-B-4	0.02	
	180	M-B-5	0.05	0.04
		M-B-6	0.03	
	240	M-B-7	0.08	0.08
		M-B-8	0.09	
Salt	60	M-S-1	0.01	0.02
		M-S-2	0.01	
	120	M-S-3	0.03	0.02
		M-S-4	0.01	
	180	M-S-5	0.03	0.04
		M-S-6	0.03	
	240	M-S-7	0.04	0.08
		M-S-8	0.05	

Table B.2 Liquid and salt contents of siltstone for uniaxial compression test.

Conditions	Duration (Days)	Specimen No.	Liquid/salt contents (%)	Average (%)
Initial	0	SY-I-1	0.00	0.00
		SY-I-2		
		SY-I-3		
Water	60	SY-W-1	4.11	3.76
		SY-W-2	3.12	
	120	SY-W-3	4.49	4.67
		SY-W-4	4.43	
	180	SY-W-5	5.67	5.68
		SY-W-6	5.08	
	240	SY-W-7	6.26	6.35
		SY-W-8	5.68	
Brine	60	SY-B-1	2.74	3.32
		SY-B-2	2.93	
	120	SY-B-3	4.24	4.47
		SY-B-4	4.32	
	180	SY-B-5	5.15	5.32
		SY-B-6	4.95	
	240	SY-B-7	5.41	5.79
		SY-B-8	5.54	
Salt	60	SY-S-1	1.68	1.30
		SY-S-2	0.93	
	120	SY-S-3	2.28	2.19
		SY-S-4	2.09	
	180	SY-S-5	1.43	2.54
		SY-S-6	3.65	
	240	SY-S-7	3.20	2.72
		SY-S-8	2.23	

Table B.3 Liquid and salt contents of sandstone for uniaxial compression test.

<table>
<tr><th>Conditions</th><th>Duration (Days)</th><th>Specimen No.</th><th>Liquid/salt contents (%)</th><th>Average (%)</th></tr>
<tr><td rowspan="3">Initial</td><td rowspan="3">0</td><td>SR-I-1</td><td rowspan="3">0.00</td><td rowspan="3">0.00</td></tr>
<tr><td>SR-I-2</td></tr>
<tr><td>SR-I-3</td></tr>
<tr><td rowspan="8">Water</td><td rowspan="2">60</td><td>SR-W-1</td><td>4.00</td><td rowspan="2">4.87</td></tr>
<tr><td>SR-W-2</td><td>5.27</td></tr>
<tr><td rowspan="2">120</td><td>SR-W-3</td><td>6.17</td><td rowspan="2">6.59</td></tr>
<tr><td>SR-W-4</td><td>6.18</td></tr>
<tr><td rowspan="2">180</td><td>SR-W-5</td><td>8.19</td><td rowspan="2">7.94</td></tr>
<tr><td>SR-W-6</td><td>6.51</td></tr>
<tr><td rowspan="2">240</td><td>SR-W-7</td><td>7.77</td><td rowspan="2">8.99</td></tr>
<tr><td>SR-W-8</td><td>8.71</td></tr>
<tr><td rowspan="8">Brine</td><td rowspan="2">60</td><td>SR-B-1</td><td>3.94</td><td rowspan="2">4.22</td></tr>
<tr><td>SR-B-2</td><td>4.14</td></tr>
<tr><td rowspan="2">120</td><td>SR-B-3</td><td>6.81</td><td rowspan="2">5.94</td></tr>
<tr><td>SR-B-4</td><td>4.36</td></tr>
<tr><td rowspan="2">180</td><td>SR-B-5</td><td>6.33</td><td rowspan="2">6.26</td></tr>
<tr><td>SR-B-6</td><td>5.45</td></tr>
<tr><td rowspan="2">240</td><td>SR-B-7</td><td>5.90</td><td rowspan="2">6.42</td></tr>
<tr><td>SR-B-8</td><td>6.15</td></tr>
<tr><td rowspan="8">Salt</td><td rowspan="2">60</td><td>SR-S-1</td><td>1.22</td><td rowspan="2">1.22</td></tr>
<tr><td>SR-S-2</td><td>1.21</td></tr>
<tr><td rowspan="2">120</td><td>SR-S-3</td><td>2.62</td><td rowspan="2">2.86</td></tr>
<tr><td>SR-S-4</td><td>3.10</td></tr>
<tr><td rowspan="2">180</td><td>SR-S-5</td><td>3.77</td><td rowspan="2">4.58</td></tr>
<tr><td>SR-S-6</td><td>5.39</td></tr>
<tr><td rowspan="2">240</td><td>SR-S-7</td><td>4.96</td><td rowspan="2">5.19</td></tr>
<tr><td>SR-S-8</td><td>5.42</td></tr>
</table>

APPENDIX C

SPECIMEN DENSITY

Table C.1 Specimen density of marble for uniaxial compression test.

Conditions	Duration (Days)	Specimen No.	Density (g/cc)	Average density (g/cc)
Initial	0	M-I-1	2.68	2.68
		M-I-2	2.67	
		M-I-3	2.66	
Water	60	M-W-1	2.71	2.71
		M-W-2	2.71	
	120	M-W-3	2.71	2.72
		M-W-4	2.72	
	180	M-W-5	2.73	2.73
		M-W-6	2.73	
	240	M-W-7	2.73	2.73
		M-W-8	2.73	
Brine	60	M-B-1	2.74	2.72
		M-B-2	2.70	
	120	M-B-3	2.73	2.73
		M-B-4	2.73	
	180	M-B-5	2.74	2.74
		M-B-6	2.74	
	240	M-B-7	2.74	2.74
		M-B-8	2.74	
Salt	60	M-S-1	2.70	2.70
		M-S-2	2.70	
	120	M-S-3	2.70	2.70
		M-S-4	2.70	
	180	M-S-5	2.71	2.71
		M-S-6	2.71	
	240	M-S-7	2.72	2.72
		M-S-8	2.72	

Table C.2 Specimen density of siltstone for uniaxial compression test.

Conditions	Duration (Days)	Specimen No.	Density (g/cc)	Average density (g/cc)
Initial	0	SY-I-1	2.23	2.24
		SY-I-2	2.25	
		SY-I-3	2.24	
Water	60	SY-W-1	2.34	2.34
		SY-W-2	2.35	
	120	SY-W-3	2.34	2.34
		SY-W-4	2.34	
	180	SY-W-5	2.37	2.36
		SY-W-6	2.35	
	240	SY-W-7	2.40	2.38
		SY-W-8	2.37	
Brine	60	SY-B-1	2.44	2.43
		SY-B-2	2.43	
	120	SY-B-3	2.42	2.44
		SY-B-4	2.46	
	180	SY-B-5	2.46	2.46
		SY-B-6	2.46	
	240	SY-B-7	2.47	2.47
		SY-B-8	2.47	
Salt	60	SY-S-1	2.30	2.30
		SY-S-2	2.30	
	120	SY-S-3	2.33	2.33
		SY-S-4	2.33	
	180	SY-S-5	2.34	2.35
		SY-S-6	2.35	
	240	SY-S-7	2.36	2.36
		SY-S-8	2.35	

Table C.3 Specimen density of sandstone for uniaxial compression test.

Conditions	Duration (Days)	Specimen No.	Density (g/cc)	Average density (g/cc)
Initial	0	SR-I-1	2.35	2.36
		SR-I-2	2.37	
		SR-I-3	2.36	
Water	60	SR-W-1	2.38	2.38
		SR-W-2	2.37	
	120	SR-W-3	2.41	2.40
		SR-W-4	2.40	
	180	SR-W-5	2.42	2.42
		SR-W-6	2.42	
	240	SR-W-7	2.45	2.45
		SR-W-8	2.45	
Brine	60	SR-B-1	2.41	2.40
		SR-B-2	2.40	
	120	SR-B-3	2.45	2.45
		SR-B-4	2.45	
	180	SR-B-5	2.47	2.46
		SR-B-6	2.45	
	240	SR-B-7	2.48	2.49
		SR-B-8	2.49	
Salt	60	SR-S-1	2.43	2.36
		SR-S-2	2.58	
	120	SR-S-3	2.38	2.38
		SR-S-4	2.38	
	180	SR-S-5	2.38	2.39
		SR-S-6	2.39	
	240	SR-S-7	2.41	2.41
		SR-S-8	2.41	

APPENDIX D

STRESS-STRAIN CRUVE

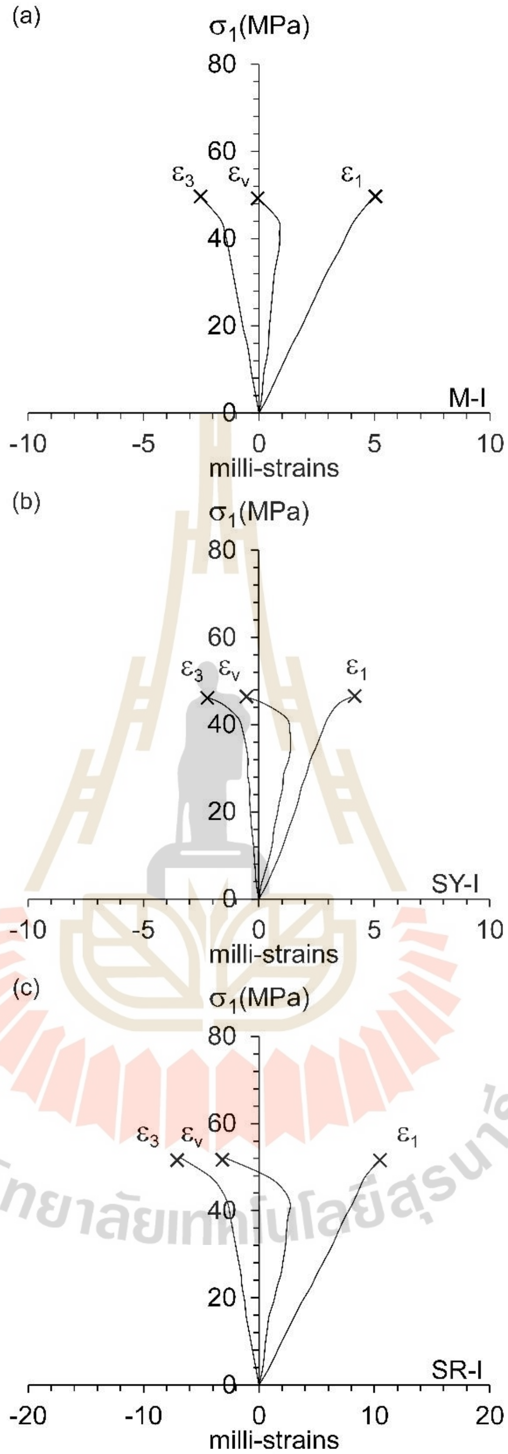

Figure D.1 Stress-strain curves of initial condition (0 Day) for marble (a), siltstone (b), and sandstone (c).

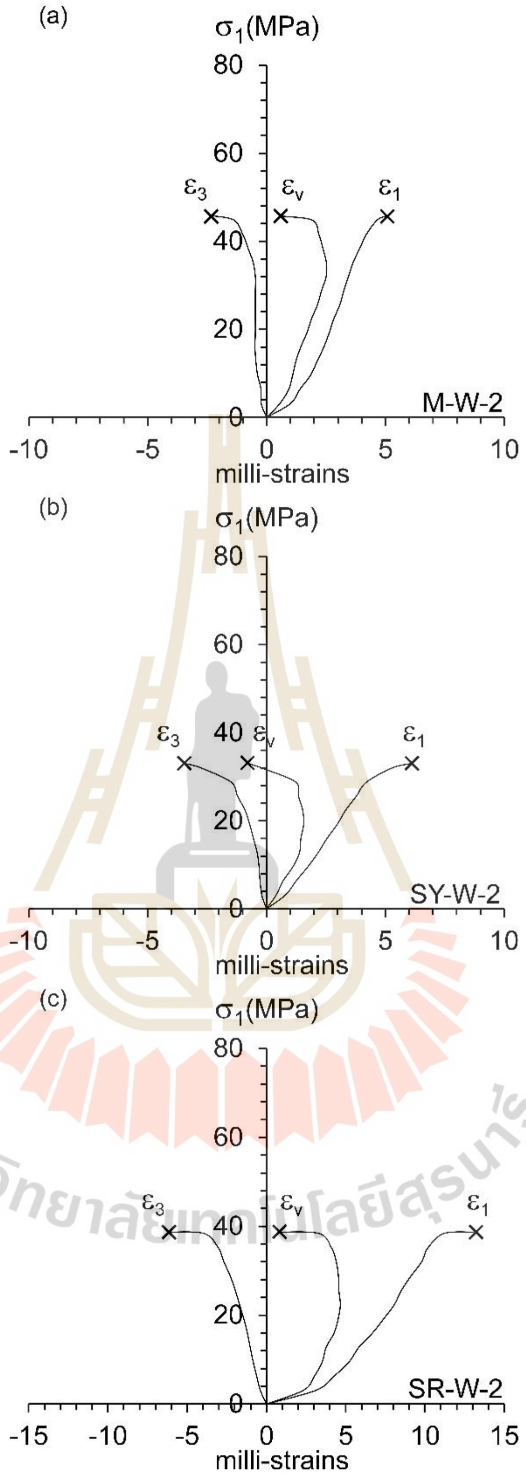

Figure D.2 Stress-strain curves of water condition on 60 days for marble (a), siltstone (b), and sandstone (c).

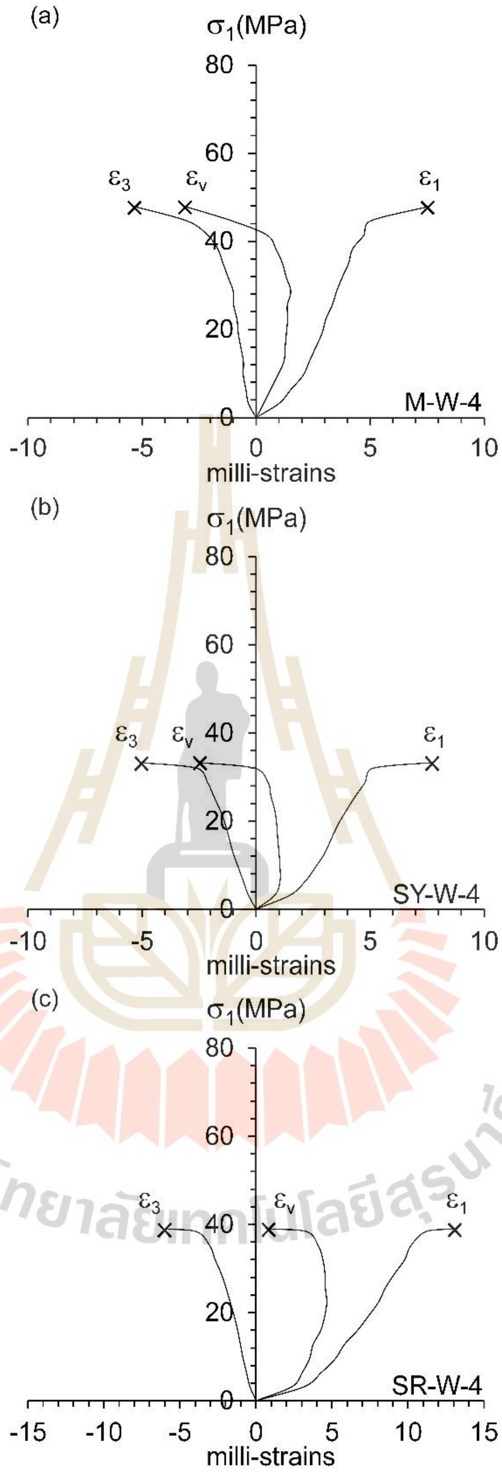

Figure D.3 Stress-strain curves of water condition on 120 days for marble (a), siltstone (b), and sandstone (c).

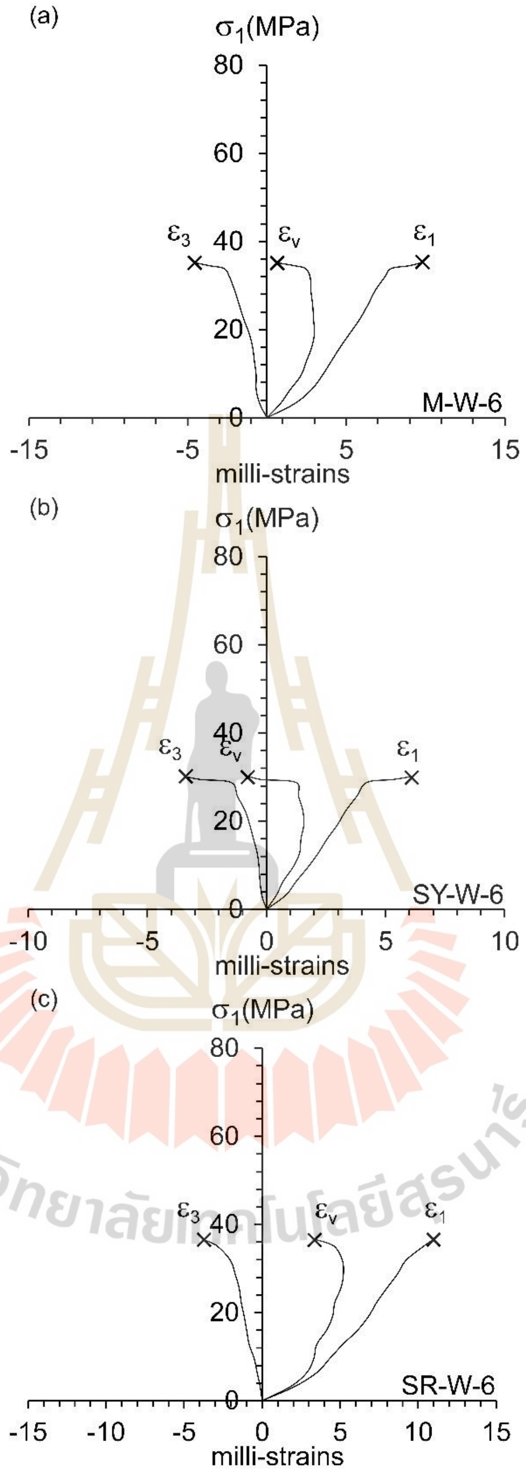

Figure D.4 Stress-strain curves of water condition on 180 days for marble (a), siltstone (b), and sandstone (c).

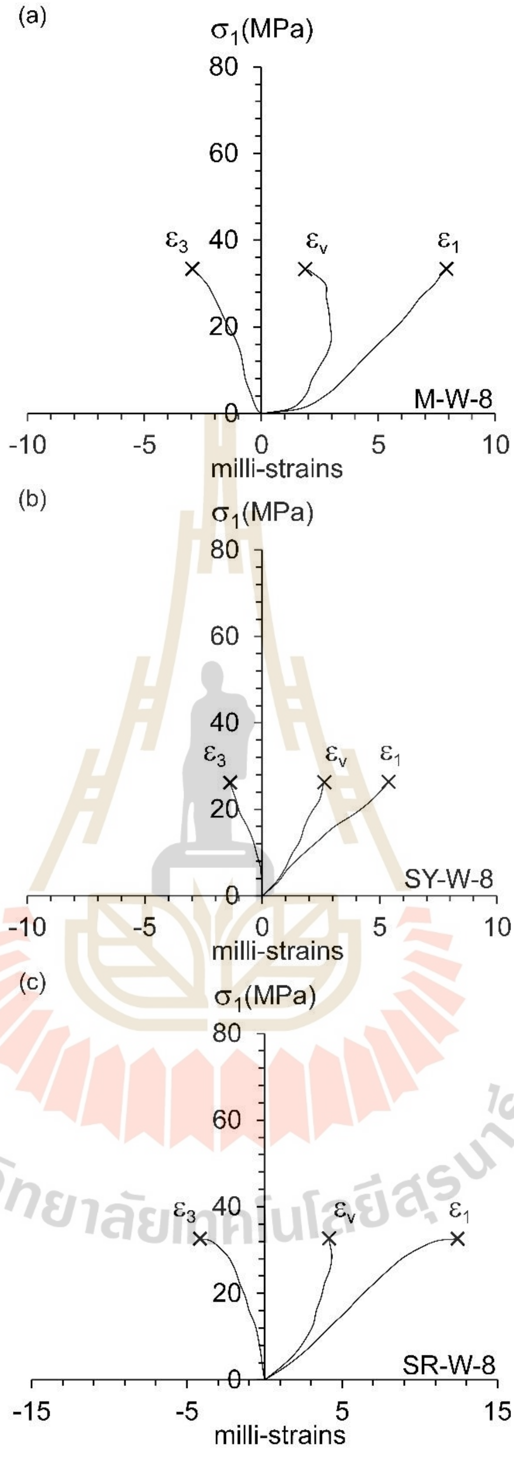

Figure D.5 Stress-strain curves of water condition on 240 days for marble (a), siltstone (b), and sandstone (c).

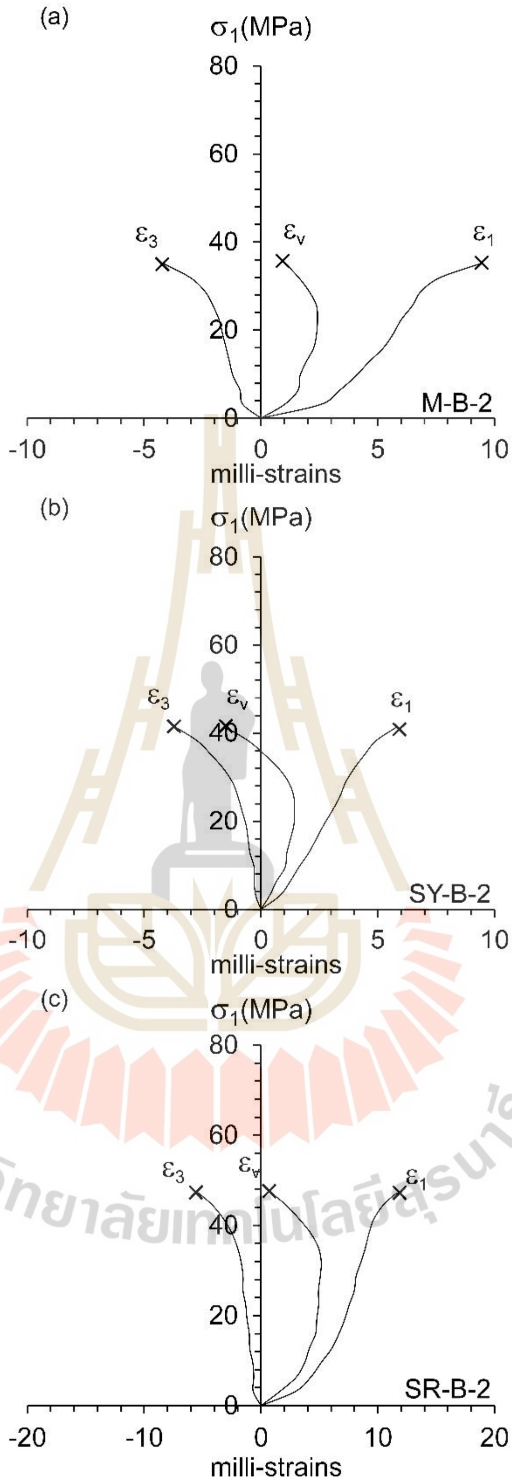

Figure D.6 Stress-strain curves of brine condition on 60 days for marble (a), siltstone (b), and sandstone (c).

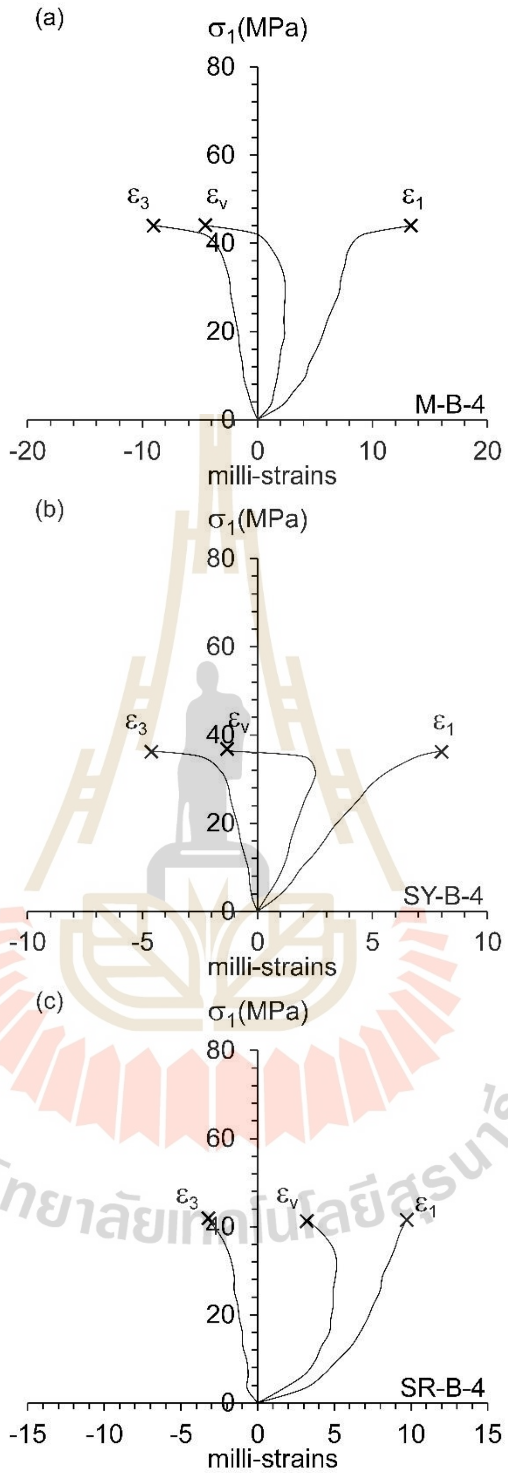

Figure D.7 Stress-strain curves of brine condition on 120 days for marble (a), siltstone (b), and sandstone (c).

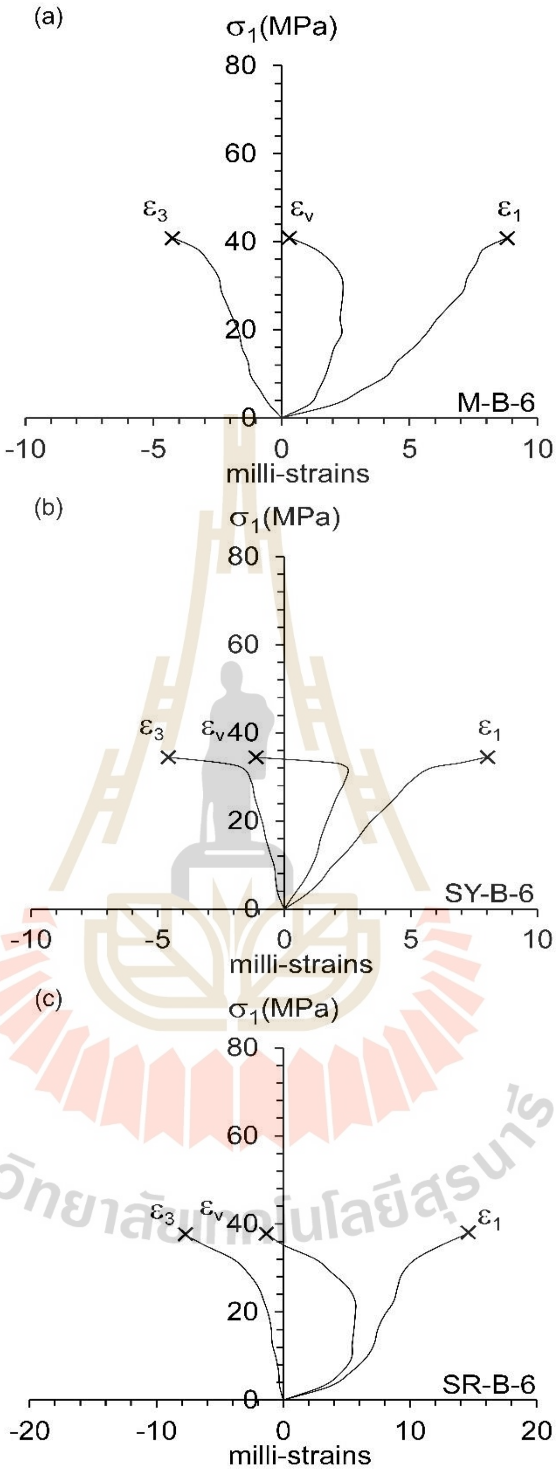

Figure D.8 Stress-strain curves of brine condition on 180 days for marble (a), siltstone (b), and sandstone (c).

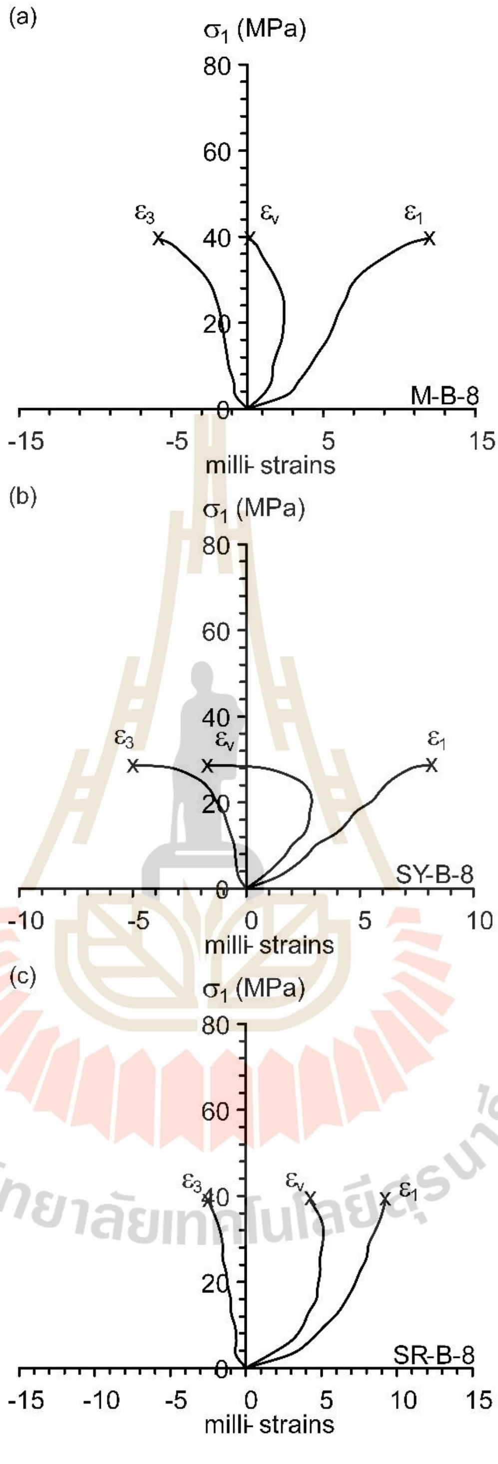

Figure D.9 Stress-strain curves of brine condition on 240 days for marble (a), siltstone (b), and sandstone (c).

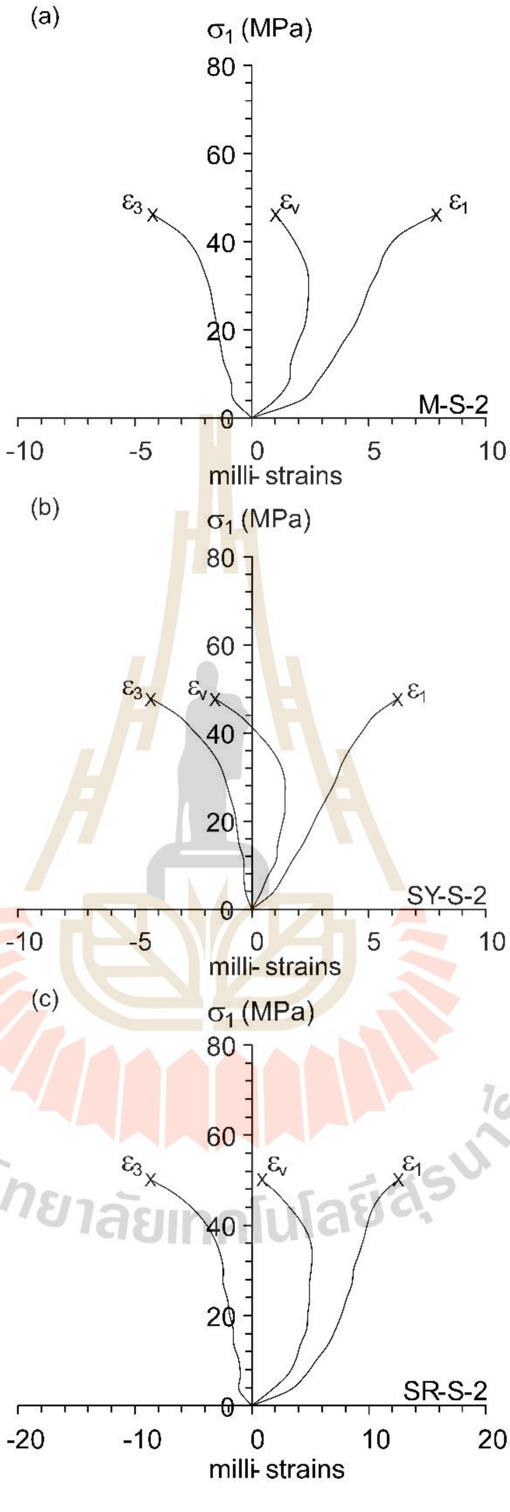

Figure D.10 Stress-strain curves of salt condition on 60 days for marble (a), siltstone (b), and sandstone (c).

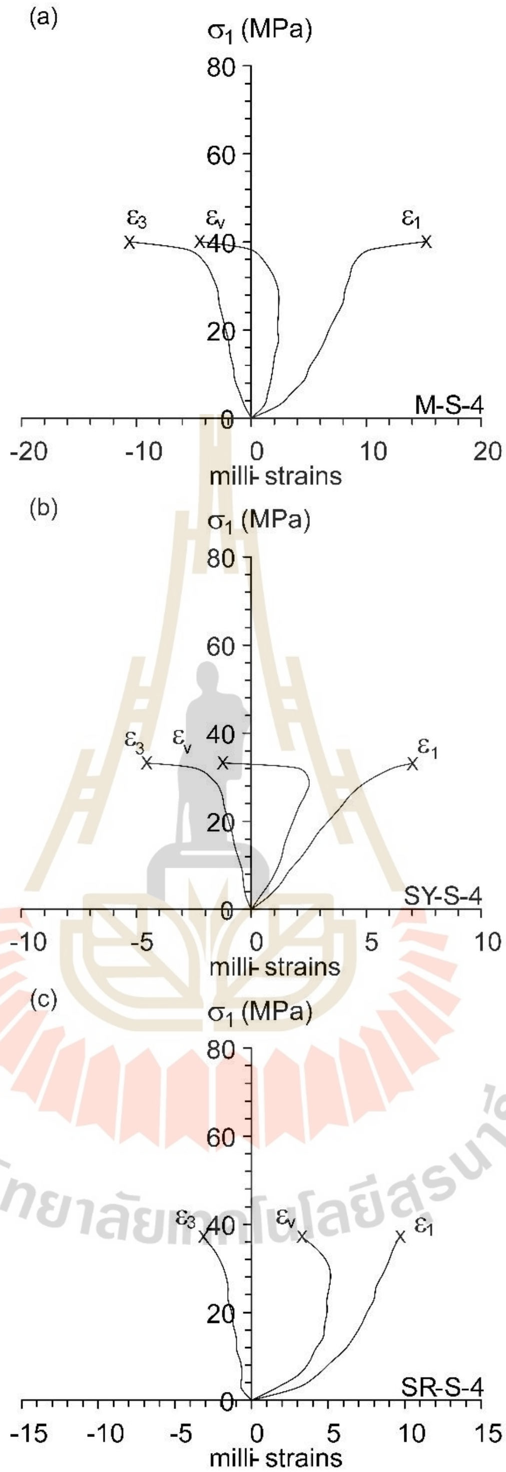

Figure D.11 Stress-strain curves of salt condition on 120 days for marble (a), siltstone (b), and sandstone (c).

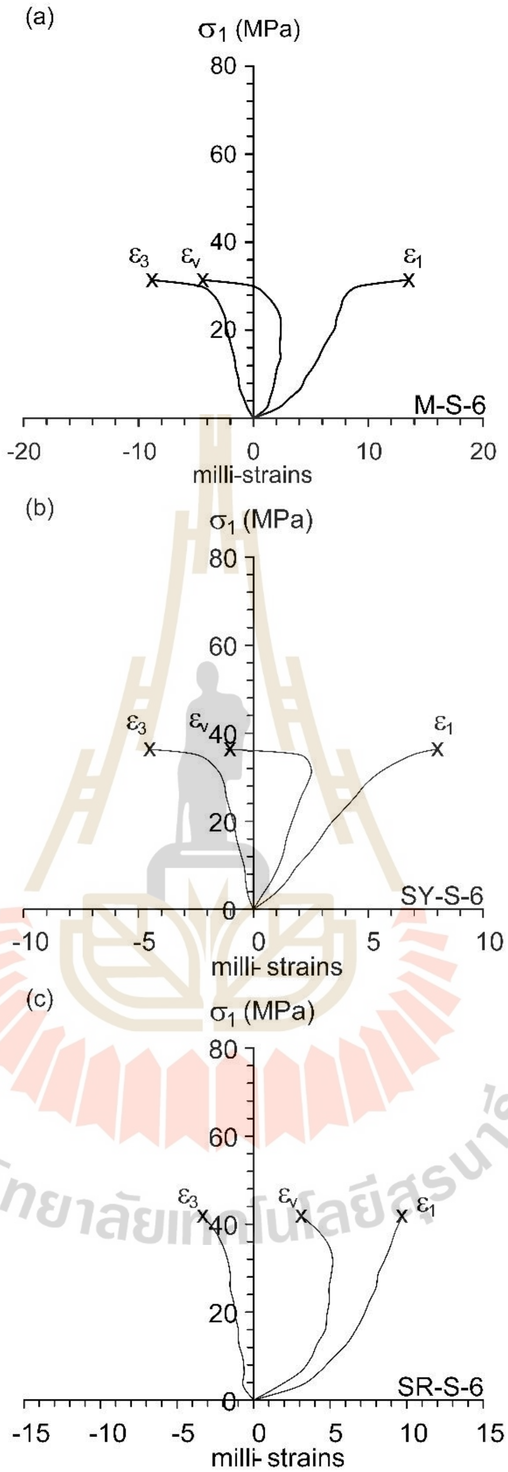

Figure D.12 Stress-strain curves of salt condition on 180 days for marble (a), siltstone (b), and sandstone (c).

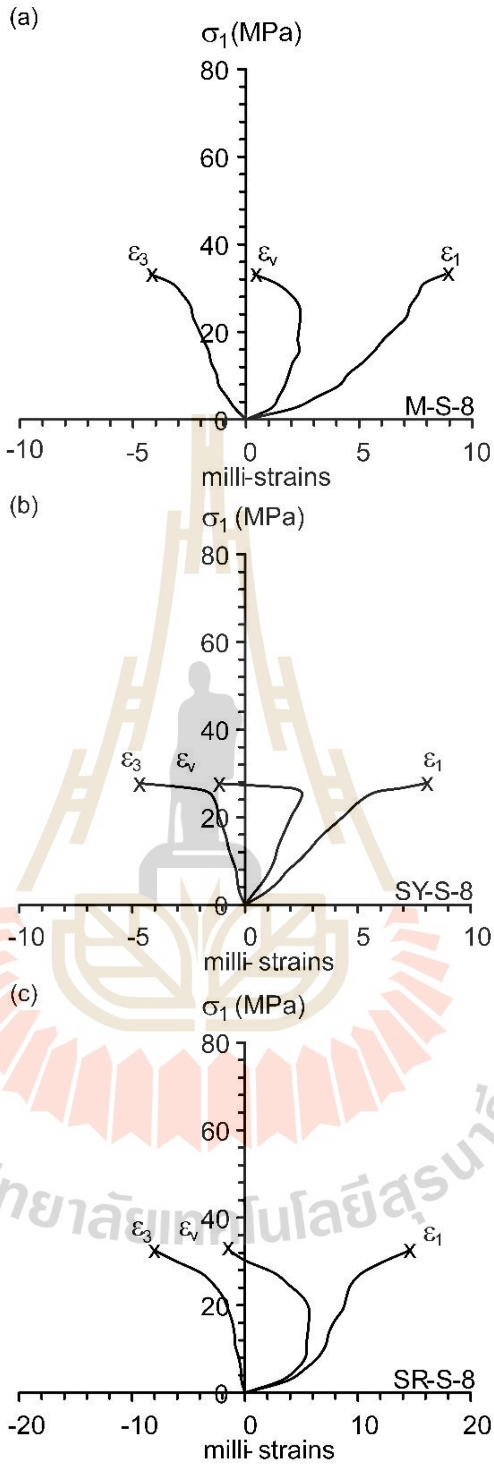

Figure D.13 Stress-strain curves of salt condition on 240 days for marble (a), siltstone (b), and sandstone (c).

APPENDIX E

UNIAXIAL COMPRESSION TEST RESULTS

Table E.1 Compressive strengths of marble for uniaxial compression test.

Conditions	Duration (Days)	Specimen No.	σ_c (MPa)	Average σ_c (MPa)
Initial	0	M-I-1	54.10	53.99
		M-I-2	53.46	
		M-I-3	54.41	
Water	60	M-W-1	48.92	47.49
		M-W-2	46.07	
	120	M-W-3	44.59	42.08
		M-W-4	39.56	
	180	M-W-5	34.14	36.73
		M-W-6	39.37	
	240	M-W-7	31.88	32.72
		M-W-8	33.50	
Brine	60	M-B-1	50.09	48.98
		M-B-2	47.86	
	120	M-B-3	47.14	44.27
		M-B-4	41.40	
	180	M-B-5	38.82	40.79
		M-B-6	42.75	
	240	M-B-7	41.44	40.82
		M-B-8	40.20	
Salt	60	M-S-1	44.63	43.09
		M-S-2	41.55	
	120	M-S-3	41.81	39.95
		M-S-4	38.08	
	180	M-S-5	33.18	35.42
		M-S-6	37.65	
	240	M-S-7	31.91	31.25
		M-S-8	30.60	

Table E.2 Compressive strengths of siltstone for uniaxial compression test.

Conditions	Duration (Days)	Specimen No.	σ_c (MPa)	Average σ_c (MPa)
Initial	0	SY-I-1	45.94	46.09
		SY-I-2	46.26	
		SY-I-3	46.07	
Water	60	SY-W-1	39.49	37.68
		SY-W-2	35.86	
	120	SY-W-3	35.26	34.09
		SY-W-4	32.92	
	180	SY-W-5	26.75	30.33
		SY-W-6	31.91	
	240	SY-W-7	21.08	26.48
		SY-W-8	31.88	
Brine	60	SY-B-1	41.48	39.87
		SY-B-2	38.25	
	120	SY-B-3	38.22	36.96
		SY-B-4	35.70	
	180	SY-B-5	34.46	34.12
		SY-B-6	33.79	
	240	SY-B-7	25.48	28.68
		SY-B-8	31.88	
Salt	60	SY-S-1	33.18	34.76
		SY-S-2	36.34	
	120	SY-S-3	30.58	29.95
		SY-S-4	27.41	
	180	SY-S-5	26.78	26.93
		SY-S-6	23.59	
	240	SY-S-7	22.33	22.32
		SY-S-8	22.31	

Table E.3 Compressive strengths of sandstone for uniaxial compression test.

Conditions	Duration (Days)	Specimen No.	σ_c (MPa)	Average σ_c (MPa)
Initial	0	SR-I-1	54.29	50.32
		SR-I-2	44.67	
		SR-I-3	52.01	
Water	60	SR-W-1	44.95	44.47
		SR-W-2	43.99	
	120	SR-W-3	39.56	38.93
		SR-W-4	38.29	
	180	SR-W-5	34.46	33.83
		SR-W-6	33.18	
	240	SR-W-7	32.57	32.24
		SR-W-8	31.91	
Brine	60	SR-B-1	47.22	45.26
		SR-B-2	43.35	
	120	SR-B-3	42.15	41.78
		SR-B-4	41.40	
	180	SR-B-5	37.97	37.78
		SR-B-6	37.58	
	240	SR-B-7	38.82	38.49
		SR-B-8	38.15	
Salt	60	SR-S-1	38.89	40.48
		SR-S-2	42.08	
	120	SR-S-3	37.01	35.94
		SR-S-4	34.87	
	180	SR-S-5	31.56	32.02
		SR-S-6	32.49	
	240	SR-S-7	29.62	30.44
		SR-S-8	31.27	

Table E.4 Elastic modulus of marble for uniaxial compression test.

Conditions	Duration (Days)	Specimen No.	E (GPa)	Average E (GPa)
Initial	0	M-I-1	11.57	12.7
		M-I-2	13.16	
		M-I-3	14.19	
Water	60	M-W-1	10.34	10.37
		M-W-2	10.39	
	120	M-W-3	9.36	8.45
		M-W-4	7.55	
	180	M-W-5	8.43	7.74
		M-W-6	6.51	
	240	M-W-7	7.23	7.23
		M-W-8	7.23	
Brine	60	M-B-1	11.12	10.26
		M-B-2	9.40	
	120	M-B-3	9.20	8.65
		M-B-4	8.10	
	180	M-B-5	7.00	7.85
		M-B-6	8.70	
	240	M-B-7	7.66	7.63
		M-B-8	7.60	
Salt	60	M-S-1	8.98	7.90
		M-S-2	6.87	
	120	M-S-3	7.17	6.68
		M-S-4	6.18	
	180	M-S-5	6.20	6.10
		M-S-6	6.00	
	240	M-S-7	5.85	5.93
		M-S-8	6.00	

Table E.5 Elastic modulus of siltstone for uniaxial compression test.

Conditions	Duration (Days)	Specimen No.	E (GPa)	Average E (GPa)
Initial	0	SY-I-1	13.31	13.63
		SY-I-2	11.72	
		SY-I-3	15.87	
Water	60	SY-W-1	7.42	7.86
		SY-W-2	8.30	
	120	SY-W-3	4.99	6.04
		SY-W-4	7.10	
	180	SY-W-5	6.51	5.43
		SY-W-6	4.35	
	240	SY-W-7	5.56	5.13
		SY-W-8	4.69	
Brine	60	SY-B-1	8.13	7.84
		SY-B-2	7.54	
	120	SY-B-3	7.32	6.74
		SY-B-4	6.15	
	180	SY-B-5	5.86	5.87
		SY-B-6	5.87	
	240	SY-B-7	5.45	5.50
		SY-B-8	5.55	
Salt	60	SY-S-1	5.70	5.85
		SY-S-2	6.00	
	120	SY-S-3	4.06	4.34
		SY-S-4	4.62	
	180	SY-S-5	4.10	3.90
		SY-S-6	3.70	
	240	SY-S-7	3.95	3.80
		SY-S-8	3.65	

Table E.6 Elastic modulus of sandstone for uniaxial compression test.

Conditions	Duration (Days)	Specimen No.	E (GPa)	Average E (GPa)
Initial	0	SR-I-1	6.74	6.12
		SR-I-2	6.41	
		SR-I-3	5.20	
Water	60	SR-W-1	4.43	4.64
		SR-W-2	4.85	
	120	SR-W-3	3.98	4.19
		SR-W-4	4.40	
	180	SR-W-5	3.98	3.60
		SR-W-6	3.21	
	240	SR-W-7	3.25	3.40
		SR-W-8	3.55	
Brine	60	SR-B-1	5.00	5.55
		SR-B-2	6.10	
	120	SR-B-3	4.54	4.86
		SR-B-4	5.18	
	180	SR-B-5	4.30	4.20
		SR-B-6	4.10	
	240	SR-B-7	4.00	4.00
		SR-B-8	4.00	
Salt	60	SR-S-1	4.76	4.10
		SR-S-2	3.48	
	120	SR-S-3	3.42	3.52
		SR-S-4	3.62	
	180	SR-S-5	3.20	3.13
		SR-S-6	3.05	
	240	SR-S-7	3.00	3.02
		SR-S-8	3.00	

Table E.7 Poisson's ratio of marble for uniaxial compression test.

Conditions	Duration (Days)	Specimen No.	ν	Average ν
Initial	0	M-I-1	0.15	0.15
		M-I-2	0.16	
		M-I-3	0.15	
Water	60	M-W-1	0.19	0.20
		M-W-2	0.20	
	120	M-W-3	0.25	0.25
		M-W-4	0.26	
	180	M-W-5	0.27	0.27
		M-W-6	0.26	
	240	M-W-7	0.27	0.27
		M-W-8	0.27	
Brine	60	M-B-1	0.21	0.23
		M-B-2	0.25	
	120	M-B-3	0.29	0.28
		M-B-4	0.27	
	180	M-B-5	0.27	0.28
		M-B-6	0.28	
	240	M-B-7	0.28	0.28
		M-B-8	0.28	
Salt	60	M-S-1	0.19	0.19
		M-S-2	0.19	
	120	M-S-3	0.20	0.23
		M-S-4	0.25	
	180	M-S-5	0.21	0.24
		M-S-6	0.26	
	240	M-S-7	0.26	0.26
		M-S-8	0.26	

Table E.8 Poisson's ratio of siltstone for uniaxial compression test.

Conditions	Duration (Days)	Specimen No.	ν	Average ν
Initial	0	SY-I-1	0.23	0.23
		SY-I-2	0.23	
		SY-I-3	0.24	
Water	60	SY-W-1	0.25	0.25
		SY-W-2	0.26	
	120	SY-W-3	0.25	0.26
		SY-W-4	0.26	
	180	SY-W-5	0.28	0.27
		SY-W-6	0.28	
	240	SY-W-7	0.27	0.28
		SY-W-8	0.28	
Brine	60	SY-B-1	0.24	0.26
		SY-B-2	0.27	
	120	SY-B-3	0.25	0.27
		SY-B-4	0.26	
	180	SY-B-5	0.27	0.28
		SY-B-6	0.28	
	240	SY-B-7	0.28	0.28
		SY-B-8	0.28	
Salt	60	SY-S-1	0.23	0.24
		SY-S-2	0.24	
	120	SY-S-3	0.26	0.25
		SY-S-4	0.24	
	180	SY-S-5	0.25	0.25
		SY-S-6	0.25	
	240	SY-S-7	0.25	0.26
		SY-S-8	0.26	

Table E.9 Poisson’s ratio of sandstone for uniaxial compression test.

Conditions	Duration (Days)	Specimen No.	ν	Average ν
Initial	0	SR-I-1	0.23	0.22
		SR-I-2	0.22	
		SR-I-3	0.21	
Water	60	SR-W-1	0.25	0.25
		SR-W-2	0.25	
	120	SR-W-3	0.27	0.27
		SR-W-4	0.28	
	180	SR-W-5	0.27	0.27
		SR-W-6	0.27	
	240	SR-W-7	0.28	0.28
		SR-W-8	0.27	
Brine	60	SR-B-1	0.24	0.26
		SR-B-2	0.27	
	120	SR-B-3	0.27	0.28
		SR-B-4	0.28	
	180	SR-B-5	0.27	0.28
		SR-B-6	0.28	
	240	SR-B-7	0.28	0.28
		SR-B-8	0.28	
Salt	60	SR-S-1	0.23	0.23
		SR-S-2	0.23	
	120	SR-S-3	0.24	0.25
		SR-S-4	0.25	
	180	SR-S-5	0.25	0.26
		SR-S-6	0.26	
	240	SR-S-7	0.26	0.26
		SR-S-8	0.26	

APPENDIX F

BRAZILLIAN TENSILE STRENGTH RESULTS

Table F.1 Tensile strengths of marble for Brazilian tension test.

Conditions	Duration (Days)	Specimen No.	σ_B (MPa)	Average σ_B (MPa)
Initial	0	M-I-1-1	7.13	6.21
		M-I-1-2	6.34	
		M-I-1-3	5.15	
Water	60	M-W-1-1	4.36	4.98
		M-W-1-2	4.60	
		M-W-1-3	4.82	
	120	M-W-2-1	4.24	4.42
		M-W-2-2	5.58	
		M-W-2-3	4.69	
	180	M-W-3-1	4.26	4.20
		M-W-3-2	3.80	
		M-W-3-3	6.50	
	240	M-W-4-1	4.23	3.94
		M-W-4-2	4.47	
		M-W-4-3	3.14	
Brine	60	M-B-1-1	4.91	5.06
		M-B-1-2	5.36	
		M-B-1-3	4.91	
	120	M-B-2-1	4.91	4.67
		M-B-2-2	4.67	
		M-B-2-3	4.42	
	180	M-B-3-1	4.93	4.40
		M-B-3-2	4.01	
		M-B-3-3	5.81	
	240	M-B-4-1	6.23	4.12
		M-B-4-2	6.45	
		M-B-4-3	2.67	

Table F.1 Tensile strengths of marble for Brazilian tension test (continue).

Conditions	Duration (Days)	Specimen No.	σ_B (MPa)	Average σ_B (MPa)
Salt	60	M-S-1-1	4.47	4.47
		M-S-1-2	4.47	
		M-S-1-3	3.57	
	120	M-S-2-1	4.91	4.14
		M-S-2-2	3.09	
		M-S-2-3	4.40	
	180	M-S-3-1	5.58	4.03
		M-S-3-2	5.14	
		M-S-3-3	4.36	
	240	M-S-4-1	4.67	3.80
		M-S-4-2	4.67	
		M-S-4-3	4.47	

Table F.2 Tensile strengths of siltstone for Brazilian tension test.

Conditions	Duration (Days)	Specimen No.	σ_B (MPa)	Average σ_B (MPa)
Initial	0	SY-I-1-1	2.47	3.15
		SY-I-1-2	2.79	
		SY-I-1-3	2.57	
Water	60	SY-W-1-1	2.46	2.20
		SY-W-1-2	2.20	
		SY-W-1-3	1.90	
	120	SY-W-2-1	2.24	1.72
		SY-W-2-2	1.79	
		SY-W-2-3	1.59	
	180	SY-W-3-1	1.56	1.38
		SY-W-3-2	1.79	
		SY-W-3-3	1.57	
	240	SY-W-4-1	1.58	1.49
		SY-W-4-2	1.56	
		SY-W-4-3	1.34	
Brine	60	SY-B-1-1	2.11	2.47
		SY-B-1-2	2.25	
		SY-B-1-3	2.24	
	120	SY-B-2-1	1.35	2.06
		SY-B-2-2	2.02	
		SY-B-2-3	1.79	
	180	SY-B-3-1	2.68	1.73
		SY-B-3-2	1.79	
		SY-B-3-3	1.77	
	240	SY-B-4-1	1.90	1.83
		SY-B-4-2	1.91	
		SY-B-4-3	1.70	

Table F.2 Tensile strengths of siltstone for Brazilian tension test (continue).

Conditions	Duration (Days)	Specimen No.	σ_B (MPa)	Average σ_B (MPa)
Salt	60	SY-S-1-1	2.69	2.10
		SY-S-1-2	2.70	
		SY-S-1-3	2.91	
	120	SY-S-2-1	1.99	1.67
		SY-S-2-2	2.43	
		SY-S-2-3	1.76	
	180	SY-S-3-1	1.88	1.28
		SY-S-3-2	1.70	
		SY-S-3-3	1.61	
	240	SY-S-4-1	1.45	1.30
		SY-S-4-2	1.35	
		SY-S-4-3	1.12	

Table F.3 Tensile strengths of sandstone for Brazilian tension test.

Conditions	Duration (Days)	Specimen No.	σ_B (MPa)	Average σ_B (MPa)
Initial	0	SR-I-1-1	4.50	4.23
		SR-I-1-2	4.06	
		SR-I-1-3	4.12	
Water	60	SR-W-1-1	2.02	2.27
		SR-W-1-2	2.49	
		SR-W-1-3	1.99	
	120	SR-W-2-1	1.79	1.87
		SR-W-2-2	1.80	
		SR-W-2-3	2.03	
	180	SR-W-3-1	2.24	1.58
		SR-W-3-2	1.76	
		SR-W-3-3	2.26	
	240	SR-W-4-1	1.35	1.46
		SR-W-4-2	1.68	
		SR-W-4-3	1.81	
Brine	60	SR-B-1-1	3.14	3.10
		SR-B-1-2	3.14	
		SR-B-1-3	3.05	
	120	SR-B-2-1	2.15	2.73
		SR-B-2-2	3.14	
		SR-B-2-3	2.90	
	180	SR-B-3-1	2.03	2.32
		SR-B-3-2	2.25	
		SR-B-3-3	1.79	
	240	SR-B-4-1	1.79	2.09
		SR-B-4-2	1.79	
		SR-B-4-3	2.68	

Table F.3 Tensile strengths of sandstone for Brazilian tension test (continue).

Conditions	Duration (Days)	Specimen No.	σ_B (MPa)	Average σ_B (MPa)
Salt	60	SR-S-1-1	3.14	2.11
		SR-S-1-2	3.14	
		SR-S-1-3	3.05	
	120	SR-S-2-1	2.70	1.66
		SR-S-2-2	2.44	
		SR-S-2-3	2.88	
	180	SR-S-3-1	3.14	1.46
		SR-S-3-2	2.47	
		SR-S-3-3	2.90	
	240	SR-S-4-1	3.14	1.39
		SR-S-4-2	2.91	
		SR-S-4-3	2.90	

APPENDIX G

LIST OF PUBLICATION

EFFECT OF BRINE SUBMERSION ON MECHANICAL PROPERTIES OF DECORATING STONES

[1]NONGPLOY PUANGTHONG, [2]LAKSIKAR SITTHIMONGKOL, [3]KIATTISAK ARTKHONGHAN, [4]KITTITEP FUENKAJORN

Geomechanics Research Unit, Suranaree University of Technology, Nakhon Ratchasima 30000, Thailand
E-mail: nongploy.puangthong@gmail.com

Abstract - The objective of this study is to determine the effects of NaCl brine submersion on mechanical properties of siltstone, sandstone and marble that have been used as decorating stones in the northeast of Thailand. Rock specimens are submerged under saturated brine for up to 240 days. Every 60 days interval, their liquid contents, strengths and elasticity are determined. Results indicate that after 240 days siltstone and sandstone specimens can absorb brine up to 6% and 9% by weight, where less than 0.1% can be absorbed by marble. Due to the effect of pore pressure both compressive and tensile strengths and elasticity of the rocks continue to decrease with increasing submersion duration. When left air-dried for 30 days further reduction of rock strengthsand elasticity are observed from the siltstone and sandstone. This is due to initiation and propagation of fissures and micro cracks caused by the growth of remaining salt crystals left in the pore spaces.

Keywords - Rock Deterioration, Salt Crystallization, Sodium Chloride Brine, Submerged Duration, Rock Strengths

I. INTRODUCTION

Rock salt near ground surface in the Maha Sarakham formation, northeast of Thailand, has caused damage to housing structures, particularly near the edges of the basins where salt depth is less than 50 m. The shallow salt beds are mostly covered by silty and sandy soils. Detailed description of the salt and geology of the basins are given by Warren [1]. During rainy season the saline groundwater can reach the ground surface and can cause flooding in some low areas. The groundwater subsides during dry season and salt crystals and powder are left on the top soil and in decorating stonesforming housingterraceand pavement. Marble, siltstone and sandstone are widely used in the area. This calls for the study of the effect of saline groundwater and remaining salt crystals on the long-term integrity of these rocks.

The objective of this study is to determine the effect of brine submersion on the mechanical properties of some decorating stones in the laboratory. Marble, siltstone and sandstone cylindrical specimens are submerged in the distilled water and saturated brine (NaCl) for up to 240 days (8 months). Liquid and salt contents are measured for every 60 days interval of submersion. Compressive and tensile strengths and elastic parameters of specimens are also determined for every 60 days. The evolutions of the mechanical properties are determined with the increase of submersion duration and liquid and salt contents. X-ray diffraction analysis is performed on specimens under each test interval to compare with those of the initial conditions (before liquid submersion).

II. SAMPLE AND BRIN PREPARATION

The rock specimens used in this study are Khoa Khad marble, Phu Phan siltstone, and Phu Phan fine-grained sandstone. They expose in the northeast of Thailand and are widely used as decorating stones in the region. For each rock type, thirty specimens are prepared to obtain cylindrical specimens with nominal dimensions of 45 mm in diameter and 90 mm in height for uniaxial compression test. Siltstone and sandstone are prepared to have bedding planes normal to loading direction. Forty-five specimens are prepared to obtained cylindrical disks with a diameter of 54 mm and thickness of 27 mm for Brazilian tension test.

Saturated brine is prepared by mixing distilled water with pure sodium chloride powder (NaCl) in plastic container. NaCl powder is added until no future dissolution occurs. The solution is continuously stired. The container is left opened to allow evaporation. The process is performed at 30 ± 1°C. Approximately 39.1% by weight of NaCl powder is used to obtain fully saturation. The brine density is measured by hydrometer (ASTM D1298) [2]. The density is 1.21 g/cc. Its viscosity is measured by marsh funnel viscometer, which is equal to 85 mPa•s (85 centipoise).

III. TEST SCHEME

After drilling and cutting all specimens are oven-dried at 105 °C for 24 hours. Their weight and dimensions are measured. The specimens for each rock type are separated into three sets, as shown in Fig. 1. Each set comprises eight cylindrical and twelve disk specimens. Specimens of set I are submerged in distilled water, and those of sets II and III are in saturated brine. Total submerging period is 240 days. Every 60 days, two cylindrical and three disk specimens from each set and each rock type are taken out from the liquid container.

The liquid contents of specimens from set I and II are determined in accordance with ASTM D2216-19 [3]. They are subsequently subjected to uniaxial compression test (ASTM 7012-14e) [4]. Brazilian tension tests (ASTM D3967-16) [5] are performed on disk specimens from the two sets.After taking out from the brine container the specimens from set III are left air-dried for 30 days, and then are subjected to the two mechanical tests as describe above. The design test scheme allows assessing the effects of water and brine saturations (sets I and II) and evaluating the effect of salt crystal growth on the mechanical response of the test specimens from set III.

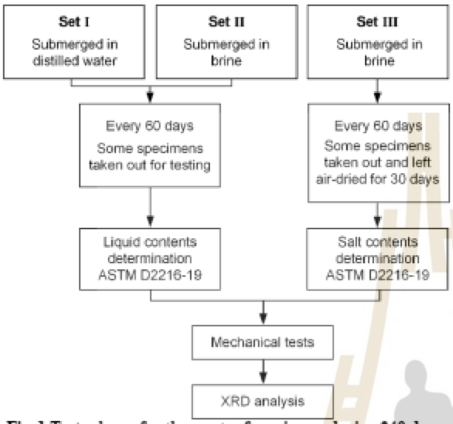

Fig. 1 Test scheme for three sets of specimens during 240 days submersion

IV. TEST RESULTS

Liquid Content

The liquid contents of specimens from sets I and II are measured immediately after they have been removed from the liquid container. The salt content of specimens from set III (after air-dried for 30 days) are measured by comparing their weight with those of the initial condition.

Fig. 2 shows the results for every 60 days interval up to 240 days. The test marble has such low porosity that less than 0.1% by weight of water and brine can infiltrate the rock matrix (Fig. 2a). Siltstone and sandstone can rapidly absorb liquid after submersion, where water can penetrate through the connective voids better than the brine for both rock types. This is probably due to that water has lower density and viscosity than brine. Under water submersion for 240 days, the water contents of siltstone and sandstone are up to 6% and 9%, respectively.The liquid contents increase with increasing submerging duration. For the specimens from set III, some pore spaces are filled with crystallized salt. The longer submerging duration, the larger amount of salt can be measured, as clearly shown in siltstone and sandstone (Figs. 2b and 2c). The diagrams in Fig. 2 also suggest that even after 240 days of liquid submersion, all specimens have not reached fully-saturated condition, as the liquid and salt contents continue to increase at 240 days of submersion.

Compression Test Results

Immediately after the liquid contents have been determined, uniaxial compression tests are performed on cylindrical specimen

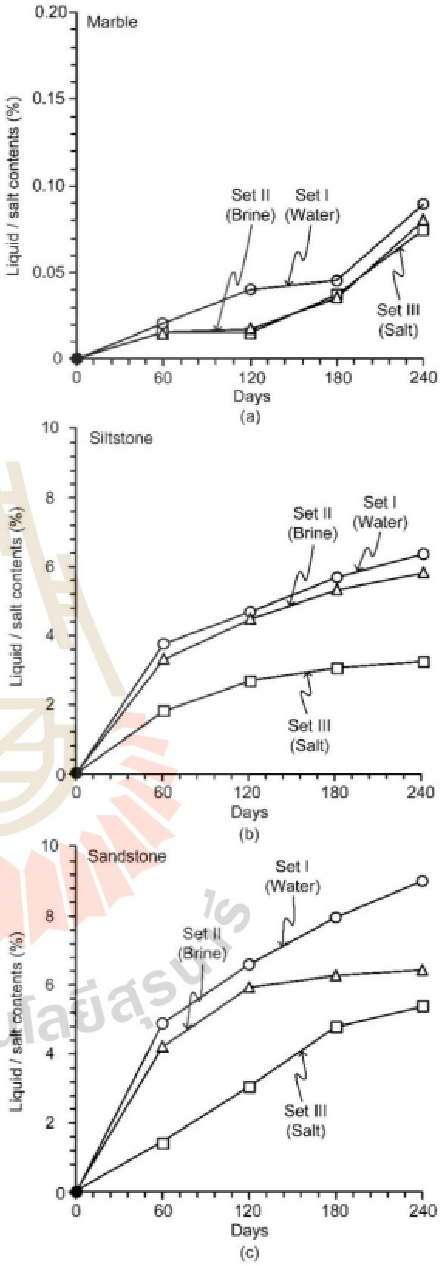

Fig. 2 Liquid and salt contents as a function of submerging duration for marble (a), siltstone (b), and sandstone (c)

from sets I and II. The specimen strength (σ_c) and elastic modulus (E) are determined for each 60 days interval. The elastic modulus is obtained from the tangent of axial stress-strain curve at about 40% to 50% of the rock strength. Fig. 3 shows the results for all rock types. Post-test specimens show combination of multiple shear and longitudinal failures. No distinctive different of failure modes has been detected among

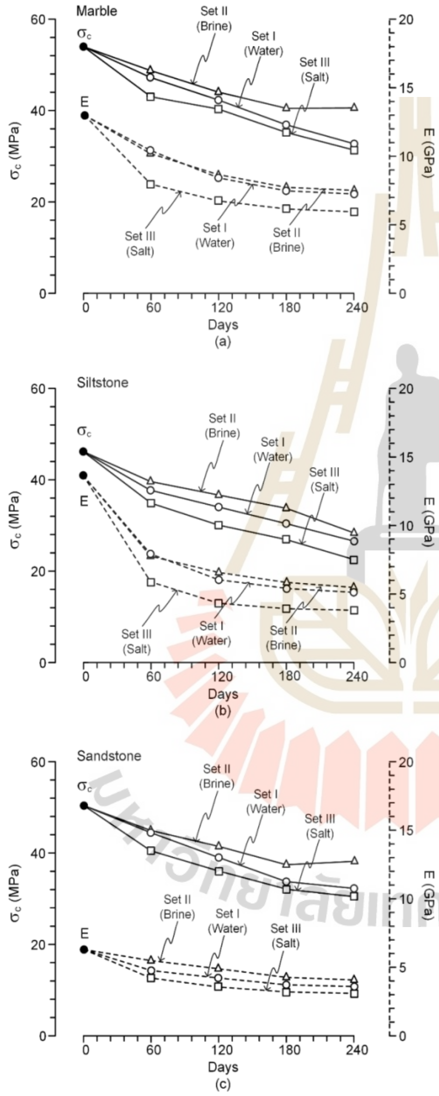

Fig. 3 Uniaxial compressive strengths (solid line) and elastic modulus (dash line) as a function of submerging duration for marble (a), siltstone (b), and sandstone (c). Solid point represents initial condition (before liquid submersion)

the specimens. Both specimen strength and elasticity continuously decrease from their initial condition (without liquid submersion), where water saturated specimens always show lower strength and elasticity than thosewith brine saturation.This is due to the effect of pore pressure,which coincide with test results obtained from other researches (Robinson [6]; Khamrat et al [7]; Liu et al [8]). Specimens with water exhibit higher effect of pore pressure than those with brine because their pore spaces contain larger volume of water as evidenced by the liquid contents measured prior to themechanical testing (see Fig. 2). The lowest strength and elasticity are obtained from the specimens containing salt crystals (set III). This holds true for all rock types and submersion durations. The mechanism that reduces the rock mechanical properties probably relates to the salt crystal growth in the pore spaces which cause initiation and propagation of fissures and inter-crystalline boundaries before the specimens are subjected to loading under uniaxial compression (Shukla et al, 2013 [9]; Sampath et al, 2018 [10]; Dinesh et al, 2022 [11]).

Liquid submersion also increases Poisson's ratios of the specimens from sets I and II (Fig. 4). Such phenomenon increases with test duration for all rock types. The Poisson's ratio is determined from the ratio of lateral-to-axial strains at about 40% to 50% of the failure stress. The increase of Poisson's ratios is due to the increase of the lateral dilation of the specimens when they are under axial loading. This is caused by the liquid pressure trapped in the pore spaces. The longer submersion duration leads to the higher internal liquid pressure, and subsequently the larger lateral dilation.

For the specimens containing salt crystals (set III), the new defects (micro-cracks and fissures) reduce the bonding inside rock matrix. As a result, the lateral dilation of specimens is greater under axial loading, as compared to those of the initial condition. Such effect also increases with submersion duration.

Brazilian Tensile Strengths

Similar to the uniaxial compression specimens, the Brazilian disk specimens from sets I and II are immediately subjected to diametral loading after their liquid contents have been measured. Fig. 5 shows the Brazilian tensile strengths (σ_B) as a function of submersion duration for all rock types. They notably decrease with increasing submersion duration. Pore pressure is again the main factor inducing the decrease of tensile strengths of specimens with increasing liquid contents. New micro-cracks and fissures induced by salt crystal growth in the pore space of specimen from set III can further reduce the rock tensile strength to be lower than those tested under wet conditions. This holds true for all rock types and test durations.

X-ray Diffraction (XRD) Analysis

Some specimens from each rock type and each test duration are ground to obtain powder finer than 0.25 mm (mesh #60). The prepared specimens are analyzed using Bruker D8 advance with TOPAS software to determine their mineral compositions in weight percent. Table 1 gives the mineral compositions of rock specimens at initial condition. Before submerging in the liquid, siltstone and sandstone are mainly composed of quartz and feldspar, while calcite and dolomite are prominent in marble (Table 1). The XRD results from other submersion durations and liquid types do not show significant change of the amounts of these main mineral compositions.

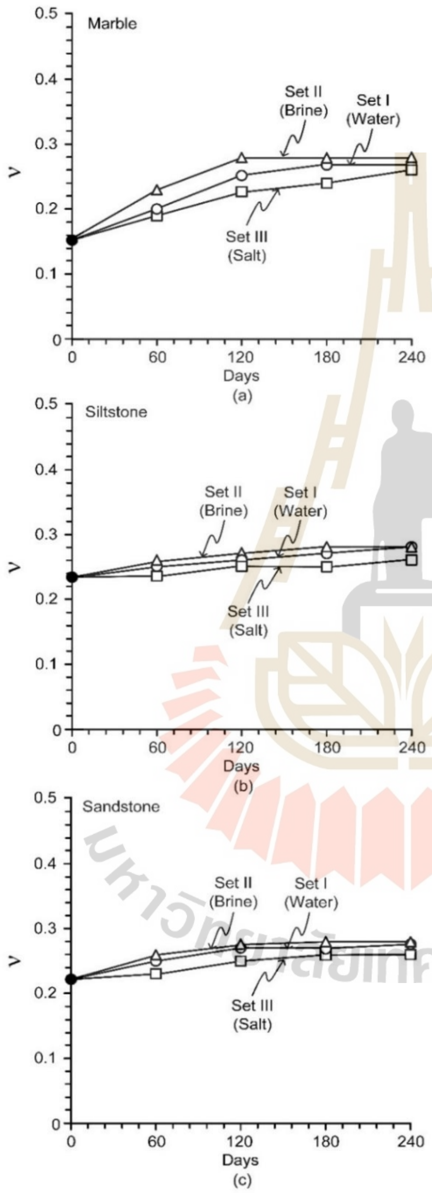

Fig 4. Poisson's ratio (ν) as a function of submerging duration for marble (a), siltstone (b), and sandstone (c).

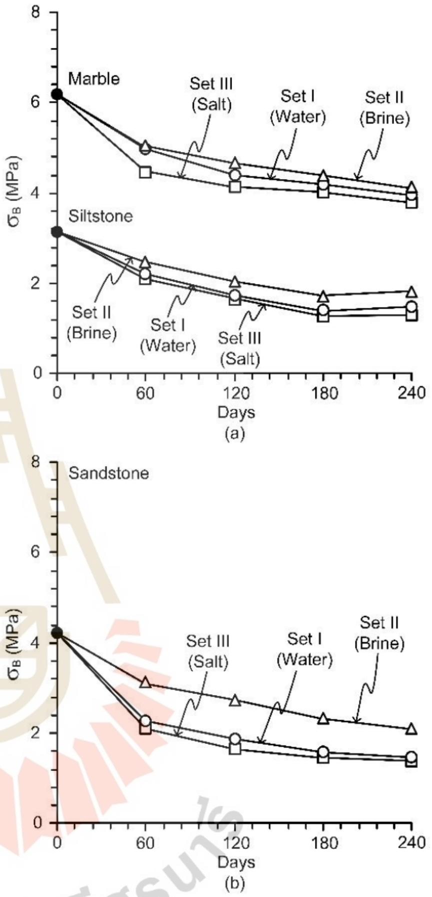

Fig 5. Brazilian tensile strengths (σ_B) as a function of submerging duration for marble, siltstone (a), and sandstone (b).

As shown in Fig. 6 the combined weight percents of quartz and feldspar remain effectively unchanged for siltstone and sandstone. Marble also shows the similar amounts of calcite and dolomite in the specimens from different test conditions. Small differences of weight percents of these key minerals can however be observed. This is probably due to the intrinsic variability among the specimens. In summary, the minerals composing the tested sandstone, siltstone and marble tend to be chemically insensitive to the water and brine, at least within the test period of 240 days.

V. DISCUSSIONS

Submersion of rock specimens in distilled water (set I) has been performed to obtain the rock mechanical properties, as affected by pore pressure to compare the results with those submerged under saturated NaCl brine under the same period. This could reveal how the brine affects the rock properties. The compressive and tensile strengths and elastic parameters of the water submerging specimens are about 5-10% lower than those obtained from the brine submersion (Figs. 3 and 4). Thisdoes not necessarily mean the brine cause less adverse effect to rock strengths and elasticity as compared to water. The strength and elasticity differences are due to the fact that the lower density and viscosity of water allow a larger amount of liquid to penetrate into the connective voids of the rocks, as compared to the higher density and viscosity of the brine. As a result, strength reduction caused by the trapped water pore pressure is more severe than that of the brine pore pressure. Sincethere is no significant alteration of the mineral composing these rocks as suggested by XRD analysis results, the strengths and elasticity of the water submersion specimens would return to their initial values after they are left air-dried. For the brine submersion specimens, the real adverse effect occurs when they are left dried. The remaining recrystallized salt expands inside the pore spaces, and hence initiates new cracks and fissure or propagates the existing ones. This is a progressive process as additional brine penetrates under increasing the submersion period. This process is however irreversible. The compressive and tensile strengths of specimens with salt crystals in pore spaces are about 35% to 50% lower than those of the initial condition, and are lower than those tested under wet conditions. Approximate extrapolation of the compressive strength-time curves suggests that the threerock types could lose their strength within 5 to 6 years. Note that this approximation is based on that the rocks are continuously under saturated brine before drying. In actual condition, however they would be subjected to yearly cycle of wet and dry which could extend their service life longer than the approximation above. Remediation of the salt crystals induced damage to these decorating rocks could be made by routinely washing these rocks with fresh water soon after they submerged under the brine.

Rock types	Mineral compositions (w%)
Marble	Calcite (55.75%), Dolomite (4.84%), Wollastonite (1.65%), Ankerite (11.40%), Actinolite (9.04%), Huntite (7.16%), Tremolite (5.79%), Chalcopyrite (2.4%), Diopside (1.43%)
Siltstone	Quartz (70.04%), Feldspar (2.21%), Clay Minerals (26.06%), Mica (1.33%), Pyrite (0.19%), Siderite (0.16%)
Sandstone	Quartz (50.99%), Feldspar (40.96%), Clay Minerals (5.3%), Mica (1.19%), Calcite (1.05%), Pyrite (0.39%), Hematite (0.12%)

Table 1Mineral compositions by X-ray diffraction analysis for initial condition.

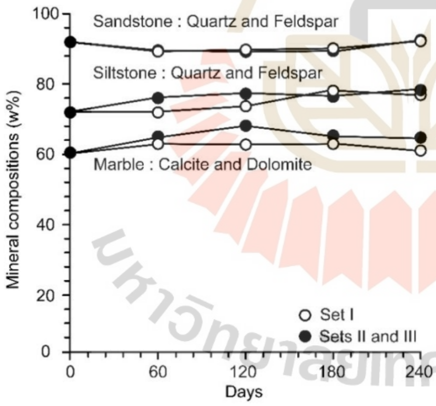

Fig. 6 Main mineral compositions observed during 240 days of submersion.

VI. CONCLUSION

Conclusions drawn from this study can be summarized as follows.

1) Siltstone and sandstone can absorb water and brine up to 6 % to 9 % by weight while less than 0.1% can be absorbed by marble through the submersion period of 240 days.
2) For all tested rocks water can infiltrate the connective voids better than brine can. This results in lower strengths and elasticity of water submersion specimens than brine submersion specimens. This is due to a high pore pressure effect for water submersion specimens.
3) The reduction of rock strength and elasticity increases with increasing submersion duration.
4) After the brine submersion specimens have been left air-dried for 30 days, they yield the lower strength and elasticity than those of the wet specimens. This is due to the initiation and propagation of fissure and micro-cracks caused by the growth of the remaining salt crystals in the pore spaces.
5) X-ray diffraction analysis shows that within the maximum continuous period of submersion in both liquids, all tested rocks show insignificant change of their mineral compositions.

ACKNOWLEDGEMENT

This work was financially supported by Suranaree University of Technology (SUT), Thailand Science Research and Innovation (TSRI), and National Science, Research and Innovation Fund (NSRF) under the grant numbers: NRIIS 179329. Permission to publish this paper is gratefully acknowledged.

REFERENCES

[1] J. Warren, "Evaporites: Their Evolution and Economics," Oxford: Blackwell Science., 1999.

[2] ASTM D1298, Standard Test Method for Density, Relative Density (Specific Gravity), or API Gravity of Crude Petroleum and Liquid Petroleum Products by Hydrometer Method, In Annual Book of ASTM Standards, West Conshohocken, PA,2016.

[3] ASTM D2216-19, Standard Test Method for Laboratory Determination of Water (Moisture) Content of Soil and Rock by Mass, In Annual Book of ASTM Standards, West Conshohocken, PA,2019.

[4] ASTM D7012-14, Standard Test Methods for Compressive Strength and Elastic Moduli of Intact Rock Core Specimens under Varying States of Stress and Temperatures, In Annual Book of ASTM Standards, West Conshohocken, PA,2014.

[5] ASTM D3967-16, Standard Test Method for Splitting Tensile Strength of Intact Rock Core Specimens, In Annual Book of ASTM Standards, West Conshohocken, PA,2016.

[6] L. H. Robinson, "Effects of pore and confining pressure on failure characteristics of sedimentary rocks," Petroleum Transactions., Vol.216, pp.26-32, 1958.

[7] S. Khamrat, S. Archeeploha, and K. Fuenkajorn, "Pore pressure effects on strength and elasticity of ornamental stones," Sci. Asia., Vol.42, pp.121-135,2016.

[8] X. Liu, K. Xue, Y. Luo, K. Long, Y. Liu, and Z. Liang, "The effect of pore pressure on the mechanical behavior of coal with burst tendency at a constant effective stress," Sustainability., Vol.14, pp.14568,2022.

[9] R. Shukla, P.G. Ranjith, S.K. Choi, A. Haque, M. Yellishetty, and L. Hong, "Mechanical behaviour of reservoir rock under brine saturation," Rock Mechanics and Rock Engineering., Vol.46, no.1, pp.83-93,2012.

[10] K. H. S. M. Sampath, M. S. A. Perera, D. Elsworth, P.G. Ranjith, S.K. Matthai, and T. Rathnaweera, "Experimental investigation on the mechanical behavior of victorian brown coal under brine saturation." Energy & Fuels., Vol.32, no.5, pp.5799-5811,2018.

[11] P. Dinesh, P. G. Ranjith, M.R. Behera, and N. Muthu, "Experimental and numerical (EFG method) studies on sedimentary rock under varied salinity conditions," Rock Mechanics and Mining Sciences., Vol.148, pp.1-21,2021.

★★★

BIOGRAPHY

Ms. Nongploy Puangthong born on November 11, 1998 in Bangkok, Thailand. She received her Bachelor's Degree in Engineering (Geological Engineering) from Suranaree University of Technology in 2020. For her post-graduate, she continued to study with a Master's degree in the Geological Engineering Program, Institute of Engineering, Suranaree university of Technology. During graduation, 2020-2023, She was a part time worker in position of research associate at the Geomechanics Research Unit, Institute of Engineering, Suranaree University of Technology.